

CHAPTER 16

Turbulence Models for Sediment Transport Engineering

D. A. Lyn

16.1 INTRODUCTION

In problems of civil engineering interest, sediment transport invariably occurs under turbulent-flow conditions. Traditional discussions (*ASCE Manual 54*; see also Chapter 2) of turbulence models have, however, been mainly restricted to the problem of determining the vertical distribution of suspended sediment in the simplest case of uniform channel flow over a plane bed. Since the appearance of *ASCE Manual 54* in 1975, there have been considerable advances in our understanding and hence modeling of complex turbulent flows, and these might be expected to have a positive impact on approaches to practical problems in sediment transport. In general, the scope of the problems that can be studied has been broadened substantially, and a larger range of engineering problems can be tackled with reasonable success. The more traditional basic questions have proven more refractory and progress in answering them has been correspondingly limited. Nevertheless, with ever-growing computational capabilities and the proliferation of commercial computational fluid dynamics (CFD) software packages, numerical modeling with turbulence models will in the foreseeable future become an increasingly important engineering tool in dealing with sediment transport problems. Hence, a basic familiarity with such models, their theoretical bases, and their limitations will be useful.

The present chapter describes the standard turbulence models currently being applied to problems involving sediment transport, focusing on so-called two-equation models, but also discussing more briefly simpler models that might be used judiciously for special problems, as well as more advanced models that may find more practical application in the future. In most applications thus far, the turbulence model has been taken without modification from fields where the use of these models is more solidly established, but where possibly important features unique to sediment transport are absent. The standard features, assumptions, and limitations of turbulence models are discussed in a number

of monographs (Rodi 1993; Hallbäck et al. 1996; Chen and Jaw 1998; Wilcox 1998; Piquet 1999; Durbin and Petterson Reif 2001), as well as review articles (Launder 1984; Speziale 1991; Hanjalic 1994; Rodi 1995; Speziale 1996; Lauder 1996; Spalart 2000), but, except for the review by the ASCE Task Committee on Turbulence Models in Hydraulic Computations (1988) and the works of Rodi, hydraulic or sedimentation engineering applications have not received much attention (see, however, the brief review by Lane 1998). General references on multiphase flows are also available (e.g., Crowe et al. 1998) that discuss aspects relevant to turbulent particulate flows, often, however, with gas-solid or bubbly flows in mind. Although the present chapter will necessarily rely heavily on these works, it will elaborate issues that may be of particular relevance to sediment-transport engineering applications. Turbulence modeling, especially for the very complicated problem involving sediment transport, is an extensive field undergoing continual development, and the present chapter can only serve as an introduction to the subject, targeted at a sedimentation engineering audience. For the most part, the discussion is restricted to classical problems in sediment-transport mechanics, emphasizing noncohesive uniform-sized sediment. The important case of depth-averaged models, in which complicating issues other than but closely related to turbulence modeling arise, is covered briefly in an appendix.

16.2 TURBULENCE, MODELS, AND PARTICULATE FLOWS

Before the mathematical models used to describe the behavior of turbulent flows in general and sediment-laden flows in particular are stated, a discussion of qualitative aspects introduces basic concepts, motivations, and terminology. Much use will be made of scaling arguments and dimensional analysis involving length scales and time scales (or velocity scales, because a combination of length and

time scales will define a velocity scale). These characteristic quantities associated with physical processes provide a measure of size and of duration. Turbulent flows exhibit a broad and continuous range of length (and time) scales corresponding loosely to the size of “eddying” motions or “eddies.” The analogy between turbulent and molecular transport, although deficient in many respects, has been important in the development of turbulence models, and it will be helpful to consider the similarities and differences between the two types of transport.

16.2.1 Qualitative Features of Turbulent Flows and Modeling Implications

In attempting to define turbulence, Tennekes and Lumley (1972) list several essential features. The instantaneous flow quantities at a point of a turbulent flow, such as velocity and pressure, fluctuate irregularly in time in such a way as to preclude predictability, except possibly in a statistical “averaged” sense. Instead of attempting to solve the complete exact governing equation, which is not feasible for practical problems, the engineer resorts to describing the flow by suitably averaged equations involving at most second-order moments, such as variances. Because the influence of higher-order statistics is presumed to be weaker, the modeler is permitted greater flexibility in formulating models of correlations involving higher-order terms (Launder 1996).

As a consequence of the averaging operation, detailed flow information is lost that may still have important transport effects, for which models, preferably simple and of wide applicability, must be developed. This much-greater effectiveness in mixing or greater “diffusivity” compared to laminar flows is the feature of turbulent flows that is often of most practical interest. The ratio of turbulent diffusivity (viscosity in the context of momentum transfer) to molecular diffusivity may be several orders of magnitude, which can be qualitatively understood in terms of the much larger length scales involved in the former compared to the latter. As a result, turbulent diffusive transport may be of comparable importance to or, in some cases, may even dominate advective transport, and the effective modeling of turbulent transport becomes essential to reliable predictions of overall transport. Turbulence models have therefore focused on predicting the effects of the large-scale motions responsible for the enhanced diffusivity.

Even though the main flow features of engineering interest, and hence the (time-)averaged equations, may be well approximated as being one- or two-dimensional, instantaneous turbulent fluctuations are essentially three-dimensional in that they are nonzero in all spatial directions. Moreover, turbulence characteristics will vary in at least one, and possibly all spatial directions; i.e., the turbulence is inhomogeneous. The characteristics in each coordinate direction also may differ from one another; i.e., the turbulence is anisotropic.

The modeling of strongly inhomogeneous and anisotropic features requires greater effort, both theoretically and computationally, and still is the subject of intensive research. The search for simpler models has often been based on assumptions of local homogeneity and isotropy, such that, in a sufficiently small volume in the flow region of interest, spatial variations and anisotropic effects may be neglected. The simple models, however, may not yield reliable results for flows far from the isotropic and homogeneous ideal.

A flow becomes turbulent at sufficiently high Reynolds number, $R = UL/v$, where U and L are appropriate velocity and length scales, and v is the fluid kinematic viscosity. In alluvial channel flows, R , based on an average velocity and the flow depth, h , can attain quite large values, because of the large length scale (h) involved. As a result, not only is the flow turbulent, but it is a high- R turbulent flow, a characteristic that has been exploited in turbulence modeling. Two aspects of high- R flows have been implicitly incorporated into most turbulence models (Launder 1996). The first is the empirical observation of high- R similarity, in which many practically important characteristics of high- R turbulent flows are largely insensitive to variations in R , or equivalently to the effects of molecular viscosity. This has implications for suspension flows, because it is known that the effective (molecular or small-scale) viscosity of a suspension may vary with the suspension concentration. For dilute suspensions, however, this effect is irrelevant as far as high- R turbulent flows are concerned, because viscous effects are unimportant in regions away from (smooth) solid boundaries. The second is that, at high R , turbulence at the smallest scales is considered locally isotropic, not being strongly influenced by the mean flow or the anisotropic large-scale turbulent motions. In smooth-channel flows, e.g., in the laboratory, however, viscous effects may be important in the near-bed region because the local R is low, and high- R model assumptions need to be reexamined. In sediment-transport applications with fine sands, viscous effects may also need to be considered in particular problems, such as the formation of ripples (Richards 1980).

In the shear flows of primary interest in hydraulic engineering, turbulent fluctuations or “kinetic energy,” which is more precisely defined later (Eq. (16-5)), may be viewed as being produced or extracted from the mean flow by the interaction of the fluctuations with large-scale mean velocity gradients. On the other hand, the fluctuations are also seen as being dissipated at the smallest scales by the action of viscosity. The process by which the energy is produced and then eventually dissipated, essentially through the stretching of vortices, is often conceptually pictured as a cascade, in which large-scale eddying motions undergo continual transformation into motions on smaller and smaller scales. Fluctuating vorticity, which accompanies this cascade, is a defining feature of turbulence. In spite of the fact that dissipation is effected through fluid viscosity, the rate of dissipation of turbulent kinetic energy, denoted by ϵ , is controlled

by the largest scales. Changes in fluid viscosity influence the scale on which dissipation occurs, but do not affect ϵ , consistent with the high- R similarity already mentioned. The importance of the large scales in determining ϵ will be reiterated throughout this chapter. When production and dissipation are in approximate balance, i.e., a local equilibrium is established, this may permit model simplification. On the other hand, strongly nonequilibrium turbulence, like strongly anisotropic turbulence, will present problems for simple turbulence models.

16.2.2 Length and Time Scales in Turbulent Sediment-Transport Problems

A familiarity with the relevant length and time (or velocity) scales is important in the discussion of turbulent flows and models. Turbulence scales characteristic of the bulk flow are usually taken to be the average or maximum velocity and the flow depth or boundary layer thickness, with time and length scales on the order of at most minutes and tens of meters, respectively. For flows where the turbulence is primarily generated by boundary shear, the shear velocity, u_* , which characterizes the local boundary shear stress, $\bar{\tau}_b$, since $u_* \equiv \sqrt{\bar{\tau}_b/\rho}$ (ρ is the fluid density), plays a particularly important role as a velocity scale. The smallest scales of turbulence are those associated with viscous dissipation of eddies, and hence are characterized by v and ϵ (with dimensions of energy per unit mass per unit time, [L^2/T^3]). The Kolmogorov scales, the smallest length and time scales in turbulent flows, are determined from these variables as $\eta_K = (\nu^3/\epsilon)^{1/4}$ and $\tau_K = (\nu/\epsilon)^{1/2}$, respectively, with typical values of $O(1 \text{ mm})$ and $O(0.05 \text{ s})$.

A comparison of turbulence scales with scales of interest in sediment-transport engineering, which may span a very wide range, provides a preliminary assessment of the importance of effects on turbulence and serves as a guide to appropriate turbulence models. Morphological time scales over which changes of engineering significance in erodible boundaries occur may be on the order of months or even years. The migration speed of bed forms is much smaller than bulk-flow velocities, and so is associated with correspondingly much longer time scales. Flood hydrographs in rivers and the corresponding sedimentographs or flow reversals in estuaries occur on time scales of hours or days. Because of the large disparities in time scales, such "long"-time-scale unsteady phenomena should not interact strongly with "short"-time-scale turbulence-generating (or -dissipating) mechanisms, and hence turbulence models developed for steady-state problems should be adequate; i.e., deficiencies in predictive abilities are likely due to other than unsteady effects. The possibly different needs of sediment transport and flow predictions need to be pointed out. Because sediment transport may occur over relatively long time scales, detailed flow features may have important implications for sediment transport, and yet, from the narrow point of view

of the gross flow, be unremarkable. Further, this does not address possible difficulties arising when problems involving large-scale unsteadiness are *deliberately* simplified and modeled as being steady. In problems involving shorter time (or length) scales, e.g., oscillatory waves with periods on the order of seconds, possible unsteady effects on turbulence may not be so easily dismissed. Because laboratory measurements play such an important role in verifying (and calibrating) turbulence models, it should also be emphasized that important length and time scales in the laboratory may differ from those in the field, and effects that may be small or negligible in the field may assume greater importance in small-scale laboratory experiments, and vice versa.

Particle length and time scales merit further discussion, because these may be comparable to turbulence scales, and so conducive to potentially strong interaction with turbulence. A characteristic length scale of a sedimenting particle is its size, d , and its time scale may be taken as the time required for it to respond to fluid velocity fluctuations, τ_p . A simple estimate of the latter is $\tau_p \sim w_s/[g(s-1)/s]$, where

w_s = terminal settling velocity;

g = the acceleration due to gravity, and

$s = \rho_s/\rho$ = relative density of the sediment.

The ratio of τ_p to a turbulence time scale is often termed a Stokes number, denoted as St ; e.g., the Stokes number based on the Kolmogorov time scale is $St_K \equiv \tau_p/\tau_K$. For fine to medium sands, $d/\eta_K = O(1)$ and $St_K = O(10^{-1})$, suggesting that these sands will follow all but the highest frequency fluctuations. For noticeable effects on the bulk flow, it might be expected that a sufficiently large suspension volume concentration, c , is necessary. A length scale indicative of concentration would be an interparticle separation distance, $l_s \sim d/c^{1/3}$, which for moderate values of $c = O(10^{-3})$ would lie in a range, $\approx 10d$, comparable to smaller turbulence scales.

16.2.3 Turbulence in Particulate Flows

The qualitative features of suspension-free or clear-water turbulent flows should also apply to turbulent suspensions transporting solid particles, at least if the suspension is sufficiently dilute, i.e., for c sufficiently small. What level of c characterizes a dilute suspension? Lumley (1973) has argued on the basis of the neglect of particle-particle interaction that c should not exceed $O(10^{-3})$, which also has been suggested by Elghobashi (1994). For problems in sediment-transport engineering, this is often satisfied over much, though not necessarily all, of the flow region of interest. In particular, in the important near-bed region, the dilute assumption is suspect, and a dense-phase flow may need to be considered.

Particles in a suspension are discrete and dispersed throughout the flow. Because the trajectories of specific individual particles are generally of no interest to the sediment transport engineer, a continuum or two-fluid treatment

of a suspension flow is attractive. The discrete particles are considered to constitute a continuum like the carrier fluid, and hence to be governed by equations of motion very similar to the equations of fluid flow. This can be achieved (just as in the case of the carrier fluid) by averaging over a representative volume containing a sufficiently large number of particles, but it also requires that the length scale, \mathcal{L}_v , of the representative volume be sufficiently small compared to important flow length scales. When combined with the dilute-suspension assumption, this requirement places a rather severe restriction on such a modeling approach. For a fine sand, $d = 0.2 \text{ mm}$; at $c = 10^{-3}$, this implies that $\mathcal{L}_v = O(1 \text{ cm})$, which is certainly much larger than η_K and, for laboratory flows, even becomes comparable to the largest scales. Thus, like much else in turbulence, the frequently used continuum models, though often effective for engineering purposes, can be difficult to justify with any semblance of rigor.

In the simplest models, encompassing the large majority of models, the particles or, in continuum models, the particulate phase is assumed to behave, like a dye, as a passive scalar, in that it does not influence the flow dynamics. At what level of c can this “one-way” coupling be justified? In a rough classification, Elghobashi (1994) suggests that $c < 10^{-6}$ for one-way coupling. This seems overly stringent, particularly in the parameter range more relevant to (aqueous) sediment transport, where density ratios are $O(1)$, but it does indicate that the usual neglect of the effects of the particulate phase on turbulence, sometimes termed turbulence modulation (or modification), should not be so casually assumed. The problem of modeling the two-way coupling, in which the particulate phase may significantly affect the flow, remains an active research topic, though mainly outside of the sediment-transport literature (e.g., Elghobashi and Abou-Arab 1983; Elghobashi and Truesdell 1993; Boivin et al. 1998). As will be discussed below, the main effect of sediment on the flow that has been considered within the sediment-transport literature is that analogous to density stratification stemming from vertical variation in particle concentration.

16.2.4 Aims and Scope of Modeling

Wilcox (1998) has defined an ideal turbulence model as one that “should introduce the minimum amount of complexity while capturing the essence of the relevant physics.” For the sediment-transport engineer, this may be interpreted as implying that a useful prediction can be obtained reliably for a reasonable expenditure of effort. Much of the following will be concerned with describing relatively complex models requiring not only possibly lengthy numerical solution but also possibly extensive data collection to specify boundary/initial conditions and for model validation. It should not necessarily be assumed that the additional effort in formulating and setting up more complex models will always result in commensurate improvements in predictions. The incomplete understanding

of turbulence without particles already sets an upper limit on what can be achieved in the modeling of the more complex problem of turbulence with particles. Similarly, limitations on our predictive ability may be set by our incomplete understanding of the most basic problems of sediment transport, such as the specification of bed load or an equilibrium bed concentration, which are needed in specifying boundary conditions.

16.3 THE REYNOLDS-AVERAGED EQUATIONS

The traditional modeling approach based on Reynolds averaging is likely to remain dominant for practical hydraulic problems. An instantaneous quantity of interest, $f(\mathbf{x}, t)$, which may be a velocity component, u_i , or a sediment concentration, $c(\mathbf{x}, t)$, is decomposed into an averaged, e.g., \bar{f} , and a random or at least unpredictable fluctuating component, f' . Here, $\mathbf{x} = x_i$, $i = 1, 2, 3$, denotes the position vector, and t denotes the time variable. Where convenient, the identifications $(x_1, x_2, x_3) = (x, y, z)$ and $(u_1, u_2, u_3) = (u, v, w)$ will be made, where x is taken to be in the streamwise direction, z in the vertical direction, opposite to the direction of gravity (or approximately in the direction away from the bed), and y in the horizontal direction perpendicular to x and z . For steady flows, the averaging can be performed over time,

$$\bar{f}(\mathbf{x}) = \lim_{T_{\text{avg}} \rightarrow \infty} \frac{1}{T_{\text{avg}}} \int_0^{T_{\text{avg}}} f(\mathbf{x}, t) dt, \quad (16-1)$$

where T_{avg} denotes the time period over which the averaging is performed. In the case of unsteady flows, an ensemble average can be taken over different realizations of conceptually the same flow, such as experiments repeated under the same conditions. For steady flows, averaging over an ensemble and averaging over time may be assumed to be equivalent and to yield the same results. Though, in Eq. (16-1), T_{avg} is formally taken as going to infinity, in practice it is sufficient that T_{avg} be much longer than any relevant turbulence time scale, but much shorter than any time scale over which the flow might be considered unsteady (Lumley and Panofsky 1964; Wilcox 1998).

16.3.1 The General Flow Equations

With the averaged continuity equation, the general three-dimensional Reynolds-averaged Navier-Stokes (RANS) equations for an incompressible fluid may be conveniently written in Cartesian tensor notation (for those unfamiliar with this notation, a brief introduction is given in Appendix I to this chapter) as

$$\frac{\partial \bar{u}_j}{\partial x_j} = 0 \quad (16-2a)$$

$$\begin{aligned} \frac{D\bar{u}_i}{Dt} &= \frac{\partial \bar{u}_i}{\partial t} + \frac{\partial (\bar{u}_i \bar{u}_j)}{\partial x_j} \\ &= -\frac{1}{\rho_{\text{ref}}} \frac{\partial \bar{p}}{\partial x_i} + \frac{\partial}{\partial x_j} \left(-\bar{u}'_i \bar{u}'_i + \frac{\mu}{\rho_{\text{ref}}} \frac{\partial \bar{u}_i}{\partial x_j} \right) + \bar{F}_i \end{aligned} \quad (16-2b)$$

where

- p = pressure;
- ρ_{ref} = reference fluid density; and
- μ = molecular dynamic viscosity.

The term \bar{F}_i represents a force per unit mass, i.e., an acceleration. Here, the summation convention is followed, where repeated roman alphabetic subscripts indicate summation over all values of the subscript. For particle-free flows, \bar{F}_i might be the gravitational body force, such as g_i , the component of gravitational acceleration in the i^{th} coordinate direction.

In the context of suspension flows, \bar{F}_i would represent interaction forces exerted on the fluid by the particles. Frequently, the effect of sediment on the flow is modeled in a manner analogous to that of a variable-density fluid. A locally averaged density, ρ_m , for the suspension can be defined as

$$\begin{aligned} \rho_m(\mathbf{x}, t) &= \rho_s c(\mathbf{x}, t) + \rho [1 - c(\mathbf{x}, t)] \\ &= \rho [1 + (s-1) c(\mathbf{x}, t)]. \end{aligned} \quad (16-3)$$

The Boussinesq approximation, which neglects inertial effects due to a variable (suspension) density, and includes only buoyancy effects, can then be invoked, with the result (using $\rho_{\text{ref}} = \rho$) that

$$\bar{F}_i = g_i \frac{(\bar{\rho}_m - \rho)}{\rho} = g_i (s-1) \bar{c}. \quad (16-4)$$

To what extent the application of Eqs. (16-2) to suspensions can be justified is debatable, but if the suspension is sufficiently dilute, then Eqs. (16-2) should at least approximately hold. Whether the dominant interaction force between fluid and solid phases can be effectively modeled with a variable-density buoyancy term as in Eq. (16-4) is more controversial. Simplified forms of Eqs. (16-2) are often used; e.g., for primarily horizontal flows, the shallow-water-wave assumption of hydrostatic pressure distribution in the vertical direction is frequently invoked (see the discussion of spatially averaged flows in Appendix II).

The basic closure problem following from the adoption of the Reynolds averaging procedure arises because of the appearance, on the right-hand side of Eq. (16-2b), of the correlation terms, $-\bar{u}'_i \bar{u}'_j$. These result from the averaging of the nonlinear advection term, $u'_i u'_j$. As expressed in Eq. (16-2b), $-\bar{u}'_i \bar{u}'_j$ is not known a priori and consequently, Eqs. (16-2) are not closed and cannot be solved as is. The

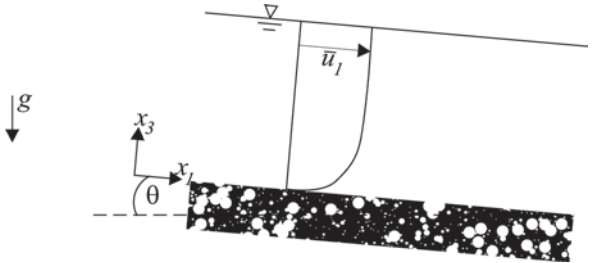


Fig. 16-1. Steady uniform flow without sediment in a wide channel on a slope θ .

nine elements of $-\bar{u}'_i \bar{u}'_j$ may be interpreted as representing effective stresses and hence $-\bar{u}'_i \bar{u}'_j$ is termed the (kinematic) Reynolds stress tensor. The three diagonal terms, $-\bar{u}'_1 \bar{u}'_1$, $-\bar{u}'_2 \bar{u}'_2$, $-\bar{u}'_3 \bar{u}'_3$, are interpreted as normal stresses, while the off-diagonal terms are interpreted as shear stresses. In general, the diagonal terms are all different in value, and hence turbulence is anisotropic. One of the most important parameters describing turbulence is obtained from the sum of the diagonal terms, namely, the turbulent kinetic energy,

$$k \equiv \frac{1}{2} \bar{u}'_i \bar{u}'_i = \frac{1}{2} \left(\bar{u}'_1 \bar{u}'_1 + \bar{u}'_2 \bar{u}'_2 + \bar{u}'_3 \bar{u}'_3 \right). \quad (16-5)$$

The Reynolds stress tensor is symmetric, so that only six of its nine terms (the diagonal terms and the three off-diagonal terms, $\bar{u}'_1 \bar{u}'_2$, $\bar{u}'_1 \bar{u}'_3$, $\bar{u}'_2 \bar{u}'_3$) are independent. Together with the four primary unknowns (the three mean velocity components, \bar{u}'_i and the mean pressure, \bar{p}), the six independent Reynolds stresses form a total of ten unknown variables, whereas Eqs. (16-2) provides only four equations. Turbulence modeling provides closure of the system by formulating sufficient additional equations, algebraic or differential, that specify $-\bar{u}'_i \bar{u}'_j$, in terms of already existing variables.

Example. In the following, the special case of a steady uniform plane-bed flow in an infinitely wide channel (Fig. 16-1) will be used recurrently as a simple illustration of the use of the model equations discussed. These illustrations will be set apart from the main text. In this special case, $\bar{u}_2 \equiv \bar{u}_3 \equiv 0$, $\partial/\partial t \equiv \partial/\partial x_1 \equiv \partial/\partial x_2 \equiv 0$. Equation (16-2a) is therefore satisfied automatically, and Eq. (16-2b) is reduced to

$$0 = \frac{\partial}{\partial x_3} \left(-\bar{u}'_1 \bar{u}'_3 + \frac{\mu}{\rho_{\text{ref}}} \frac{\partial \bar{u}_1}{\partial x_3} \right) + g \sin \theta \quad (16-6a)$$

$$0 = \frac{\partial}{\partial x_3} \left(-\bar{u}'_2 \bar{u}'_3 \right) \quad (16-6b)$$

$$0 = \frac{1}{\rho_{\text{ref}}} + \frac{\partial \bar{p}}{\partial x_3} + \frac{\partial}{\partial x_3} \left(-\bar{u}'_3 \bar{u}'_3 \right) - g \cos \theta. \quad (16-6c)$$

This involves five unknowns (\bar{u}_1 , \bar{p} , $\bar{u}'_1 \bar{u}'_3$, $\bar{u}'_2 \bar{u}'_3$, $\bar{u}'_3 \bar{u}'_3$) with only three equations. From Eq. (16-6b) and the boundary

condition at the bottom, $-\overline{u'_2 u'_3}$ is found to be identically zero, and from Eq. (16-6c), the pressure distribution may be treated as hydrostatic because $\partial(\overline{u'_3 u'_3})/\partial x_3$ is small. Interest is therefore focused on Eq. (16-6a), which still involves two unknowns, $\overline{u'_1}$ and $\overline{u'_1 u'_3}$, and therefore is not closed.

16.3.2 Equation(s) for the Sediment Model

The basic flow equations, the continuity and Navier-Stokes equations describing (fluid) mass and momentum conservation, may be considered exact at least for a pure fluid, and very plausible for the fluid phase in a dilute suspension. In contrast, much remains unclear as far as the basic governing equations for sediment are concerned. Unlike "molecular" scalars like temperature or salinity, sediment constitutes a separate physical phase, the motion of which may not necessarily be the same as the motion of the fluid. The large bulk of the work on sediment transport modeling has been based on a continuum approach, similar to that taken with a molecular species. In analogy with the treatment of the latter, only a sediment mass conservation equation is taken, without mention of sediment momentum conservation equation. To further complicate the picture, the discrete nature of the solid phase permits an alternative (Lagrangian) modeling approach, in which the motion of individual particles is tracked. Thus, even before any attempt at the modeling of turbulent transport of sediment, the choice and justification of even the basic sediment equations must be addressed.

16.3.2.1 The Continuum Approach The continuum or two-fluid approach treats the discrete solid phase as a continuum, described by a possibly spatially and temporally varying local (either point or depth-averaged or cross-sectionally averaged) sediment concentration, $c(\mathbf{x},t)$. A differential conservation equation is then heuristically derived, which governs the temporal evolution and/or the change in spatial distribution of c . Most commonly, the sediment is treated in a manner analogous to a molecular species, assuming that the particulate phase moves with the fluid, with, however, a special model for particle settling, which is characterized solely by a constant settling velocity, w_s . In problems where sediment heterogeneity may play an important role, the problem may be attacked by modeling different size classes, such that the α^{th} size class would be characterized by its own settling velocity, $(w_s)_\alpha$. The standard Reynolds-averaged model equation describing the conservation of sediment in the α^{th} size class is thus written as

$$\begin{aligned} \frac{D\bar{c}_\alpha}{Dt} &= \frac{\partial \bar{c}_\alpha}{\partial t} + \frac{\partial (\bar{u}_j \bar{c}_\alpha)}{\partial x_j} \\ &= \frac{\partial (-\overline{u'_j u'_\alpha})}{\partial x_j} + \frac{\partial [(w_s)_\alpha \bar{c}_\alpha]}{\partial z} + \bar{R}_\alpha. \end{aligned} \quad (16-7)$$

Here, the summation convention is not applied with repeated Greek subscripts (α). The source (sink) term, \bar{R}_α , represents a reaction or transformation term, such as might be considered in cases involving particle coagulation, breakup, or entrainment from a heterogeneous bed, that may cause a change in the concentration of particles in any given size class. From Eq. (16-7), the settling term (the second term on the extreme right-hand side) might also be viewed as a somewhat special reaction term for a molecular species. The total solid-phase volume concentration, \bar{c} , can be obtained by summation as

$$\bar{c} = \sum_\alpha \bar{c}_\alpha. \quad (16-8)$$

In spite of its wide use and its intuitive physical interpretation and hence appeal, the theoretical basis of Eq. (16-7) deserves further examination. The questions surrounding the continuum approximation have already been discussed in Section 16.2.3. Even if a continuum model is adopted, the question remains of whether it suffices to formulate only a mass conservation equation for sediment, or whether a more consistent two-phase flow approach including not only sediment kinematics but also sediment dynamics is necessary. The latter would necessitate an equal treatment of the continuous solid phase with its own momentum conservation equation. In particulate flows, it is empirically observed that, even with the settling velocity taken into account, the mean particle velocity differs from the fluid velocity (e.g., Muste and Patel 1997), such that the implicit assumption of Eq. (16-7) of equal particle and fluid velocities is clearly violated. The velocity difference for aqueous suspensions of small sand particles is however generally small, $O(w_s)$, and so it is not clear if and when a detailed treatment of sediment dynamics would be required. A general discussion of the theoretical basis of two-phase flow models is given by Drew (1983) and Crowe et al. (1998). In practical sediment transport computations, the latter approach has rarely been taken, though two-phase flow models have been proposed (Drew 1975; McTigue 1981; Kobayashi and Seo 1985; Greimann et al. 1999; Hsu et al. 2003) and simple cases, such as uniform flow over a plane bed, have been analyzed. Subtle differences from the conventional approach can lead to confusion (see, e.g., the discussion between Celik 1982 and McTigue 1982); whereas Eq. (16-7) is conventionally interpreted as a *kinematic* sediment conservation equation, the two-phase modeler may view it (or at least its simplified form in the uniform-flow case) as resulting from a *dynamic* momentum balance. The main difficulty in the two-phase flow approach, however, is similar to that of turbulence closure, in that modeling assumptions regarding the interaction between phases must be made to close the governing system of equations, but these are often impossible to confirm experimentally in any detail.

16.3.2.2 The Settling Velocity in a Turbulent Suspension Even if Eq. (16-7) is accepted as an intuitively plausible model for describing sediment transport, it remains

to specify w_s . The simplest choice of w_s , which therefore has been the most popular, is that corresponding to the settling of an isolated equivalent-spherical particle in a stagnant fluid of infinite extent, and formulae for this are available (see Chapter 2, where other effects on w_s , such as those due to shape, are discussed). In a turbulent suspension, however, these assumptions are not strictly satisfied. For the present chapter, the effects due to concentration and turbulence (already discussed in *ASCE Manual 54*) are relevant. Presumably, if the dilute assumption implicit in the standard models is valid, then effects of concentration are likely negligible (though the effect of preferential particle clustering in a turbulent flow (Wang and Maxey 1993) might need to be considered). On the other hand, numerical simulations (Wang and Maxey 1993) have shown an effect of turbulence on w_s , with w_s increasing by as much as 40% over the fall velocity in a stagnant fluid. Unfortunately, these results have been obtained for small heavy particles ($d < \eta_K$, and $s \gg 1$) in homogeneous isotropic turbulence, which is not in the parameter range of greatest interest in sediment transport applications.

Since the publication of *ASCE Manual 54*, experimental studies of settling velocities of particles in water have been few. Boillat and Graf (1981; 1982) conducted experiments of spherical particle settling in stagnant water and in an approximately homogeneous turbulent flow for a range of particle Reynolds numbers, $200 \leq w_s d/\nu = R_p \leq 20,000$, which for typical particle parameters would correspond to the size range of coarse sands and larger. The observed drag coefficients, C_D , which can be simply related to w_s , in the stagnant-water case were consistently larger than those given by the standard drag curve for spheres. Relative to the stagnant-water C_D , the turbulent-flow C_D was generally reduced, corresponding to a larger w_s , though an increased C_D , corresponding to a smaller w_s , was often observed when $R_p \approx 2,000$. Although it was argued that both the intensity and the length scale of the turbulence influence C_D , a simple dimensionless correlation could not be found. In a similar study, Yang and Shy (2003) examined a range of smaller $R_p < 40$, and observed increases in w_s (relative to still-water values) with increasing St_K with a maximum increase of up to 7% for $St_K \approx 1$, but also found that decreases might occur for much larger St_K . The limited experimental evidence should be regarded with some caution, but does indicate that the use of a w_s based on stagnant-fluid condition may involve uncertainties of $O(10\%)$. Moreover, since most practical applications involve inhomogeneous turbulence, such that the settling particle is constantly adjusting to a changing turbulence environment, the practical implications of such results remain to be explored.

16.3.2.3 Lagrangian Models In this approach, the motion of individual particles is determined by writing a model equation of motion for an individual particle:

$$m_p \frac{d(u_i)_p}{dt_p} = (F_i)_p. \quad (16-9)$$

The subscript, p , refers to a particle quantity; hence, $(u_i)_p$ is the instantaneous velocity of a particle, m_p is mass, and $(F_i)_p$ denotes the sum of forces acting on the particle. In a popular variant of the Bassett-Boussinesq-Oseen (BBO) equation for a spherical particle of radius a , the forces are modeled as

$$(F_i)_p = m_p \left[\underbrace{\frac{3}{8} \frac{C_D}{a_s} \{(u_i)_f - (u_i)_p\} |(u_i)_f - (u_i)_p|}_I \right] + \underbrace{m_f \left[\frac{d(u_i)_f}{dt} \right]}_{II} + \underbrace{\frac{1}{2} m_f \left[\frac{d(u_i)_f}{dt} - \frac{d(u_i)_p}{dt_p} \right]}_{III} + \underbrace{6a^2 (\pi \rho \mu)^{1/2} \int_{t_{p_0}}^{t_p} \frac{d[(u_i)_f - (u_i)_p]/d\tau}{\sqrt{t_p - \tau}} d\tau}_{IV} + \underbrace{(m_p - m_f) g_i}_V \quad (16-10)$$

including (I) a drag force (i.e., in the direction of relative velocity), (II) forces due to fluid pressure gradient and viscous stresses, (III) virtual mass forces, (IV) the Bassett force due to unsteady relative acceleration, and (V) gravitational forces (Hinze 1975; Elghobashi and Truesdell 1993; Frey et al. 1993). In Eq. (16-10), the subscript f refers to a fluid quantity, C_D is the drag coefficient, and $d(u_i)_f/dt$ is the total instantaneous acceleration of the fluid as seen by the particle at $(x_i)_p$. The BBO equation is intended for a single isolated particle, and cannot be rigorously justified outside of the Stokes regime (Clift et al. 1978). Lift forces, i.e., those acting in a direction normal to the relative velocity, may also be important, but are more difficult to model because they may arise from different mechanisms, such as shear and particle rotation (Clift et al. 1978; Stock 1996). Wiberg and Smith (1985; 1989) proposed a model for saltating particles, neglecting the Bassett force and direct viscous forces but including an empirical expression for a lift force stemming only from shear. The possible importance of other lift mechanisms was also discussed. A similar study by Sekine and Kikkawa (1992) argued, however, that, at least for saltation, lift forces are negligible. For the case where $s \gg 1$, frequently encountered in the literature on two-phase flows, terms (II), (III), and (IV) are negligible, but for the conditions of interest in aqueous sediment transport, where $s = O(1)$, a priori neglecting any one of these terms is difficult to justify generally. Rigorous applications to turbulent flows require additional restrictions, including $d/\eta_K \ll 1$ (Maxey 1993; Elghobashi 1994; Stock 1996).

A solution of Eq. (16-9) can then be used to determine the trajectory, $(x_i)_p$, of the particle by integrating

$$\frac{d(x_i)_p}{dt_p} = (u_i)_p - (Z_{u'_1})_p, \quad (16-11)$$

where $(Z_{u'_1})_p$ is a random velocity-fluctuation term that models the stochastic motion of particle, if $(u_i)_p$ is assumed to be entirely deterministic.

In addition to the question of the settling velocity in turbulent flows dealt with in the preceding subsection, two other main classes of problems have been studied with the Lagrangian approach. The question of the diffusivity of solid particles in a turbulent flow relative to the diffusivity of fluid particles is a classical problem, discussed by Lumley (1973) and Hinze (1975), and more recently by Squires and Eaton (1991) and Mei and Adrian (1995). An early review in a more specifically sediment hydraulic context was given by Alonso (1981). These studies are of some relevance because they illuminate theoretically one of the empirical parameters in the transport models to be discussed later, namely the turbulent Schmidt number, $(\sigma_r)_s$, for turbulent diffusion of solid particles. The turbulent Schmidt number is defined and discussed in greater detail in Section 16.4.1.3. Under rather restrictive idealized assumptions, they predict that the particle diffusivity is less than or equal to the fluid diffusivity (i.e., $(\sigma_r)_s \geq 1$) for sedimenting particles. Unfortunately, the experimental evidence is somewhat equivocal regarding this prediction.

The other major class of problems that have been examined by means of Lagrangian models is the saltation of particles and the resulting bed load (e.g., van Rijn 1984b; Wiberg and Smith 1985). Typically, simplified versions of Eq. (16-10) were used. Rather more problematic, Eqs. (16-9) to (16-11) were integrated with time-averaged models of the fluid velocity instead of an instantaneous velocity, and did not include any stochastic component. It is not clear that the averaged, much less the instantaneous, trajectory of a particle in a turbulent flow can be predicted from such a procedure, but such a Lagrangian approach may provide an alternative more physically based starting point for developing bedload formulae. In a somewhat different application, Frey et al. (1993) computed the steady flow in a model sedimentation tank, and, based on this flow field, studied particle transport using Eqs. (16-9) to (16-11), including a stochastic component. Some of their results are given in Section 16.5.2.

16.3.3 Auxiliary Equations: Boundary Conditions—Introductory Discussion

The governing equations for the flow and the sediment (Eqs. (16-2) and (16-7)) form a system of partial differential equations that requires a specification of boundary conditions on the entire boundary of the domain being considered. Conditions at inlet and outlet boundaries are problem-dependent, and, for practical computations, are best based on laboratory or field measurements. If these are not available,

then the problem of specifying these boundary conditions may be alleviated by choosing the boundaries of the computational domain sufficiently far from the region of greatest interest, such that the computational results in this region are not sensitive to exact details of the inlet and outlet conditions. For special problems, spatially periodic conditions in which inlet and outlet conditions are identical may be reasonable.

A boundary condition of special interest in sediment-transport problems is that at the bed, or at a solid boundary. The standard condition at a solid boundary, namely zero velocity, remains applicable to the instantaneous velocity, as well as to the mean and the fluctuating components. Because of the dominance of viscous effects, the elements of the Reynolds stress tensor tend to zero as the solid wall is approached. Although these wall conditions are undisputed, difficulties arise in its implementation in practical computations. For high- R problems, large gradients occur in the region adjacent to the solid boundary, and hence lead to difficulties in numerical resolution. For the rough-boundary flows of most interest in sediment transport, the detailed geometric representation of the rough wall is not feasible, and a fictitious boundary is used for modeling purposes, so that an exact bed boundary condition is not necessarily helpful. As might be expected from the preceding discussion of the uncertainties in the modeling of suspended sediment transport, an exact boundary condition on the sediment concentration at the bed is not available. The deformability of the bed/boundary due to an erodible bed introduces a further complication, such that if the details of the bed forms and their motion are of interest, then, just as in the case of the water surface, an additional boundary condition is required. In most applications, however, a simplified approach is taken in which bed details, whether small-scale sand-grain roughness or large-scale bed form, are ignored, and only their effect on the bulk flow is modeled.

The other boundary of special interest is the water surface. In most cases, a simplified approach is taken in which the water surface is treated as a rigid, i.e., nondeformable, shear-free plane lid, the location of which is known a priori. This is often implemented by treating the water surface as a plane of symmetry, with zero applied shear, analogous to the centerline of a pipe flow. In steady flows, this approximation can be justified when the appropriate Froude number is small and the direct effect of spatial variations in water surface elevations is negligible. If the water surface is treated more exactly as a free, i.e., deformable, surface, then the computational effort will be much more significant. In addition to a dynamic boundary condition, a kinematic boundary condition needs to be satisfied. These conditions per se are not unique to turbulent flows, and so are not discussed further here; the reader is referred to Liggett (1994) for details. Turbulence at a water surface, however, differs from that at a pipe centerline, so that if the effects of free-surface turbulence are of interest, then special models of free-surface turbulence may be required, even when a rigid-lid approximation is made.

In sediment transport applications, interest is usually focused on the near-bed region rather than on the free-surface region, and so detailed turbulence modeling of the latter is generally not necessary.

16.4 TURBULENCE CLOSURE MODELS

16.4.1 The Boussinesq Eddy-Viscosity Model

The turbulence closure problem arises because of the presence of the Reynolds stress tensor, $-\bar{u}'_i \bar{u}'_j$, in the governing flow equations (Eq. (16-2)). Further, the effectiveness of turbulent transport relative to molecular transport has been remarked as perhaps the most important characteristic of turbulence for engineering purposes. The analogy between molecular and turbulent diffusivity has played a pervasive, some would say pernicious, role in turbulence modeling, but before this analogy is explicitly made, the basic features of molecular diffusive transport are recalled.

16.4.1.1 Molecular Transport of Momentum Consider a pure-shear steady laminar flow (Fig. 16-2), in which only a single component of velocity is nonzero and varies only in one coordinate direction, $\mathbf{u} = (u_1(x_3), 0, 0)$. The only nonzero shear stress is

$$\tau_{13} = \tau_{31} = \mu \frac{du_1}{dx_3} = \nu \frac{d(\rho u_1)}{dx_3}. \quad (16-12)$$

This constitutive equation (for a Newtonian fluid) relates the only nonzero shear stress *linearly* to the strain rate (here simply the velocity gradient) through the transport coefficient, μ , or its kinematic variant, $\nu = \mu/\rho$, which are *properties of the fluid*. Equation (16-12) is an example of a gradient-transport model, in which a flux, here the shear stress, which can be interpreted as a (negative) momentum flux, is related to a gradient of the quantity being transported, here the momentum per unit volume, i.e., ρu_1 .

At the molecular level, this shear stress or momentum flux is effected by molecules in random motion. If the instantaneous fluctuating velocities of molecules in the x_1 and x_3 directions are denoted as u''_1 and u''_3 , then the shear stress can also be written as $\tau_{12} = \rho u''_1 u''_3$, exactly analogously to a Reynolds shear stress. Moreover, for ideal gases, a rigorous result can be obtained for ν using kinetic theory, namely,

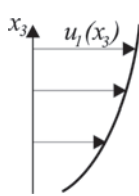


Fig. 16-2. Laminar shear flow.

$$\nu \propto u_{th} \mathcal{L}_{mfp} \quad (16-13)$$

where

u_{th} = average molecular thermal velocity and
 \mathcal{L}_{mfp} = molecular mean free path, i.e., the average distance a molecule travels before a collision with another molecule.

This motivates an analogous treatment of turbulent transport, which is effected by random fluid motion rather than random molecular motion. Equation (16-13), however, can only be justified if the length scale over which u_1 varies is much larger than \mathcal{L}_{mfp} and the time scale of the mean flow (measured by $(du_1/dx_3)^{-1}$) is much longer than molecular time scales (measured by $(u_{th}/\mathcal{L}_{mfp})^{-1}$). This is evidently satisfied for the case of molecular transport, but, as will be argued below, the equivalent condition is clearly not satisfied in the case of turbulent transport.

16.4.1.2 The Eddy Viscosity For multidimensional problems, the analogy between molecular and turbulent transport can be expressed in a general form as

$$-\bar{u}'_i \bar{u}'_j = \nu_t (2\bar{S}_{ij}) - \frac{2}{3} k \delta_{ij} \\ = \nu_t \left(\frac{\partial \bar{u}_i}{\partial x_j} + \frac{\partial \bar{u}_j}{\partial x_i} \right) - \frac{2}{3} k \delta_{ij} \quad (16-14)$$

which will be termed the Boussinesq eddy-viscosity model (BEVM), where ν_t denotes a (kinematic) turbulent eddy viscosity. An expanded version of Eq. (16-14) is given in Appendix I as Eq. (16-79). The mean strain-rate tensor

$$\bar{S}_{ij} = \frac{1}{2} \left(\frac{\partial \bar{u}_i}{\partial x_j} + \frac{\partial \bar{u}_j}{\partial x_i} \right) \quad (16-15)$$

and the Kronecker delta tensor $\delta_{ij}=1$ for $i = j$ and $\delta_{ij} = 0$ for $i \neq j$. Eq. (16-14) specifies the Reynolds stress tensor in terms of gradients of the mean flow, and thus makes progress in closing the system, Eq. (16-2). It remains to specify ν_t , which is no longer a fluid property like its molecular counterpart, ν , but rather depends on the local flow state. Hence, ν_t will in general vary spatially within a flow and differ in different types of flows even with the same fluid.

The term, $(2/3)k\delta_{ij}$, is necessary for consistency with the definition of the turbulent kinetic energy (Eq. (16-5), since the sum $\bar{u}'_i \bar{u}'_j = 2k$), and acts as an effective pressure. When Eq. (16-14) is substituted into Eqs. (16-2), this term can be absorbed into the pressure-gradient term. Hence, even though k appears explicitly in Eq. (16-14), it does not necessarily have to be determined independently.

Example. When Eq. (16-14) is applied to a steady plane uniform flow, the only relevant elements of $-\bar{u}'_i \bar{u}'_j$ are obtained as

$$-\bar{u}'_1 \bar{u}'_3 = \nu_t \frac{\partial \bar{u}_1}{\partial x_3} \quad (16-16a)$$

$$-\overline{u'_2 u'_3} = \nu_t \frac{\partial \bar{u}_2}{\partial x_3} \quad (16-16b)$$

$$-\overline{u'_3 u'_3} = 2\nu_t \frac{\partial \bar{u}_3}{\partial x_3} - \frac{2}{3} k \quad (16-16c)$$

thereby yielding for momentum conservation

$$\begin{aligned} 0 &= \frac{\partial}{\partial x_3} \left[(\nu_t + \nu) \frac{\partial \bar{u}_1}{\partial x_3} \right] + g \sin \theta \\ &= \frac{\partial}{\partial x_3} \left(\frac{\bar{\tau}_{13}}{\rho_{ref}} \right) + g \sin \theta \end{aligned} \quad (16-17a)$$

$$0 = -\frac{\partial}{\partial x_3} \left(\frac{\bar{P}}{\rho_{ref}} \right) - g \cos \theta \quad (16-17b)$$

In Eqs. (16-17), the conditions, $\bar{u}_2 = \bar{u}_3 = 0$, $\nu = \mu/\rho_{ref}$ have been used, an effective pressure has been redefined as $\bar{p} = \bar{p} + (2/3)\rho_{ref} k$, and $\bar{\tau}_{13} = \rho_{ref} (\nu_t + \nu)(\partial \bar{u}_1 / \partial x_3)$. To solve for \bar{u}_1 , a specification for ν_t is still needed. Equations (16-17) can be integrated over x_3 , and, with the imposition of the condition that, at $x_3 = 0$, $\bar{\tau}_{13} = \rho_{ref} u_*^2$, where $u_* = \sqrt{gh \sin \theta}$ is the shear velocity, and at the free surface, $x_3 = h$, $\bar{\tau}_{13} = 0$, the following result is obtained:

$$\frac{\bar{\tau}_{13}}{\rho_{ref}} = u_*^2 \left(1 - \frac{x_3}{h} \right) \quad (16-18a)$$

$$\approx -\overline{u'_1 u'_3} \quad (16-18b)$$

where the second relation assumes a region sufficiently far from the bed that molecular viscous effects are negligible. Equations (16-18) already point to u_* as the appropriate scale for the turbulent velocity fluctuations in wall-bounded flows.

16.4.1.3 The Eddy Diffusivity and the Turbulent Schmidt Number A close analogy holds between the viscous transport of momentum and the diffusive (molecular) transport of heat or a solute species. In laminar flows, both momentum and mass diffusion are typically assumed to follow a gradient-transport law, with constant transport coefficients that are properties of the fluid and, in the case of mass transport, of the solute. The ratio of the molecular kinematic viscosity to the molecular diffusivity, termed the Schmidt number and denoted as σ , is necessarily constant, depending again only on the carrier fluid and the solute.

With the analogies between laminar and turbulent transport of momentum, and between mass and momentum transport, the extension of Eq. (16-14) to mass (sediment) transport applications in turbulent flows is naturally motivated. Unlike momentum, which is a vector, mass or concentration is a scalar. The turbulent mass fluxes are therefore assumed to follow a gradient-transport law of the form

$$\overline{u'_j c'} = -\epsilon_c \frac{\partial \bar{c}}{\partial x_j} = -\frac{\nu_t}{\sigma_t} \frac{\partial \bar{c}}{\partial x_j} \quad (16-19)$$

where the eddy diffusivity, ϵ_c , is specified as being proportional to the turbulent kinematic viscosity, ν_t . The turbulent Schmidt number, σ_t , is defined as the ratio of the turbulent eddy viscosity to the turbulent diffusivity of the relevant transported scalar,

$$\sigma_t = \frac{\nu_t}{\epsilon_c} \quad (16-20)$$

In traditional sediment transport hydraulics, the reciprocal of σ_t , denoted as β_s , is more often encountered; i.e., $\epsilon_s = \beta_s \nu_t = [1/(\sigma_t)_s] \nu_t$. Unlike its laminar counterpart, σ_t will not depend solely on fluid and species properties, but, like ν_t , may in general depend on local flow conditions. It is usually assumed to be constant spatially, though the justification for this is based more on convenience and ignorance than on theory. Another complication arises from the anisotropy of particle diffusivity for sedimenting particles, whereby vertical diffusivity differs from horizontal diffusivity (Lumley 1973). Further, because the large-scale transport and mixing effected by turbulent eddies is relatively insensitive to the transported quantity, whether momentum, heat, or mass, σ_t is $O(1)$ in contrast to σ , which may vary widely, e.g., for salt in water, $\sigma = O(10^3)$. A strict interpretation of the Reynolds analogy between momentum and mass turbulent transport would imply $\sigma_t = 1$.

The appropriate turbulent Schmidt number for sediment, $(\sigma_t)_s = 1/\beta_s$, has been much debated, and various prescriptions have been given (see the discussion in Davies 1995). Most studies (e.g., Li and Davies 1996; Olsen and Kjellesvig 1999; Wu et al. 2000) have simply chosen $(\sigma_t)_s = 1$, implicitly assuming the strict Reynolds analogy. Such a choice could plausibly be justified if d/η_K and w_s/u_* were sufficiently small. On the other hand, for a molecular scalar, e.g., an average value of $\sigma_t = 0.7$ is given by Launder (1978). For boundary-layer flows, which may be particularly relevant to the channel flows of sediment transport, the model of Rotta (1964) prescribes a σ_t varying from 0.9 in the near-wall region to a value of 0.5 toward the outer edge of the boundary layer.

The estimation of $(\sigma_t)_s$ from measurements is still problematic. Its basic definition (Eqs. 16-19) relies on local estimates of sediment and momentum fluxes that require estimation of gradients from noisy and often sparse point measurements. Consequently, these estimates can be erratic, but have the advantages that no additional model assumptions need to be made and a spatially variable $(\sigma_t)_s$ is allowed. Traditionally, β_s has been estimated by assuming specific velocity and concentration profiles for uniform sediment-laden flows over a plane bed and fitting these to measured profiles in uniform sediment-laden flow. Such an integral approach results in smoother estimates but rests on

dubious profile assumptions. Unfortunately, these different approaches may yield quite disparate estimates. An estimate of β_s based on fitting to a Rouse-type profile may be significantly *smaller* than an estimate based on local gradients.

Based on the flume studies of Coleman (1970), in which sediment diffusivity was estimated from local gradients, van Rijn (1984c) proposed that

$$(\beta_s)_{vR} = 1 + 2 (w_s/u_*)^2, \quad 0.1 < w_s/u_* < 1 \quad (16-21)$$

Two aspects of the Coleman data deserve mention: (1) the relatively small width-to-depth ratio (< 3) raises questions regarding the effects of secondary currents, and (2) the lack of an equilibrium sand bed raises doubts regarding the extent to which the flows studied were actually "saturated," and therefore applicable to real equilibrium-bed cases. One version of the earlier model of Einstein and Chien (1954) related the fitted Rouse exponent, Z_R , to $(Z_R)_{\text{ref}} \equiv w_s/\kappa u_*$, and can be expressed as

$$\begin{aligned} (\beta_s)_{E-C} &= \exp \left[\frac{(Z_R)_{\text{ref}} C_{E-C}}{\sqrt{\pi}} \right] \\ &+ (Z_R)_{\text{ref}} C_{E-C} \operatorname{erf} \left[\frac{(Z_R)_{\text{ref}} C_{E-C}}{\sqrt{\pi}} \right] \end{aligned} \quad (16-22)$$

with

$$C_{E,C} = \ln 1.3.$$

Both relations satisfy $(\sigma_t)_s \leq 1$, and $(\sigma_t)_s \rightarrow 1$ as $w_s/u_* \rightarrow 0$.

Local estimates of $(\sigma_t)_s$ from uniform flows over a plane equilibrium beds are plotted in Fig. 16-3a; a large scatter is evident. The data of Cellino and Graf (1999) are interesting as an example of direct measurements of momentum and sediment fluxes using acoustic Doppler techniques. Their values, however, seem excessive (values in the region $z/h < 0.4$ consistently exceed 3, and so are not plotted) and remains to be independently supported. Experimental evidence for spatial variation in $(\sigma_t)_s$ is particularly strong in the Barton and Lin (1955) and Cellino and Graf (1999) data, with $(\sigma_t)_s$ decreasing toward the

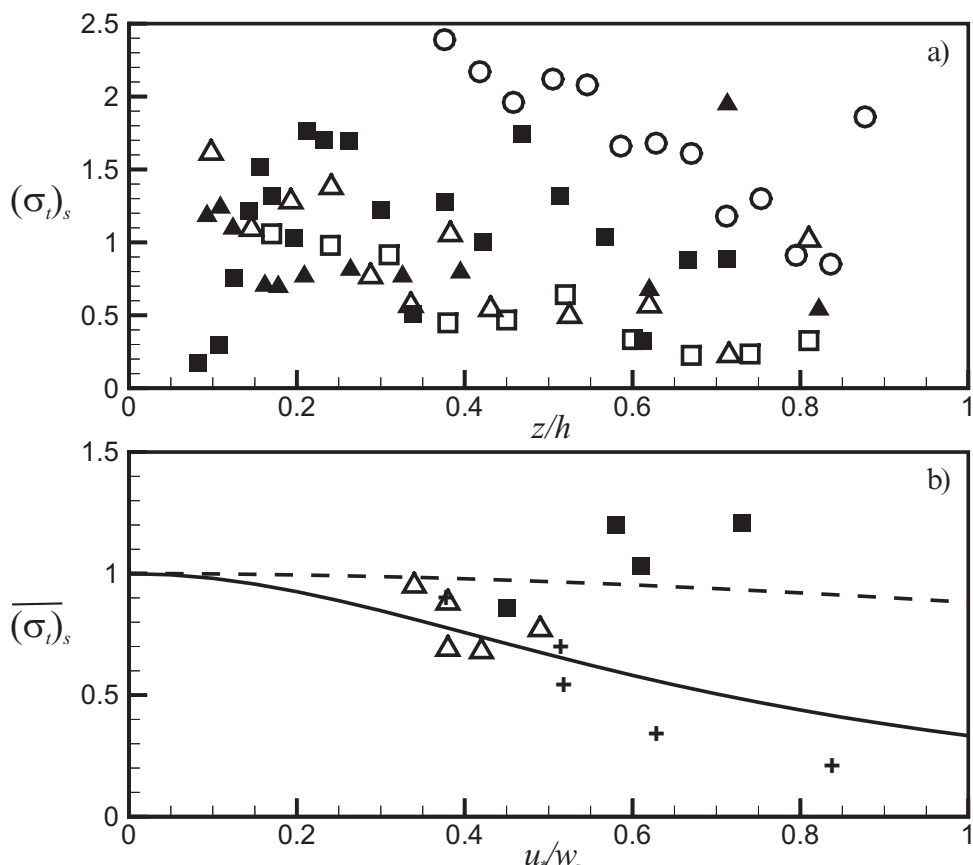


Fig. 16-3. (a) Local estimates of $(\sigma_t)_s$ for uniform flow over a plane equilibrium bed as a function of relative distance, z/h , from the bed: O, Cellino and Graf (1999, $u_*/w_s = 0.27$, Run SAT S015); ■, Lyn (1988, $u_*/w_s = 0.73$, Run EQ2565); ▲, Lyn (1988, $u_*/w_s = 0.45$, Run EQ1665); □, Barton and Lin (1955, $u_*/w_s = 0.52$, Run 31); △, Barton and Lin (1955, $u_*/w_s = 0.36$, Run 36). (b) Averaged (over $0.1 < z/h < 0.5$) values of $(\sigma_t)_s$ as a function of u_*/w_s ; △ Barton and Lin (1955); +, Coleman (1970), ■, Lyn (1988).

free surface, a variation consistent with the already-mentioned Rotta model for a flat-plate boundary-layer flow. Though scatter clouds the issue, the data, especially in the practically important near-bed region, point to the possibility of $(\sigma_t)_s > 1$, contrary to both Eqs. (16-21) and (16-22). For a spatially varying $(\sigma_t)_s$, the question of its dependence on u_*/w_s becomes complicated. The Lyn (1988) data generally indicate an increase in $(\sigma_t)_s$ with increasing u_*/w_s , whereas the Barton and Lin (1955) data exhibit the opposite tendency. The two studies, however, cover somewhat different ranges of u_*/w_s , and so the observed trends may not be entirely inconsistent.

As a simplification, the modeler may elect to use a constant averaged value of $(\sigma_t)_s$. Figure 16.3b shows values of $(\bar{\sigma}_t)_s$ (averaged over $0.1 \leq y/h \leq 0.5$, because this region carries the bulk of the suspended sediment) for different values of u_*/w_s . Also plotted are curves corresponding to Eqs. (16-21) and (16-22) (for the latter, a value of $\kappa = 0.4$ has been assumed). The different behavior of $(\sigma_t)_s$ with respect to u_*/w_s in the different studies discussed above can still be seen in the averaged quantities. The van Rijn model not surprisingly agrees well with the Coleman data on which it was based. The behavior of the Einstein–Chien model, which was based on traditional fitting to a Rouse profile, relative to the van Rijn model is also expected in that integral estimates of β_s based on the Rouse profile will generally yield values closer to unity than local estimates (assuming a clear-water value of $\kappa \approx 0.4$).

The preceding was concerned only with uniform flows homogeneous in the streamwise direction. In nonuniform flows, even more complications may be expected. That the appropriate value of $(\sigma_t)_s$ may vary not only with distance from the wall but also in the streamwise direction was observed by Celik and Rodi (1988), who simulated the experiments of Jobson and Sayre (1970) and found that better predictions were achieved with different values of $(\sigma_t)_s$ at different streamwise stations. Ouillon and le Guennec (1996), simulating the same experiment, showed that the \bar{c} -profiles nearer the inlet can even be well predicted by choosing $(\sigma_t)_s = \infty$, i.e., without any turbulent transport. They also found that agreement with measurements was improved by choosing different values of $(\sigma_t)_s$, ranging from 0.6 to 1, depending on the type of flow–bed interaction, i.e., on whether deposition to or entrainment from the bed was occurring. In practical computations with the $k-\epsilon$ model to be described, and where $(\sigma_t)_s$ is interpreted more as a model-tuning parameter that might compensate for model deficiencies and hence might be model-dependent, then experience indicates that $(\sigma_t)_s \leq 1$ (or $\beta_s \geq 1$) will yield better results, though a definitive conclusion is still to be reached.

In view of the difficulties associated with specifying $(\sigma_t)_s$, alternative approaches that avoid it altogether or attempt to specify it more completely might be sought. The conceptual model of Lyn (1988) does not rely on an eddy-diffusivity model and hence does not require a $(\sigma_t)_s$, but makes quite restrictive similarity assumptions that apply only in simple flows such as uniform plane-bed flows. Two-phase-flow

models, such as that of Greimann et al. (1999), may offer some guidance, because an explicit expression for $(\sigma_t)_s$ in terms of local flow and suspension parameters can be derived, though other constant(s) may need to be specified. A second-order model (a brief introductory discussion of second-order modeling is given in Section 16.4.7) for sediment concentration could also conceivably do without an eddy-diffusivity model. This would, however, not only likely require specifying *other* model “constants” but even in second-order turbulence models for single-phase flows, isotropic-turbulent-viscosity models with turbulent Schmidt numbers remain popular for numerical reasons (see the discussion in Lien and Leschziner 1994).

Example. For the simple uniform-flow case, Eq. (16-7) with Eq. (16-19) reduces to

$$\begin{aligned} 0 &= \frac{\partial(w_s \bar{c})}{\partial z} + \frac{\partial(-\bar{w}' c')}{\partial z} \\ &= \frac{\partial(w_s \bar{c})}{\partial z} + \frac{\partial}{\partial z} \left(\frac{v_t}{\sigma_c} \frac{\partial \bar{c}}{\partial z} \right) \end{aligned} \quad (16-23)$$

where u'_3 and x_3 have been rewritten as w' and z , respectively. This can be integrated once, and, with the imposition of a no-flux condition at the water surface, yields the familiar

$$-\bar{w}' c' + w_s \bar{c} = \frac{v_t}{(\sigma_t)_s} \frac{d\bar{c}}{dz} + w_s \bar{c} = 0 \quad (16-24)$$

As with the momentum equations, a complete solution awaits a specification of v_t (and $(\sigma_t)_s$).

16.4.2 The Specification of the Eddy Viscosity: Zero-Equation Models

A kinematic viscosity (or diffusivity) may be considered as a product of a velocity scale, u , and a length scale, \mathcal{L} . A prescription of v_t will in general involve specifying these two scales in terms of quantities, either already known or for which equations are already available. The additional equations governing these scales may be formulated either as algebraic equations or as differential transport equations, and hence eddy-viscosity models have conventionally been classified as zero-, one-, or two-equation models depending on the number of differential transport equations used in specifying u and \mathcal{L} .

16.4.2.1 Constant-Eddy-Viscosity Models Not surprisingly, the oldest turbulence models are zero-equation models, because the computational requirements are least severe. The simplest of these assume that the turbulent velocity and length scales, and hence the eddy viscosity, are effectively constant over the entire flow region of interest. The main difficulty then is the choice of an appropriate value. Calibration with measurements, possibly combined with

dimensionally based scaling arguments to extend the range of application, is recommended. In fully developed wall-bounded wide channel flows, a common choice involves the product of the shear velocity and the depth, $v_t \propto u_* h$. For depth-averaged models (see Appendix II), this choice for a constant horizontal eddy viscosity is often justified as the result of integrating the classic parabolic mixing-length eddy-viscosity model, discussed below, which gives the proportionality constant as $\kappa/6$, where κ is the von Kármán constant. Observed horizontal diffusivities tend to indicate a larger proportionality constant (Fischer et al. 1979), and so, for practical computations, calibration is recommended. This simplest of models is unlikely to be successful where flow details strongly influenced by turbulence, e.g., separation and reattachment, are of primary interest; where turbulence plays a secondary role, this may prove to be an economical if limited model.

16.4.2.2 Mixing-Length Models The classic zero-equation model, which remains important in current discussions of turbulence in sediment-laden flows, is the mixing-length model. Originally introduced within the context of simple turbulent shear layers by Prandtl (1925), the mixing length, \mathcal{L}_m , may be motivated in a scaling of turbulent velocity fluctuations with mean velocity gradients as $u', w' \sim \mathcal{L}_m \partial \bar{u} / \partial z$, where u' is the velocity fluctuation in the dominant streamwise direction, w' the corresponding fluctuation in the (z) direction across the shear layer. In this way, with the only significant correlation term $u' w' \sim [\mathcal{L}_m (\partial \bar{u} / \partial z)]^2 \sim v_t (\partial \bar{u} / \partial z)$, and with a choice of the velocity scale as $Y = \mathcal{L}_m \partial \bar{u} / \partial z$, the eddy viscosity can be specified as

$$v_t = \mathcal{L}_m \mathcal{U} = \mathcal{L}_m^2 \frac{\partial \bar{u}}{\partial z}. \quad (16-25)$$

To close the model, it remains only to specify \mathcal{L}_m . Physically, \mathcal{L}_m may be thought of as the size of a typical turbulent eddy at any given location. In a simple shear flow with a single dominant velocity gradient, \mathcal{L}_m can usually be related to a length scale across the shear layer (in the z -coordinate direction). In the important case of channel flows, this might be chosen as proportional to the distance z from the bed in the near-bed ("inner") region, i.e., $\mathcal{L}_m \propto z$, or the flow depth, h , in the "outer" bulk-flow region, i.e., $\mathcal{L}_m \propto h$.

For plane uniform flows, with $\mathcal{L}_m \propto z$ or $\mathcal{L}_m = \kappa z$, where the von Kármán constant, κ , is the proportionality constant, and also $\tau_{13} \approx \rho u_*^2$ (from Eq. 16-18 in the near-bed region and neglecting viscous effects), the momentum equation in the streamwise direction becomes

$$-\overline{u'w'} = v_t \frac{d\bar{u}}{dz} = \left(\kappa z \frac{d\bar{u}}{dz} \right)^2 = u_*^2. \quad (16-26)$$

The specification of v_t has thus closed the system of equations, permitting a solution for the velocity profile. Simplification and then integration of Eq. (16-26) yield the well-known logarithmic law for the velocity profile in the near-bed region

(see Chapter 2). In spite of the apparent relation to molecular transport, a detailed mechanistic analogy between turbulent and molecular transport cannot be sustained. As previously noted, a key assumption of molecular momentum transport is that the relevant length scale for molecular viscosity, the mean free path, is much smaller than the length scale over which the strain rate or velocity gradient is defined. On the other hand, \mathcal{L}_m is of the same order of magnitude as the length scale over which the velocity gradient is defined, and hence the mixing length model cannot be justified by analogy with molecular transport. As has been emphasized by Tennekes and Lumley (1972), the success of the mixing-length model results from the existence of a single dominant velocity and a single dominant length scale, from which an eddy viscosity can be unambiguously formulated from dimensional considerations. In this case, u_* and z are identified as the relevant velocity and length scales, and consequently, $v_t \propto u_* z$, which when substituted in to Eq. (16-26) also reproduces the logarithmic velocity profile.

The specification, $v_t = \kappa u_* z$, can only be justified for the near-bed region (but outside of the viscous region). This exemplifies the problem of defining the turbulent length scale in a mixing-length model. Multiple length scales are important in a channel flow; e.g., the viscous length scale, v/u_* , in the viscous sublayer, and the flow depth, h , in addition to z , and the classic mixing-length model of $\mathcal{L}_m \propto z$ can be applied only in the intermediate layer, where the local length scale is dominant. To develop an expression for v_t that may be extended to the outer region, a somewhat circular approach is conventionally taken. Equation (16-26) is first extended to $v_t (\partial \bar{u} / \partial z) = u_*^2 (1 - z/h)$. The logarithmic velocity profile is taken as an empirical observation, such that $\partial \bar{u} / \partial z = u_* / \kappa z$. It follows then that

$$v_t = u_*^2 \left(\frac{1 - z/h}{d\bar{u} / dz} \right) = \kappa u_* z (1 - z/h) \quad (16-27)$$

which is the classic parabolic eddy viscosity for open-channel flows, on which the traditional Ippen-Rouse suspended sediment concentration profile (see Chapter 2) is based. The measurements of Nezu and Rodi (1986) agree reasonably well with this expression, though agreement could be improved with a more appropriate velocity model (Fig. 16-4(a)) through the addition of a wake component, characterized by a wake coefficient, Π , to the logarithmic velocity profile. Equation (16-27) is also the basis of the constant-eddy-viscosity depth-averaged models, since depth-averaging of Eq. (16-27) yields $\kappa u_* h / 6$. With similar reasoning, the following expression for the mixing length, \mathcal{L}_m , can be obtained:

$$\mathcal{L}_m = \kappa z [1 - (z/h)]^{1/2} \quad (16-28)$$

Again, measurements show reasonable agreement with Eq. (16-28) (Fig. 16-4(b)). Equation (16-27) has also been applied to unsteady oscillating boundary flows under waves,

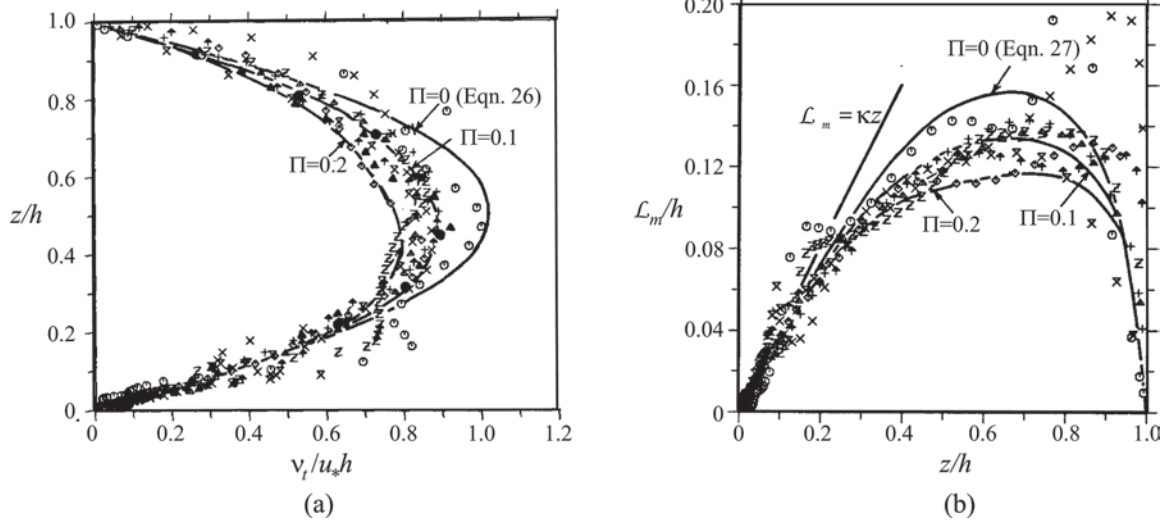


Fig. 16-4. (a) Nondimensional eddy viscosity, ν_t/u_*h , and (b) mixing length, \mathcal{L}_m/h , in a clear-water flow in a straight open channel (adapted from Nezu and Rodi 1986). Symbols are measurements; lines are theory based on a model mean velocity profile, incorporating a log-law and a wake component, with Π being the wake coefficient in the model velocity profile.

with u_* and $h = \delta_w$, where δ_w is the wave boundary layer thickness, both of which are allowed to vary in time (Fredsoe et al. 1985).

16.4.2.3 Turbulence Modulation and the Stably Stratified-Flow Analogy The effect of the suspension on the turbulent flow, sometimes termed turbulence modulation or modification, has been discussed extensively since the experimental work of Vanoni (1946), which showed a distinct steepening of the velocity profile in sediment-laden flows compared to

profiles in clear-water flows. The traditional approach has been to model this effect by a reduced mixing length, via a reduced κ , and to develop a correlation for κ , e.g., as a function of a ratio of the energy required to suspend particles to the total energy dissipated by the flow (Einstein and Chien 1955). Figure 16-5 compares the eddy viscosity and mixing length for clear-water and suspension flows, plotted in semilogarithmic coordinates to emphasize the near-bed region. There is much scatter, but the evidence, if any, for a reduced eddy viscosity and mixing length

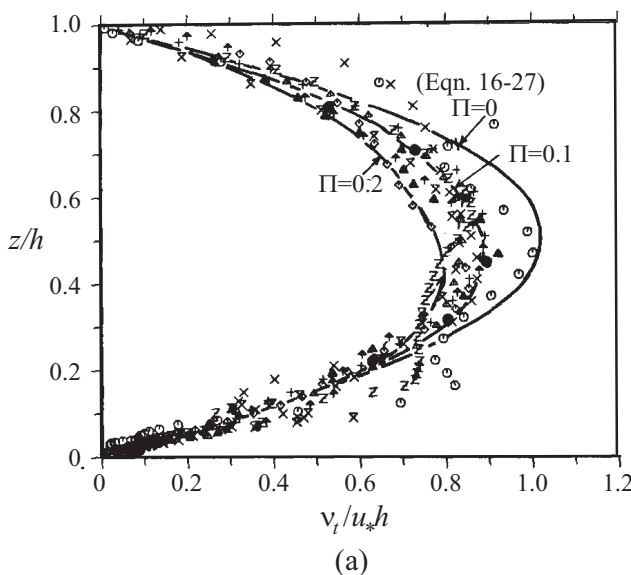


Fig. 16-5. (a) Nondimensional eddy viscosity, ν_t/u_*h , and (b) mixing length, \mathcal{L}_m/h , in a sediment-laden flow in a straight open channel (estimated from the data of Lyn 1988; open symbols: clear-water flow, filled symbols: sediment-laden flow).

is primarily in the inner region. The results of Cellino and Graf (1999) for a case with a smaller sand size and heavier load indicate a more substantial reduction in eddy viscosity over a more extensive region.

Only two models explicitly using the mixing-length approach are here discussed. Like the traditional model, both may be interpreted as resulting in a reduced mixing length, but whereas the traditional model assumes a constant proportional reduction over the entire depth, the two models propose a reduction dependent on local suspension conditions, either on the local concentration (van Rijn 1984c) or the local concentration gradient (Smith and McLean 1977). The van Rijn model modifies the standard eddy viscosity for flows without sediment, $(v_t)_0$, by a function, ϕ , dependent on the local mean suspended sediment concentration, \bar{c} , to obtain an eddy viscosity for a suspension, $(v_t)_s$, as follows:

$$(v_t)_s = \phi(v_t)_0 = \left[1 - 2\left(\frac{\bar{c}}{c_0}\right)^{0.4} + \left(\frac{\bar{c}}{c_0}\right)^{0.8} \right] (v_t)_0 \quad (16-29)$$

where c_0 is the maximum possible volumetric sediment concentration, taken to be 0.65. The physical basis for Eq. (16-29) is obscure, and van Rijn (1984c) admitted that it "does not give optimal agreement for the entire profile," conjecturing that the expression for ϕ is "somewhat too simple."

Example. As has been noted, an analogy between a sediment-laden flow and the flow of a variable-density fluid has been drawn frequently by numerous researchers (e.g., Barenblatt 1953; Lumley 1973). For uniform flow, with variations only in the vertical, the effective density of the suspension, ρ_m (Eq. 16-3), decreases away from the bed as \bar{c} decreases with increasing z . Vertical turbulent momentum transport is therefore inhibited relative to the non-stratified (neutral) case because fluid of vertically varying density displaced from its original elevation experiences a restoring buoyancy force acting to return it to its original elevation: i.e., the flow is stably stratified. The reduced vertical transport results in a velocity profile steeper than the neutral case, which, as noted above, is observed in sediment-laden flows. The analogy is attractive not only for its intuitive appeal, but also because it allows the application of results from a large literature on turbulent, stably (thermally or saline) density-stratified flows in atmospheric and oceanographic applications (Monin and Yaglom 1971; Turner 1973).

Smith and McLean (1977) proposed a density-stratified-flow model for sediment-laden flows, in which the effective mixing length is reduced, but, unlike the van Rijn model, the reduction is correlated with a suspension (gradient) Richardson number, Ri_s , defined as

$$Ri_s = -\frac{g}{\rho_{ref}} \frac{\partial \rho_m / \partial z}{(\partial \bar{u} / \partial z)^2} = -g(s-1) \frac{\partial \bar{c} / \partial z}{(\partial \bar{u} / \partial z)^2} \quad (16-30)$$

where ρ_{ref} has been taken to be ρ . Barenblatt (1996) has suggested that Ri_s be called the Kolmogorov number. As will become clearer below, for stable stratification, $Ri_s > 0$ can be interpreted as being proportional to the ratio of the local rate of energy expenditure needed to overcome a stable stratification and the local rate of production of k (similar to the traditional Einstein–Chien (1955) model). In the Smith–McLean model,

$$(v_t)_s = \left[1 - \alpha_m \left\{ \frac{\epsilon_s}{(v_t)_s} \right\} Ri_s \right] (v_t)_0 \quad (16-31)$$

where α_m is a model constant. Here, $\epsilon_s/(v_t)_s$ is seen as equivalent to $1/(\sigma_t)_s$, but, contrary to the usual practice where $(\sigma_t)_s$ is assumed constant in space (e.g., as in the van Rijn model), $\epsilon_s/(v_t)_s$ can be expressed as a spatially varying function in terms of other model parameters. Villaret and Trowbridge (1991) analyzed the performance of this model (actually a perturbation solution of this model, since, for most of the laboratory flows examined, $Ri_s \ll 1$) in fitting an extensive series of laboratory measurements from various studies. They found some support for the stratified-flow model, but their results indicate that α_m might vary considerably, detracting from one of the main advantages of this model.

In contrast to the traditional approach, in which the solution for the velocity profile is effectively decoupled from the solution for the suspended sediment concentration profile, both the van Rijn and the Smith–McLean models require a fully coupled treatment, in which the relevant momentum and sediment equations are solved simultaneously. These two models may be expressed respectively as follows:

Van Rijn model:

$$[(v_t)_0 \phi] \frac{d\bar{u}}{dz} = u_*^2 \left(1 - \frac{z}{h} \right) \quad (16-32a)$$

$$[(\beta_s)_{vR} (v_t)_0 \phi] \frac{d\bar{c}}{dz} = -w_s \bar{c} \quad (16-32b)$$

Smith–McLean model:

$$\begin{aligned} (v_t)_s \frac{d\bar{u}}{dz} &= (v_t)_0 \left[1 - \alpha_m \left\{ \frac{\epsilon_s}{(v_t)_s} \right\} Ri_s \right] \frac{d\bar{u}}{dz} \\ &= u_*^2 \left(1 - \frac{z}{h} \right) \end{aligned} \quad (16-33a)$$

$$\varepsilon_s \frac{d\bar{c}}{dz} = (\nu_t)_0 \left[1 - \alpha_s \left\{ \frac{\varepsilon_s}{(\nu_t)_s} \right\} \text{Ri}_s \right] \frac{dc}{dz} \quad (16-33b)$$

$$= -w_s \bar{c}$$

where α_s is another model constant.

A comparison of the predictions of the van Rijn and Smith-McLean models with two measured velocity and concentration profiles for flows under equilibrium-bed (capacity or saturated) conditions is given in Fig. 16-6. The experimental parameters are given in Table 16-1. In these computations, different models of $(\nu_t)_0$ were used. The $(\nu_t)_0$ of van Rijn (1984b) was used for the van Rijn model, whereas the $(\nu_t)_0$ of Villaret and Trowbridge (1991) was used for the Smith-McLean model. Bottom boundary conditions were based on measured velocity and concentration, and α_m and α_s were taken as 6.9 and 9.2, as specified in McLean (1992). According to the classification scheme of Soulsby and Wainwright (1987), based on u_* and d , both of the experiments should exhibit some stratification effects ($u_* \approx 4$ cm/s and $d_{50} \approx 0.18\text{--}0.19$ mm). Estimates of local flux Richardson numbers from the measurements indicate values exceeding $O(0.01)$ in both experiments. Both models perform reasonably well for both the velocity and concentration data of Barton and Lin, although slight systematic deviation of the data from predictions might be seen. The van Rijn model does somewhat better in predicting concentrations than the Smith-McLean model, which underestimates concentrations in the outer flow ($z/h = O(1)$), due to the reduced mixing caused by stable stratification. The Barton-Lin data were used in the calibration of the van Rijn model, and so good performance might be expected. Both models do comparatively poorly for the Lyn velocity data, which exhibit a much more pronounced deviation from the log-law profile that is, however, confined to the near-bed region. At the measured concentration values, both models predict profiles quite close to the classic log-law profile. Hence when the measured velocity at the lowest point is imposed as a boundary condition, there is notable disparity between measured and predicted profiles. Nevertheless, the Lyn concentration data are quite well reproduced by the Smith-McLean model, where as the van Rijn model predictions are substantially in error, attributable to the overly large β_s value given by Eq. (16-21) and the associated enhanced vertical sediment transport.

The problem of predicting the velocity and concentration profiles in a suspension flow over a nominally plane bed is still largely unresolved. Two other related aspects of uniform sediment-laden flows over plane beds shed light on appropriate models, namely flow resistance, e.g., parameterized by a friction factor, f_{DW} , and the root mean square of vertical velocity fluctuations, $\sqrt{w'^2}$. In their purest (and simplest) form, the stably stratified-flow models predict

Table 16-1 Experimental Parameters for Equilibrium Plane-Bed Flows

Parameter	Barton and Lin (1955) Run 36	Lyn (1988) Run 1957EQ
Median sediment size, d_{50} (mm)	0.18	0.19
Depth, h (cm)	16.2	5.7
Shear velocity, u_* (cm/s)	5.6	3.95
$\bar{c}(z/h = 0.1) (\times 10^{-3})$	3.1	1.1
Slope, $S (\times 10^{-3})$	2.10	2.95
$R_* = u^* h / v (\times 10^3)$	9.1	2.3
$F = U / \sqrt{gh_0}$	0.21	0.90

a decrease in f_{DW} (e.g., Itakura and Kishi 1980; McLean 1992) and a reduction in $\sqrt{w'^2}$ in suspension flows. The choice of an appropriate benchmark or reference for comparison is important, because, unlike stratification due to temperature or salinity, density stratification in sediment-laden flows may be only one of several factors influencing flow characteristics. In the case of flow resistance, if the basis of comparison is a clear-water flow of the same depth and a roughness height equal to the *median grain size*, d_{50} , as is commonly done in clear-water flows, then the empirical evidence argues *against* this prediction of the stably stratified flow models (see the discussion below of boundary conditions for further details). In the case of $\sqrt{w'^2}$, the laser-Doppler studies of Lyn (1993) and Bennett et al. (1998) indicate either no significant effect or indeed the opposite effect, namely, a slight increase in, contrary to that expected from stably stratified-flow analogies. On the other hand, Cellino and Graf (1999), using an acoustic Doppler technique, did observe a marked reduction in $\sqrt{w'^2}/\mu_*$, and so the experimental evidence is at present inconclusive. Measurements of turbulence characteristics in the most interesting flow region, i.e., the near-wall region, in a sediment-laden flow over a plane sand bed in equilibrium with the suspension present very difficult challenges to all experimental techniques, and hence any such measurements should be considered with some caution.

The stably stratified flow analogy has been discussed here within the context of mixing-length models, but similar comments would also apply to the more sophisticated models discussed below, since they, as will be seen, may often be simplified to essentially mixing-length models for uniform-flow problems.

16.4.2.4 Limitations of Mixing-Length Models The success of the mixing-length model rests on the dominance of a single velocity and a single length scale, which also, as will be seen below, reflects a local equilibrium between production and dissipation of turbulent kinetic energy.

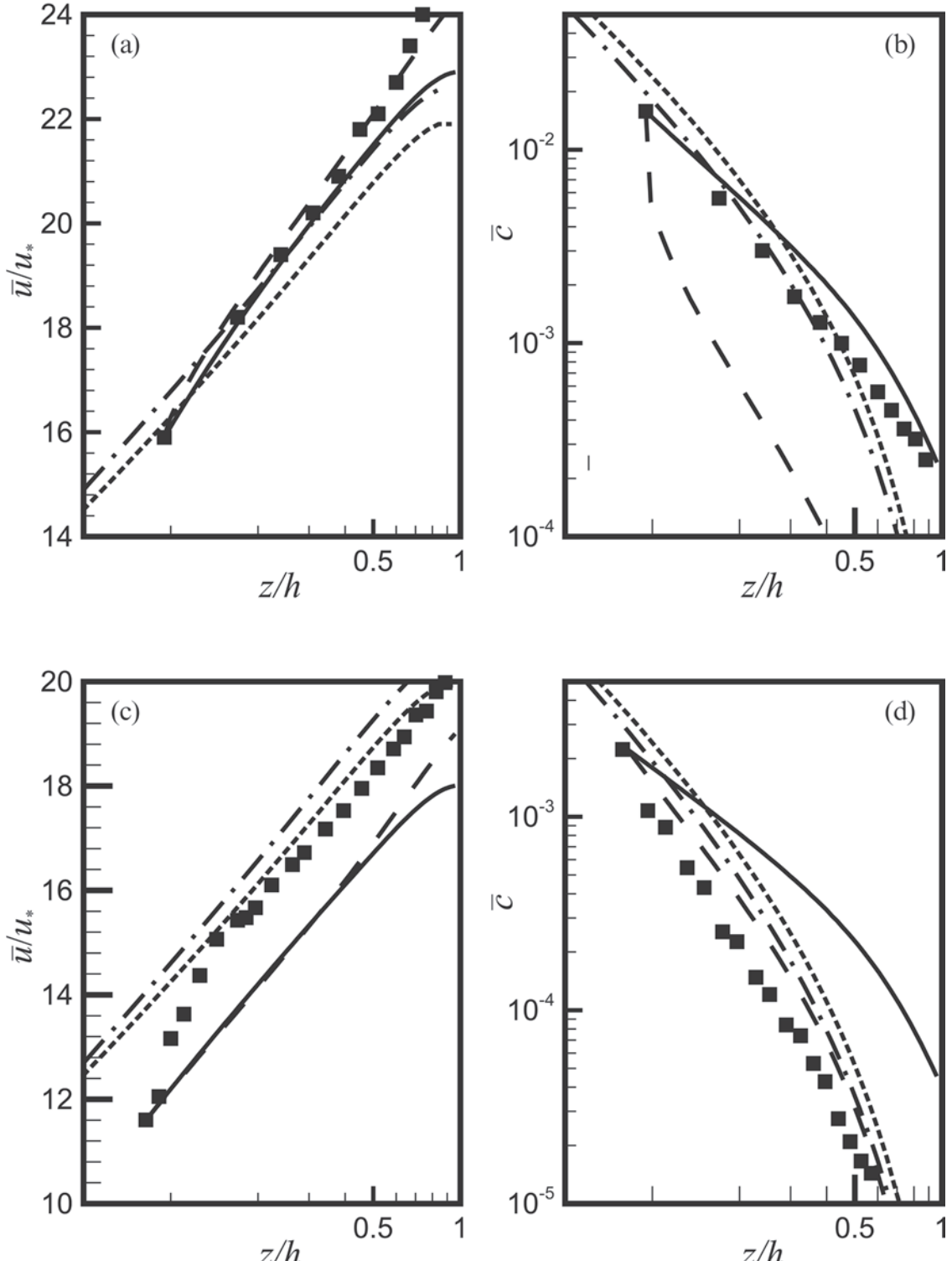


Fig. 16-6. Comparison of model predictions for steady uniform sediment-laden flows of (a) and (c) dimensionless velocity, \bar{u}/u_* , and (b) and (d) concentration, \bar{c} . Data (filled symbols) in (a) and (b) from Barton and Lin (1955), Run 36; data in (c) and (d) from Lyn (1988), Run 1957EQ. — : van Rijn model; —— : Smith-McLean model; ... : standard $k-\epsilon$ model; - - - : $k-\epsilon$ model including buoyancy.

In multidimensional problems with strong spatial variation in more than one coordinate direction, the mixing-length model will likely perform poorly. Generalizations of Eq. (16-25) to multidimensional flows have been proposed, but the practical difficulty of specifying \mathcal{L}_m for complicated flows remains. Nonequilibrium problems where history/transport effects are important will also present difficulties because of the time required to relax to an equilibrium state, which introduces another time (or velocity) scale into the problem. On the other hand, a great deal of practical experience has been accumulated with such models in a wide variety of problems, the computational demands are attractive, and reasonable predictions can be obtained with some degree of experience and judgment on the part of the modeler. The problem of turbulence modulation does illustrate the fundamental weakness of mixing-length models (as well as other more sophisticated models) in that the appropriate mixing length when the flow is sediment-laden is not clear, even for the simplest case of a fully developed uniform wall-bounded flow.

16.4.3 The Specification of the Eddy Viscosity: One-Equation Models

An algebraic specification of the eddy viscosity, as in zero-equation models, may be interpreted as implicitly assuming a local equilibrium where v_t is determined entirely by local flow conditions. Nonequilibrium effects imply that the flow characteristics at a point may be significantly affected by the history of fluid parcels passing through that point. Zero-equation turbulence models are poorly suited to model such effects in any general way. An alternative approach seeks to include these effects in a differential rather than algebraic specification of the velocity scale, the length scale, or both. In one-equation models, a single differential equation for a turbulence quantity is formulated in addition to the momentum equations. Most frequently, the quantity chosen is the turbulent kinetic energy, k , the square root of which provides a velocity scale.

16.4.3.1 The Equation for Turbulent Kinetic Energy

An exact equation for k can be derived from the Navier-Stokes equations (Hinze 1975; Kundu 1990):

$$\begin{aligned} \frac{Dk}{Dt} &= \frac{\partial k}{\partial t} + \frac{\partial(\bar{u}_j k)}{\partial x_j} \\ &= -\frac{\partial}{\partial x_j} \left(\frac{1}{2} \bar{u}'_i \bar{u}'_i \bar{u}'_j + \frac{1}{\rho_{\text{ref}}} \bar{u}'_j p' - 2v \bar{u}'_i s'_{ij} \right) \\ &\quad + P_k - \epsilon + G_k \end{aligned} \quad (16-34)$$

where

$$s'_{ij} = (\partial u'_i / \partial x_j + \partial u'_j / \partial x_i) / 2 \text{ fluctuating strain-rate tensor}$$

The rate of production, P_k , of k by the interaction of the Reynolds stresses with the mean strain rate is given by

$$\begin{aligned} P_k &= -\bar{u}'_i \bar{u}'_j S_{ij} = -\bar{u}'_i \bar{u}'_j \left[\frac{1}{2} \left(\frac{\partial \bar{u}_i}{\partial x_j} + \frac{\partial \bar{u}_j}{\partial x_i} \right) \right] \\ &= -\bar{u}'_i \bar{u}'_j \frac{\partial \bar{u}_i}{\partial x_j} \end{aligned} \quad (16-35)$$

(see Appendix I, Eq. (16-82) for an expanded version of Eq. (16-35)). The rate of dissipation, ϵ , of k by viscosity can be expressed as

$$\begin{aligned} \epsilon &= 2v \overline{s'_{ij} s'_{ij}} \\ &= \frac{v}{2} \overline{\left(\frac{\partial u'_i}{\partial x_j} + \frac{\partial u'_j}{\partial x_i} \right) \left(\frac{\partial u'_i}{\partial x_j} + \frac{\partial u'_j}{\partial x_i} \right)} \\ &= v \overline{\left(\frac{\partial u'_i}{\partial x_j} + \frac{\partial u'_j}{\partial x_i} \right) \frac{\partial u'_i}{\partial x_j}} . \end{aligned} \quad (16-36)$$

The last term in Eq. (16-34), G_k , represents any other source or sink of k that may be due to additional forces, e.g., due to the presence of particles. If buoyancy effects are important, then

$$G_k = (G_k)_\rho = \frac{g_i}{\rho_{\text{ref}}} \overline{u'_i \rho'} . \quad (16-37)$$

The ratio $(G_k)_\rho / P$ is termed the flux Richardson number. If, as has been assumed in several models, the sole effect of particles in suspension on the k -budget is analogous to that caused by buoyancy, then

$$\frac{g_i}{\rho_{\text{ref}}} \overline{u'_i \rho'} = g_i (s-1) \overline{u'_i \rho'} . \quad (16-38)$$

Because Eq. (16-34) contains extra correlation terms (the triple velocity correlation, $\bar{u}'_i \bar{u}'_j \bar{u}'_l$, and the pressure-velocity correlation, $\bar{u}'_i p'$, as well as ϵ) that are not known, it is not immediately useful. For a one-equation model based on Eq. (16-34), the length scale, \mathcal{L} , is specified algebraically, and so the extra correlation terms must be expressed in terms of k and/or \mathcal{L} for a closed system of equations. The terms involving the triple velocity and pressure-velocity correlations are interpreted as turbulent "diffusive" transport terms that do not increase or decrease the overall level of k but only redistribute k over the flow region of interest. A diffusion model for these terms together can be motivated, namely,

$$\frac{1}{2} \overline{u'_i u'_j u'_l} + \frac{1}{\rho_{\text{ref}}} \overline{u'_j p'} = -\frac{v_t}{\sigma_k} \frac{\partial k}{\partial x_j} \quad (16-39)$$

where the turbulent Schmidt number for k , σ_k , is defined by Eq. (16-39) and is usually assumed constant. The model for the rate of dissipation (sink) term, ϵ , is obtained from a dimensional scaling argument as

$$\epsilon = c_D \frac{k^{3/2}}{\mathcal{L}} \quad (16-40)$$

with c_D an empirically determined model constant. With these model choices, the inclusion of a buoyancy effect for suspensions, and the neglect of the viscous diffusive term (justifiable for high- \mathbf{R} applications), the equation for k becomes

$$\begin{aligned} \frac{Dk}{Dt} &= \frac{\partial k}{\partial t} + \frac{\partial(\bar{u}_j k)}{\partial x_j} \\ &= \frac{\partial}{\partial x_j} \left(\frac{v_t}{\sigma_k} \frac{\partial k}{\partial x_j} \right) + v_t \left(\frac{\partial \bar{u}_i}{\partial x_j} + \frac{\partial \bar{u}_j}{\partial x_i} \right) \frac{\partial \bar{u}_i}{\partial x_j} \\ &\quad - g_i(s-1) \frac{v_t}{(\sigma_t)_s} \frac{\partial \bar{c}}{\partial x_i} - c_D \frac{k^{3/2}}{\mathcal{L}} \end{aligned} \quad (16-41)$$

where the standard eddy viscosity (Eq. (16-14)) or diffusivity (Eq. (16-19)) model has been applied to eliminate the Reynolds stress term, $-\bar{u}'_i \bar{u}'_j$, and the buoyancy flux term, $\bar{u}'_i c'$. In this form, the ratio, $(G_k)_\rho/P$, becomes proportional to the gradient Richardson number, Ri_s , already introduced in the discussion of zero-equation models. The solution of Eq. (16-41) for k provides the required μ , and so v_t is evaluated as

$$v_t = c'_\mu \sqrt{k} \mathcal{L} \quad (16-42)$$

where c'_μ is a model constant. The choice of c_D and c'_μ is constrained by the requirement for consistency in the case of local equilibrium, as will be elaborated below.

16.4.3.2 Local Equilibrium and Mixing-Length Models In Eq. (16-34) or (16-41), the left-hand side of the equation and the diffusive term (the first term on the right-hand side of the equation) represent the transport terms that become important in nonequilibrium problems. In cases where these effects may be neglected, i.e., those for which the mixing-length model might be appropriate, Eq. (16-41) reduces to

$$\begin{aligned} 0 &= P_k + (G_k)_\rho - \epsilon \\ &= v_t \left(\frac{\partial \bar{u}_i}{\partial x_j} + \frac{\partial \bar{u}_j}{\partial x_i} \right) \frac{\partial \bar{u}_i}{\partial x_j} \\ &\quad + g(s-1) \frac{v_t}{(\sigma_t)_s} \frac{\partial \bar{c}}{\partial z} - c_D \frac{k^{3/2}}{\mathcal{L}}. \end{aligned} \quad (16-43)$$

Example. For the plane uniform-flow case, Eq. (16-43) becomes

$$\begin{aligned} P_k + (G_k)_\rho &= \epsilon \quad \text{or} \quad v_t \left(\frac{d\bar{u}}{dz} \right)^2 + g(s-1) \frac{v_t}{(\sigma_t)_s} \frac{\partial \bar{c}}{\partial z} \\ &= c_D \frac{k^{3/2}}{\mathcal{L}} \end{aligned} \quad (16-44)$$

which, together with Eq. (16-42), becomes

$$\begin{aligned} v_t &= \sqrt{\frac{(c'_\mu)^3}{c_D} \mathcal{L}^2 \frac{d\bar{u}}{dz} \left[1 - \frac{1}{(\sigma_t)_s} \text{Ri}_s \right]^{1/2}} \\ &= (v_t)_0 \left[1 - \frac{1}{(\sigma_t)_s} \text{Ri}_s \right]^{1/2} \end{aligned} \quad (16-45)$$

where

$(v_t)_0$ = eddy viscosity in the absence of buoyancy effects.

If $\text{Ri}_s = 0$, then Eq. (16-45) reproduces the standard model. If \mathcal{L} is taken as κz , then for consistency with the mixing-length model, the constants c'_μ and c_D must be chosen so that $(c'_\mu)^3/c_D = 1$, and cannot be chosen independently. For nonzero but small Ri_s , $[1 - \text{Ri}_s/(\sigma_t)_s]^{1/2}$ can be expanded in a power series in Ri_s , and a relationship of the same form as Eq. (16-31) is obtained. The inclusion of buoyancy effects adds another relevant velocity (or length) scale, e.g., $\sqrt{g(s-1)\mathcal{L}^2(\partial \bar{c}/\partial z)}$, to the problem, and so introduces an ambiguity into the mixing-length model, which, as was argued above, relies on the dominance of a single velocity and a single length scale. An interesting alternative approach was taken by Barenblatt (1953; reported in Monin and Yaglom 1971 and in Barenblatt 1996), who sought similarity solutions to Eq. (16-44). With $k \sim u_*^2$, $\mathcal{L} \sim z$, and $v_t \sim \sqrt{k} \mathcal{L} \sim u_* z$, these could be found when $\bar{c} \sim 1/z$ and $\partial \bar{u} / \partial z \sim 1/z$, equivalent to a constant Ri_s , though the implications, practical or theoretical, of this result remain unclear.

16.4.3.3 Applications of a One-Equation Model Because of their intermediate nature between the simpler zero-equation model and the more complete two-equation model, one-equation models not making the local-equilibrium assumption have not been as commonly used in hydraulic or sediment-transport engineering as either of the other two model types. Two examples may, however, be cited. In a study of sand-wave evolution due to sediment transport, Johns et al. (1990) applied a quasi-two-dimensional model based on Eqs. (16-41) and (16-42) including buoyancy effects. Nonequilibrium transport effects might be expected because of the streamwise spatial variations in flow over bed

forms. All turbulent Schmidt numbers were assumed to be unity, whereas $c_D = (c'_\mu)^3 = 0.15$, with $c'_\mu = 0.53$. The length scale was determined from a von Kármán type relationship (see the discussion in Rodi 1993),

$$\mathcal{L} = \frac{-\kappa\sqrt{k}/\mathcal{L}}{d(\sqrt{k}/\mathcal{L})/dz} \quad (16-46)$$

which is not algebraic, but is not specified by means of a partial differential transport equation. Some of their numerical results are briefly mentioned in Section 16.5.1. The second example is due to Li and Davies (1996), who were interested in predicting sediment transport in combined wave-current flows. In this case, nonequilibrium effects might be expected because of the unsteadiness in problems with surface waves. The stratification analogy was also made, so that $(G_k)_\rho$ was included. The variable $(\sigma)_s$ was assumed to be unity, but $\sigma_k = 1.37$, while $c_D = (c'_\mu)^3 = 0.097$, corresponding to $c'_\mu = 0.46$. Wilcox (1998) reported on early one-equation models with values of c_D taken in the range from 0.07 to 0.09 and with $c'_\mu = 1$, where Rodi (1993) indicated that the product $c'_\mu c_D \approx 0.08$. The length scale, motivated by Eq. (16-28), was given by

$$\mathcal{L} = \left(1 - \frac{z}{h}\right)^{1/2} \kappa\sqrt{k} \left(z_0 k_0^{-1/2} + \int_{z_0}^z k^{-1/2} d\eta\right) \quad (16-47)$$

where z_0 is a bottom roughness scale. Some results with this model will be given in Section 16.5.4. Further developments of this model are sketched in Villaret and Davies (1995) and tested on even simpler steady unidirectional flows, with still rather mixed results, as will be seen in Section 16.4.7. Both Eqs. (16-46) and (16-47) differ from classic mixing-length specifications and attempt to incorporate information obtained in the solution of k in the specification of \mathcal{L} , so that Λ can vary in both space and time depending on flow conditions, as characterized by the local value of k . In particular, buoyancy effects that affect k will therefore also affect \mathcal{L} .

16.4.3.4 Limitations of One-Equation Models The current verdict on one-equation models in comparison to mixing-length models remains rather negative in that the improvements in predictions tend to be rather marginal (Bradshaw 1997; Wilcox 1998). As with the mixing-length model, the main problem lies in the length-scale specification, which becomes increasingly difficult in complex flow problems. In both of the above examples, the length-scale specification was guided by results for a plane-bed uniform-flow case; in more complicated flows, the specification is more difficult to motivate. This problem can be circumvented by formulating a transport equation directly for the eddy viscosity, rather than for k , such that a second equation for the length scale is not necessary. The model of Spalart and Allmaras (1992; see also the discussion in Spalart 2000), following this logic, has revived interest in one-equation

models for aeronautical problems, but does not seem to have been adopted so far in hydraulics or sediment transport, and so is not discussed further.

16.4.4 The Specification of the Eddy-Viscosity: Two-Equation Models

If the logic leading to the development of the k -equation is followed, then the problem of determining the relevant length scale can be resolved by formulating an additional transport equation for a quantity that would, possibly in combination with k , provide a length scale. Rodi (1993) has noted that any quantity of the form $k^m \mathcal{L}^n$, where m and n are arbitrary exponents, would lead to dimensionally consistent equations of the same form. The presence of ϵ in the k equation as an unknown variable leads naturally to its choice as the quantity for which a transport equation is developed. An exact equation for ϵ can be derived from the Navier-Stokes equations, but its dominant correlation terms are impossible to measure in the laboratory (though they could be evaluated from results of numerical simulations), so model proposals cannot rely on experimental observations for guidance (Lauder 1984; Wilcox 1998). Further, because viscous dissipation occurs on the smallest scales, the relevance of the exact terms for specifying \mathcal{L} is questionable, which is characteristic of the larger energy-carrying scales that determine the level of overall dissipation (recall the qualitative discussion of dissipation in Section 16.2.1). It has therefore been conventionally preferred to formulate a surrogate equation for ϵ along the lines of the k -equation, based primarily on dimensional analysis and appropriate asymptotic behavior, e.g., in the ideal case of homogeneous high- R turbulence (Lauder 1984). The strict identification of ϵ with the rate of dissipation of k , however, becomes more tenuous.

16.4.4.1 The Equation for ϵ The standard model equation for ϵ , incorporating the eddy viscosity model and, as usual, neglecting viscous transport terms in high- R flows, is thus of the form

$$\begin{aligned} \frac{D\epsilon}{Dt} &= \frac{\partial \epsilon}{\partial t} + \frac{\partial (\bar{u}_j \epsilon)}{\partial x_j} \\ &= \frac{\partial}{\partial x_j} \left(\frac{v_t}{\sigma_\epsilon} \frac{\partial \epsilon}{\partial x_j} \right) + P_\epsilon - D_\epsilon + G_\epsilon \end{aligned} \quad (16-48)$$

where σ_ϵ is the turbulent Schmidt number for the diffusive transport of ϵ . The production-of-dissipation term, P_ϵ , is necessary because, if k is being produced and the level of k increases in time, then the level of ϵ must also increase in order ultimately to limit the level of k . A simple model of $P_\epsilon \propto P_k$ may therefore be motivated, but for dimensional consistency, a multiplicative factor of ϵ/k , which may be interpreted as a turbulence frequency, is needed, such that

$$\begin{aligned} P_\epsilon &= c_{1\epsilon} \frac{\epsilon}{k} P_k \\ &= c_{1\epsilon} \left(\frac{\epsilon}{k} \right) \left[v_t \left(\frac{\partial \bar{u}_i}{\partial x_j} + \frac{\partial \bar{u}_j}{\partial x_i} \right) \right] \frac{\partial \bar{u}_i}{\partial x_j} \end{aligned} \quad (16-49)$$

where

$c_{1\epsilon}$ = a model constant.

The destruction-of-dissipation term, D_ϵ , is similarly modeled as

$$D_\epsilon = c_{2\epsilon} \left(\frac{\epsilon}{k} \right) \epsilon = c_{2\epsilon} \frac{\epsilon^2}{k} \quad (16-50)$$

where

$c_{2\epsilon}$ = another model constant.

Like the corresponding term in the k -equation, the last term in Eq. (16-48), G_ϵ , reflects the effect on ϵ of other forces or strains. In the case of buoyancy effects, $G_\epsilon = (G_\epsilon)_\rho$, the modeling of which, however, still remains open. That a term similar to P_ϵ but proportional to $(G_\epsilon)_\rho$ is desirable is commonly accepted, particularly where buoyancy production is concerned, i.e., in *unstable* stratification. Rodi (1993) recommended that

$$(G_\epsilon)_\rho = c_{1\epsilon} \frac{\epsilon}{k} [(G_k)_\rho (1 + c_{3\epsilon} R i_s) + c_{3\epsilon} R i_s P_k] \quad (16-51)$$

where

$c_{3\epsilon}$ = yet another model constant.

More often (Burchard and Baumert 1995; Chen and Jaw 1996), a simpler model for $(G_\epsilon)_\rho$, which can be viewed as a special case of Eq. (16-51) for horizontal flows, is applied:

$$(G_\epsilon)_\rho = c_{1\epsilon} c_{3\epsilon} \frac{\epsilon}{k} (G_k)_\rho \quad (16-52)$$

16.4.4.2 The Standard $k-\epsilon$ Model and the Closure Constants The buoyancy-extended $k-\epsilon$ model consists of Eq. (16-41) with the original ϵ rather than its model, $k^{3/2}/\mathcal{L}$, and Eq. (16-48). With $u = \sqrt{k}$ and $\mathcal{L} = k^{3/2}/\epsilon$, this yields

$$v_t = c_\mu \sqrt{k} \left(\frac{k^{3/2}}{\epsilon} \right) = c_\mu \frac{k^2}{\epsilon} \quad (16-53)$$

with c_μ a further model constant. In total, the standard model without buoyancy extensions requires five model constants: the two coefficients in the source and sink terms of the ϵ equation, $c_{1\epsilon}$ and $c_{2\epsilon}$, the coefficient, c_μ , in the eddy viscosity specification, and the turbulent Schmidt numbers for k and ϵ , σ_k

and σ_ϵ . The first three are chosen to agree with experimental observations in special (asymptotic) flow cases where the model equations simplify, such as equilibrium shear layers (where $P_k = \epsilon$), grid-generated wind-tunnel turbulence (where $P_k = 0$ and diffusive terms are zero), and the log-law region in wall-bounded flow (where $P_k \approx \epsilon$ and other terms are negligible). The remaining constants, σ_k and σ_ϵ , were tuned or calibrated to a variety of flows. The standard values for the $k-\epsilon$ model constants are given in Table 16-2, together with the value of the von Kármán constant, κ , resulting from the use of the standard constants. The range in values of κ may be surprising, though there have been some recent discussions on this topic (see, e.g., the review of Patel 1998). Other values of the closure constants have been suggested based on other considerations. From the case of homogeneous shear flows, Tennekes (1989) has offered an interesting scaling argument based on the special case of homogeneous shear flows for the choice, $c_{1\epsilon} = 3/2$, which is very close to the standard value for the various models in Table (16-2). Similarly, theoretical models for grid-generated turbulence at high R (Speziale and Bernard 1992) suggest, in spite of experimental evidence to the contrary, that $c_{2\epsilon} = 2$, which has been adopted in some models. Nevertheless, because the first three constants are generally tuned to the same types of flows, their values shown in Table 16-2 are quite similar. The values of the closure constants are *not* independent, and changes in one constant may for consistency require changes in other constants, similar to what was seen earlier for one-equation models.

Because of the prominence of the stratified-flow analogy in sediment-transport literature, the closure constant, $c_{3\epsilon}$, merits special discussion, which will be limited to the simpler model of Eq. (16-52). In the unstable case, where the density gradient is positive in the direction opposite to gravity, which might be assumed in models of sediment dumping or inflows, turbulence is generated by negative buoyancy, $(G_k)_\rho > 0$, and $c_{3\epsilon} > 0$. In this case, there seems to be general agreement with the value of $c_{3\epsilon} = 1$ (Rodi 1987; Burchard et al. 1998). For the more common case of stable stratification, which is of greater interest in sediment transport in alluvial channels, there is substantial variation in values used, with even the sign being in dispute. Baumert and Peters (2000) listed nine different choices ranging from -1.4 to 1.45, with the most common choice being $c_{3\epsilon} = 0$, but generally non-negative. Chen and Jaw (1998), who give an extended discussion of turbulent buoyant flows, recommended values in the range from 1 to 1.33 (note that the notation for $c_{3\epsilon}$ may vary; what is denoted here as $c_{1\epsilon} c_{3\epsilon}$ is denoted in Chen and Jaw as $c_{3\epsilon}$). A theoretical argument based again on the special case of strictly stationary ("full equilibrium") homogeneous stably stratified shear flows has been advanced by Burchard and Baumert (1995) for a negative value and the value of -1.4 was proposed (note that this value is given for a $k-\epsilon$ model with nonstandard choices of the other closure constants, so caution is advised in using this value with the standard model). Needless to say, a standard choice of $c_{3\epsilon}$

Table 16-2 Effective^a Closure Constants for the Standard $k-\epsilon$, the RNG $k-\epsilon$, the $k-\omega$, and the Mellor-Yamada (M-Y) Models, together with the Corresponding Value for the Von Kármán Constant, κ

Model	c_μ	$c_{1\epsilon}$	$c_{2\epsilon}$	σ_k	σ_ϵ	κ
Standard	0.09	1.44	1.92	1.0	1.3	0.43
RNG	0.085	1.42	1.68	0.72	0.72	0.39
$k-\omega$	0.09	1.56	1.83	2.2	0.41	
M-Y ^b	0.095	1.6	2	2	2	0.40

^aThe $k-\omega$ and Mellor-Yamada models differ in formulation from the $k-\epsilon$ model, and hence the closure constants for the different models cannot be considered as exactly equivalent.

^bThis refers to the Mellor-Yamada level 2 1/2 model for non-density-stratified flows, with the stability functions of Galperin et al. (1988).

has not as yet been established, and some sensitivity analysis with respect to its value is recommended.

That the closure coefficients satisfy constraints established in special asymptotic cases of homogeneous flows or flows in local equilibrium is certainly necessary; that they then should apply to flows far from the asymptotic conditions assumed, as Wilcox (1998) has remarked, that the model possess a degree of universality that may be grossly optimistic. The possibility that the closure constants may be functions of local dimensionless parameters reflecting the deviation of conditions from the asymptotic cases is naturally motivated (Hanjalic 1994; Bradshaw 1997). In near-wall models (Launder 1984, 1996; Patel et al. 1985; Wilcox 1998) that must deal with viscous effects, the closure constants are commonly assumed to vary with a local turbulent Reynolds number. For stratified flows, the Mellor-Yamada models discussed below propose what might be interpreted as a c_μ varying with Richardson flux numbers. For highly nonequilibrium flows, the closure constants might be taken to vary with $(P_k/\epsilon) - 1$ (or more simply, P_k/ϵ), which is a measure of the distance from local equilibrium (see also the discussion in Rodi 1993). A more systematic theoretical justification for the last two proposals can be based on algebraic stress models, which will also be dealt with below.

16.4.5 The Treatment of Boundary Conditions and Auxiliary Model Equations

The following is restricted to boundary conditions at the bed and at the free surface. The conventional approach to dealing with the condition at a solid surface, namely, through the use of so-called wall functions, is outlined. For sediment-transport problems, the difficulty of specifying a boundary condition for the sediment conservation equation, Eq. (16-7), must also be confronted. Because the boundary condition on Eq. (16-7) is conventionally not applied at the bed, Eq. (16-7) only treats suspended load (see Chapter 2 for a definition), and so if total load is of interest, then a

bed-load relationship is also required. If further a mobile erodible bed is to be simulated, then an additional equation for the bed evolution, similar to a dynamic equation at a free surface, must be included.

16.4.5.1 The Treatment of the Near-Bed Region: Flow and Turbulence The problems of imposing an exact-flow boundary condition have been discussed previously. The solution most commonly applied is the so-called wall functions approach, based on an equilibrium model for the near-wall flow, and the wall boundary conditions are imposed, not at the wall, but at a level outside of the viscous region. The traditional local-equilibrium model, $P_k = \epsilon$ and $d\bar{u}/dz = u_*/\kappa z$, is assumed to apply in a constant-shear-stress layer, where the boundary conditions are to be imposed, with the result that the necessary boundary conditions for \bar{u}_i , k , and ϵ are expressed as

$$\frac{V_w}{u_*} = \frac{1}{\kappa} \ln \frac{z_w u_*}{v} + B(d_r^+),$$

$$k_w = \frac{u_*^2}{c_\mu^{1/2}}, \quad \epsilon_w = \frac{u_*^3}{\kappa z_w} \quad (16-54)$$

where the w -subscript refers to the level where the boundary conditions are imposed, V_w is the magnitude of the velocity, with direction opposite to that of the shear stress, and B , the integration constant in the log-law velocity profile, is a function of the roughness Reynolds number, $d_r^+ \equiv u_* d_r / v$ where d_r is an equivalent roughness height. Various specifications of B are available; one due to Cebeci and Bradshaw (1977) and used by Wu et al. (2000) can be expressed as

$$\frac{B_s - B}{B_s - B_r + (1/\kappa) \ln d_r^+}$$

$$= \begin{cases} 0, & d_r^+ < 9/4, \text{ (smooth)}, \\ \sin \left[\frac{\pi}{2} \frac{\ln(4d_r^+/9)}{\ln 40} \right], & 9/4 \leq d_r^+ < 90, \text{ (transitionally rough)}, \\ 1, & 90 \leq d_r^+, \text{ (fully rough)} \end{cases} \quad (16-55)$$

Equation (16-55) is an interpolation formula for B , with B_s and B_r being the well-known integration constants in the log-law profile for hydraulically smooth and rough flows, taken to be 5.2 and 8.5. A slight inconsistency is noted in that Eq. (16-55) presumably is based on $\kappa = 0.41$, whereas the standard $k-\epsilon$ model constants are based on $\kappa = 0.43$.

This single-layer wall-function approach can be extended by the use of multilayer models, in which different functional forms for k , ϵ , and V_w are assumed in each layer (e.g., in Cheong and Xue 1997). In Eq. (16-54), u_* is to be determined as part of the solution, but this is accomplished via a momentum balance in the near-wall region. To be consistent with this equilibrium model, the nearest boundary point in the computational grid should be placed in a region where the log-law is presumed valid, e.g., $z_w u_* / v \gtrsim 40$ for a smooth wall or $z_w / d_r \gtrsim 2$ for a rough wall, though mild violations of these conditions do not seem to affect results significantly.

Several questions arise in the application of this traditional approach to treating the near-wall region. The log-law profile does not necessarily always hold in wall-bounded flows, e.g., in the recirculation region of separated flows of interest in flows over bed-forms. Measurements in smooth-walled backward-facing-step flows (Devenport and Sutton 1991; Jovic and Driver 1995), confirmed by direct numerical simulations (Le et al. 1997), also show that when the log-law profile first becomes reestablished, the associated constant is not necessarily the same as that (B_s) in an equilibrium wall-bounded flow. From the particular perspective of sediment-transport problems, z_w may be located in a high-concentration region, where particle-particle interactions are strong, and Eq. (16-54) can hardly be justified. Even if this is avoided by a judicious choice of z_w , the classic question of the appropriateness of the log law and/or the constancy of κ in a sediment-laden flow, discussed previously in Section 16-4.2.3, reappears. A related issue is the appropriate choice of wall roughness height, d_r . On a fixed (nonerodible) nominally plane bed characterized by homogeneous roughness in a flow without sediment, the choice of d_r is straightforward, namely, the equivalent median sand size, d_{50} . Experimental evidence indicates that, even on a nominally plane bed, flow resistance is increased in a sediment-transporting flow compared to an equivalent fixed-bed clear-water flow. While the deviation from the classic log-law profile may have contributed significantly to this increased flow resistance (Lyn 1991), an interpretation or parameterization in terms of an effective roughness height much larger than d_{50} is widely accepted in practice. Van Rijn (1982) listed six widely varying prescriptions for the effective roughness height for flow over plane alluvial beds, finally recommending an average value of $3d_{90}$ (see also Chapter 2). An alternative approach (Smith and McLean 1977; Dietrich 1982; Wiberg and Rubin 1989; see also Chapter 2), better

known in coastal and oceanographical applications and in some respects more physically based, proposes a roughness height parameter that may be interpreted in terms of a saltation height, and hence may vary with both particle and flow parameters. The difficulties become more acute when bed forms are present and the details of the bed geometry are not simulated. In this case, not only must an effective roughness height including the form resistance of bed forms be given, the choice of the level at which the flow boundary conditions are to be imposed also becomes much more problematic. Although crude specifications, e.g., the van Rijn (1984c) proposal used by Wu et al. (2000), are available, these leave much to be desired.

In the turbulence-modeling literature, the development of low-Reynolds-number corrections to the standard $k-\epsilon$ model, primarily with the aim of obviating the use of wall functions, has attracted much attention (Lauder 1984, 1996; Patel et al., 1985; Chen and Jaw 1998; Wilcox 1998). Here, low Reynolds number refers to the near-wall flow, where the local Reynolds number, based on the distance to a wall, becomes small, indicative of the increasing importance of viscous effects. Because of the complications noted above in sediment-transport problems, the advantages of such a more sophisticated treatment of the boundary becomes debatable.

16.4.5.2 Boundary Conditions for the Sediment Equation The condition on the suspended sediment concentration, \bar{c} , at the free surface is invariably a no-flux condition; in contrast, the condition at the bed or the near-bed region remains a vexing problem. In a manner similar to the wall-function approach to the flow boundary conditions, the bottom boundary condition for sediment is imposed at a level above the bed. This is already familiar from the traditional Ippen-Rouse profile, for which the boundary condition is usually applied at a reference level above the bed, $z = z_b$ (see Chapter 2). An “equilibrium” concentration condition,

$$\bar{c}|_{z=z_b} = \bar{c}_{\text{eq}} \quad (16-56)$$

has often been chosen (e.g., Li and Davies 1996; Olsen and Kjellesvig 1999), where an equation similar to that which might be traditionally used to close the Ippen-Rouse profile would be used for \bar{c}_{eq} . Alternatively, a net vertical sediment flux per unit area, $J_s|_b$, might be defined at $z = z_b$:

$$J_s|_b = w_s(E_s - \bar{c}_b) \quad (16-57)$$

where

E_s = entrainment concentration and
 \bar{c}_b = local concentration at $z = z_b$.

With w_s known and \bar{c}_b part of the solution for \bar{c} , the only quantity to be externally specified is the entrainment concentration, E_s . Somewhat similarly to the treatment of flow quantities, a local-equilibrium hypothesis can be motivated in which the flow entrains as much as it possibly can (Celik and Rodi 1988), such that $E_s = \bar{c}_{eq}$, for which, as noted already, several prescriptions are available. A condition essentially equivalent to Eq. (16-57) can be expressed as a diffusive-flux condition (e.g., Murray et al. 1991) in which the combination $w_s E_s$ is termed a pickup function, which is then empirically obtained (e.g., van Rijn 1984a). Other variants of Eq. (16-57) and their practical implementation are discussed in Chapter 15. A somewhat different formulation has been adopted in unsteady sediment transport in coastal engineering applications (e.g., Hagatun and Eidsvik 1986; Davies et al. 1997; Savioli and Justesen 1997b) in which

$$\bar{c}|_{z=z_b} = \max(\bar{c}_{eq}, \bar{c}_{ws}) \quad (16-58)$$

where

\bar{c}_{eq} = equilibrium bed concentration associated with the time-varying ('instantaneous') bed shear stress, whereas

\bar{c}_{ws} = concentration if only a settling flux (i.e., independent of the bed shear stress) is imposed.

Equation (16-58) aims to model a lag between settling and entrainment, such that the suspension is not always in equilibrium with the time-varying bed stress, e.g., during periods of small bed shear stress, when settling might dominate. This can also be modeled in Eq. (16-57), and so the advantage of Eq. (16-58) compared to Eq. (16-57) is not clear. Savioli and Justesen (1997b) suggested that \bar{c}_{ws} is not only due to a settling flux, but also affected by turbulent diffusion; details were, however, not given, and some tuning was found necessary.

The question remains at what level this "bottom" boundary condition is to be imposed. As may also be said of the flow boundary conditions, this level should be located at or possibly above the lower limit of the applicability of the field equations (in this case, the advection-diffusion for sediment, Eq. (16-7)), but this remains controversial. The traditional bed-load formulae proposed in the sediment-transport literature, e.g., for a reference or equilibrium concentration, have been calibrated at specific levels, which have not necessarily been chosen with the needs of modern computational fluid dynamics or turbulence models in mind. For example, for flows over plane beds, the classic Einstein total-load model specifies the lower limit of the suspended load at $z_b = 2d_{50}$, with $\bar{c}|_{z=z_b}$ taken from the Einstein bed-load model (see Chapter 2). On the other hand, $z_b = 2d_{50}$ may not be consistent with the local equilibrium model assumed in the flow boundary conditions, or even with the validity of the

field equations. The reference level for the bottom concentration boundary condition need not be located at the same level as the flow boundary conditions (Wu et al. 2000), but the two types of boundary conditions must be formulated in a consistent manner, which may place constraints on the near-bottom grid.

Bed forms complicate the issue of boundary conditions. If individual bed forms are modeled, then conditions similar to Eq. (16-57) (or even Eq. (16-56)) could conceivably be imposed, though the local equilibrium assumption (and hence \bar{c}_{eq}) would be difficult to justify in the vicinity of the separated flow region. In all fairness, however, such an approach may be said to be equally justified (or unjustified) as the log-law velocity profile wall-function model imposed on the flow. If, as in most practical computations, individual bed forms are *not* modeled and hence details of the near-bed flow are sacrificed for simplicity, then, if Eq. (16-57) or Eq. (16-56) is imposed, then these conditions should be interpreted cautiously because, when a fictitious plane bed is assumed, they implicitly invoke spatial averaging. The application of equations for \bar{c}_{eq} based on plane-bed flows is thus rather questionable, and alternative specifications of \bar{c}_{eq} based on flows over bed forms, which might vary sensitively with bedform characteristics, should be considered. The fictitious level at which the sediment boundary condition is to be imposed becomes even more difficult to specify in this case.

16.4.5.3 Bed-Load Transport and Erodible-Bed Modeling If the total load is of interest, or if a mobile erodible bed is to be modeled, then a bed-load model is necessary. In the present context, the bed-load region may be defined as that below the level at which the bottom sediment boundary condition is imposed. The turbulence model and the flow and transport computations discussed above are directly concerned only with suspended load, and, in most if not all models, only indirectly affect bed-load transport through the estimate of the bed shear stress, $\bar{\tau}_b$. Conventional bed-load formulae in most models were developed for use in problems where only bulk quantities such as $\bar{\tau}_b$ were available. An interesting attempt to incorporate information about turbulence characteristics into bed-load models has been reported by Mendoza and Shen (1988). For flow models using wall functions (Eq. (16-54)), the turbulence quantities, k_w and ϵ_w , are defined in terms of $\bar{\tau}_b$, and so, unless z_b is chosen to be significantly higher than z_w , the turbulence model will still only affect bed load through $\bar{\tau}_b$.

For modeling of the erodible bed, a conservation equation for the overall bed-material load, including the effect of deformation and temporal evolution of the bed, is formulated, typically in the form of an Exner equation (see Chapter 2 and particularly Chapter 15 for an extensive discussion) relating changes in bed elevation to spatial variations in total load. Alternatively, because the suspended load is presumably already modeled (e.g., by Eq. (16-7)), a bed-load conservation equation can be formulated. A simple form of such an equation can be expressed as

$$\begin{aligned} \frac{\partial}{\partial t} [(1-p)z_{\text{bed}} + (\bar{c}|_{z=z_b} z b)] \\ + \frac{\partial Q_{sbx}}{\partial x} + \frac{\partial Q_{sby}}{\partial y} = - J_{s|b} \end{aligned} \quad (16-59)$$

where

- p = porosity of the bed;
- z_{bed} = elevation of the bed;
- z = height measured from the local bed elevation, such that z_b is the thickness of the bed-load layer; and
- Q_{sbx} and Q_{sby} = volumetric sediment flux or discharge in the bed-load layer in the Cartesian coordinate directions x and y .

The sediment concentration in the bed-load layer has been assumed constant in Eq. (16-59) with a value equal to $\bar{c}|_{z=z_b}$. This storage term involving $\bar{c}|_{z=z_b}$ is often omitted as being negligible compared to the transport terms involving Q_{sbx} and Q_{sby} . Equation (16-59) can be considered an equation for the unknown z_{bed} , but involves Q_{sbx} and Q_{sby} , which need to be specified in terms of known quantities. A local-equilibrium assumption is usually made, wherein these are related to traditional bed-load transport functions, incorporating appropriate coordinate transformations (Wu et al. 2000). More sophisticated erodible-bed models, such as those that attempt to include nonequilibrium effects (Armanini and di Silvio 1998) have been proposed in the wider sediment-transport context. Similarly, the very practical problem of modeling the exchange of heterogeneous sediment between the bed and the flow is not addressed but receives extensive attention in Chapter 15. At the present stage of model development, these issues are only indirectly affected by the turbulence model and will not be dealt with further here.

Example. For the horizontally homogeneous unsteady case, the complete $k-\epsilon$ -model system of equations, including buoyancy effects only in the k -equation but neglecting viscous diffusion, may be written as

$$\frac{\partial \bar{u}}{\partial t} = \frac{1}{\rho} \frac{\partial \bar{p}}{\partial x} + \frac{\partial}{\partial z} \left(v_t \frac{\partial \bar{u}}{\partial z} \right) \quad (16-60a)$$

$$\begin{aligned} \frac{\partial k}{\partial t} = \frac{\partial}{\partial z} \left(\frac{v_t}{\sigma_k} \frac{\partial k}{\partial z} \right) + v_t \left(\frac{\partial \bar{u}}{\partial z} \right)^2 \\ + g(s-1) \left[\frac{v_t}{(\sigma_t)_s} \frac{\partial \bar{c}}{\partial z} \right] - \epsilon \end{aligned} \quad (16-60b)$$

$$\begin{aligned} \frac{\partial \epsilon}{\partial t} = \frac{\partial}{\partial z} \left(\frac{v_t}{\sigma_\epsilon} \frac{\partial \epsilon}{\partial z} \right) \\ + c_{1\epsilon} \frac{\epsilon}{k} \left[vt \left(\frac{\partial \bar{u}}{\partial z} \right)^2 \right] - c_{2\epsilon} \frac{\epsilon^2}{k} \end{aligned} \quad (16-60c)$$

$$\frac{\partial \bar{c}}{\partial t} = \frac{\partial}{\partial z} \left[\frac{v_t}{(\sigma_t)_s} \frac{\partial \bar{c}}{\partial z} \right] + \frac{\partial (w_s \bar{c})}{\partial z}. \quad (16-60d)$$

Together with the relationship for v_t , Eq. (16-53), and an equation for \bar{p} , the system is closed with four equations in four unknowns, \bar{u} , \bar{c} , k , and ϵ . For an oscillatory flow (further discussed in Section (16-5.4)), \bar{p} would be related to an imposed free-stream velocity by a Bernoulli equation. For a steady mean flow down a plane inclined at an angle θ , the transient terms are zero and the pressure-gradient term can be replaced by a gravitational-force term, $g \sin \theta$.

The results of two $k-\epsilon$ computations, one with and one without buoyancy effects included in the k -equation (but $c_{3\epsilon} = 0$), for the same two steady laboratory flows previously examined with the van Rijn and Smith-McLean models are shown in Fig. (16-6). The boundary conditions imposed were standard (Eqs. (16-54) with the van Rijn value of $d_r = 3d_{90}$, Eq. (16-61), Eq. (16-56) imposed at $z_b = 3d_{90}$, and $(\sigma_t)_s = 1$) for the two computations. Thus, unlike the previous computations with the van Rijn and Smith-McLean models, which "benefited" from the measurements being used as boundary conditions, the present computations are complete predictions. The velocity predictions for the standard $k-\epsilon$ model agree well with measurements in both cases for the outer flow, but a tendency to overestimate velocities closer to the boundary is noted, very apparent for the Lyn data, but also seen in the Barton-Lin data. The flow boundary conditions are the same in the buoyancy-extended model, leading to predictions of larger velocities and smaller concentrations compared to the standard model because of a reduced eddy viscosity/diffusivity. In both cases, this leads to a deterioration in agreement with the velocity data, though the concentration predictions are improved. This does not necessarily imply a virtue or deficiency in the buoyancy-extended $k-\epsilon$ model as such. Much of the credit for the good agreement or blame for the discrepancies should not necessarily be attributed to the turbulence model as such but to the boundary conditions and the choice of model parameters (the choice of d_r and \bar{c}_{ref} and $(\sigma_t)_s$). Viewed from this perspective, the differences between the predictions of the mixing-length models and the two-equation models are not as large as might at first be thought. As already pointed out, for the simple uniform-flow case, the $k-\epsilon$ model reduces to the mixing-length model because of local equilibrium. Thus, a comparison of the two types of models should focus on differences in predicted slopes rather than predicted values because the latter are

directly affected by boundary conditions. Not surprisingly, the predicted slopes of the two types of models are quite similar. The case of uniform flow over a flat bed is perhaps the simplest case of sediment-laden flow, and so is not a particularly stringent test of a turbulence model. Figure (16-6) shows what might be achieved with a $k-\epsilon$ model under the best of circumstances—in more complicated flows, larger discrepancies might be encountered.

16.4.5.4 Free-Surface Conditions The free surface is often treated as a symmetry plane, exactly analogous to the centerline of a pipe, such that, in the absence of wind shear, fluxes across the surface are set to zero. The turbulence in the vicinity of a free surface differs, however, from that in the vicinity of a pipe centerline due to a damping of vertical velocity fluctuations and a consequent flattening of turbulent eddies, somewhat similar to that occurring at a rigid wall. The resulting reduction in length scale has been modeled by imposing a condition on ϵ at the free surface, namely,

$$\epsilon_{fs} = \frac{k_{fs}^{3/2}}{c_{fse} h}, \quad (16-61)$$

where k_{fs} is the turbulent kinetic energy at the free surface and c_{fse} is a constant, with a recommended value of 0.43 (Celik and Rodi 1988; Wu et al. 2000). Equation (16-61) which may be compared with the corresponding condition at the bed, reduces the length scale at the free surface relative to the situation when a simple symmetry condition is imposed. Celik and Rodi (1984, 1988) also proposed a direct reduction in ν_t through a reduction in c_μ by a factor depending on a surface damping function and the ratio ρ/ϵ .

16.4.6 Deficiencies of the Boussinesq Eddy-Viscosity and $k-\epsilon$ Models and Some Alternatives

The weaknesses of the Boussinesq eddy-viscosity (BEVM) and $k-\epsilon$ models are discussed, and several alternative two-equation models developed to remedy some of these weaknesses are described. Because these have not yet been as widely adopted, only a select sample will be discussed here, and only rather briefly. The ϵ -equation, not surprisingly, has been the focus of modeling, either being entirely replaced or modified by additional terms. As noted above, an equation for any generic “length-scale” quantity of the form $k^m L^n$, can form the basis for a two-equation model, and the two models discussed below that differ in form from the $k-\epsilon$ model may be interpreted in terms of particular choices of m and n . The k -equation is usually retained, with either no modification or only such modification as to make it consistent with the new or revised length-scale equation.

16.4.6.1 Weaknesses of the Boussinesq Eddy-Viscosity and $k-\epsilon$ Models It was noted in connection with mixing-length models that nonequilibrium and anisotropic turbulence would cause problems. To a perhaps distressingly large extent, this remains true even when the BEVM model

is coupled with the more sophisticated $k-\epsilon$ model. Like the mixing-length model, the BEVM model was motivated primarily by thin shear flows, and the BEVM model usually performs well in predicting the important fluxes across shear-dominated flows. Fluxes in the other directions may not be so well predicted (Haroutunian and Engelman 1993). Flows in which differences in normal stresses are important, i.e., highly anisotropic flows, will pose difficulties for the standard models. These may include problems where turbulence-generated secondary currents play an important role, e.g., flows in compound channels. When extra strains, such as buoyancy forces, or when rapid changes in strain are imposed, model performance may also deteriorate (Wilcox 1998). As evident from the preceding sections, the effects of buoyancy may be relevant to suspension flows. Even if buoyancy is not accepted as the dominant mechanism for turbulence modification in sediment-laden flows, it may be argued on general physical grounds that the responsible mechanism is related to sedimentation in a gravitational field, and hence is expected to have an anisotropic effect on the flow field.

These deficiencies can be traced to the assumption of isotropy inherent in the BEVM, to the use of only scalar quantities, k and ϵ , to characterize the turbulence, and to the specification of the linear relationship between $\bar{u}'\bar{u}'$ and only the mean strain rate. Because of the extent of model assumptions in the development of the ϵ -equation, it has been the subject of much criticism, with modifications or alternatives often being proposed. As noted previously, the use of wall-functions has also been criticized because they tend to be justified only under fairly limited conditions. From the specific sediment-transport point of view, whether the stratification model and the assumed log-law wall-function model are appropriate remains unclear. Although much has been said of the anisotropic nature of real turbulent flows, the possible anisotropy of diffusive transport of settling particles even in isotropic turbulence should also be mentioned.

16.4.6.2 The $k-\omega$ Model The $k-\omega$ model, associated with Wilcox (and discussed at length in his 1998 book), is perhaps the major alternative to the $k-\epsilon$ model as far as two-equation models for engineering applications are concerned. It is based on an equation for ω , which is interpreted as a frequency scale proportional to ϵ/k , the rate of dissipation per unit turbulent kinetic energy:

$$\begin{aligned} \frac{d\omega}{dt} &= \frac{\partial\omega}{\partial t} + \frac{\partial(\bar{u}_j \omega)}{\partial x_j} \\ &= \frac{\partial}{\partial x_j} \left(\frac{\nu_t}{\sigma_\omega} \frac{\partial\omega}{\partial x_j} \right) + c_{1\omega} \frac{\omega}{k} P_k - c_{2\omega} \omega^2 \end{aligned} \quad (16-62)$$

Whereas the ϵ -equation in the $k-\epsilon$ model may be interpreted as an equation for $k^{3/2} L^{-1}$, i.e., $m = 3/2$ and $n = -1$, the

ω -equation corresponds to an equation for $k^{-1/2} \mathcal{L}$, or $m = -1/2$ and $n = 1$. With the additional model relations

$$\epsilon = c_{kw} k \omega \quad \text{and} \quad v_t = \frac{k}{\omega} \quad (16-63)$$

the $k-\omega$ model is completely specified. Like the $k-\epsilon$ model, there are five closure coefficients, $c_{k\omega} = 0.09$, $c_{1\omega} = 5/9$, $c_{2\omega} = 3/40$, and the two turbulent Schmidt numbers, $\sigma_k = 2 = \sigma_\omega$. A frequently cited advantage of the $k-\omega$ model for wall-bounded flow applications is that, without the need to use wall-functions, integration to the wall is feasible. For the transitionally rough-wall flows of most interest in sediment-transport applications, the boundary conditions to be applied at the bed are the no-slip conditions for the velocity components, together with

$$k = 0, \quad \omega = u_*^2 S_r / v \quad (16-64)$$

where S_r is a parameter, analogous to E_r for the $k-\epsilon$ model (Eq. 16-55), that is correlated with the wall roughness, namely,

$$S_r = \begin{cases} (50/d_r^+)^2, & d_r^+ < 25 \\ 100/d_r^+, & d_r^+ \geq 25. \end{cases} \quad (16-65)$$

With the specification, Eq. (16-65) and boundary conditions, Eq. (16-64) the $k-\omega$ model reproduces the standard log-law for transitionally and fully rough flows for parallel or nearly parallel flows of a homogeneous fluid, such as clear-water boundary-layer or channel flows. Importantly, however, unlike the wall-functions approach, log-law behavior is *not* explicitly imposed on the flow. Yoon and Patel (1996) note that a fine grid close to the wall is necessary because of large spatial gradients. This does not imply that the flow very near the wall is being resolved, because individual roughness elements are not modeled; hence, the results very near the wall must be interpreted cautiously because the solution is only physically meaningful at some distance from the modeled wall. In addition to Wilcox (1998), Patel (1998) discusses the performance of the $k-\omega$ and $k-\epsilon$ models for wall-bounded flows in general, and, for rough walls in particular. Because it avoids explicitly assuming a log-law velocity profile at the wall, it may be advantageous in separated flows where it is known that the log-law profile does not hold in recirculating regions. Nevertheless, in a study of the backward-facing-step flow, Speziale and Thangam (1992) concluded that, at least for this flow, the use of wall functions does not entail major errors in spite of flow separation. The problems peculiar to sediment-transport applications discussed before, such as the appropriate roughness height in sediment-laden flows or dealing with bed forms, not to mention the question of turbulence modification, still need to be addressed. A well-known

weakness of the $k-\omega$ model is its extreme sensitivity to free-stream boundary conditions, and so it should not be applied without modifications to flows with interfaces between turbulent and nonturbulent flows, e.g., boundary-layer flows, free shear flows. For alluvial-channel flows, this should be of little concern, but may require more consideration in the coastal or lacustrine context.

16.4.6.3 The RNG Model Since its introduction by Yakhot and Orszag (1986), the renormalization group (RNG or RG) approach to developing turbulence models has attracted much attention (Speziale and Thangam, 1992; Yakhot and Orszag 1992), as well as skepticism (McComb 1990; Hanjalic 1994; Bradshaw 1997). The standard $k-\epsilon$ model is apparently derived, with only changes in the values of the closure coefficients (see Table 16-2) and, in its latest version, the addition of a term involving the mean strain rate ϵ -equation, namely,

$$G = (G_\epsilon)_{RNG} = - c_\mu \frac{\epsilon^2}{k} \left[\frac{\eta^3 (1 - \eta/\eta_0)}{1 + c_{RNG} \eta^3} \right] \quad (16-66)$$

where $\eta = S k/\epsilon$, and the two additional model constants, $\eta_0 = 4.38$, obtained from an analysis of homogeneous shear flow, and $c_{RNG} = 0.015$, the value of which was chosen to match a von Kármán constant, $\kappa = 0.39$ (a value of $c_{RNG} = 0.012$ would yield $\kappa = 0.4$).

A formidable, even impenetrable theory notwithstanding, the RNG results rely on an asymptotic perturbation argument for a small parameter, but the argument is then applied with a finite (not small) value of that parameter. On one hand, this is similar to the standard procedure of determining the closure constants from simple flows and applying the model to complex flows (see the discussion in Section 16-4-4); on the other hand, the claims to theoretical rigor and superiority vis-à-vis the standard procedure suffer accordingly. Although the RNG approach points to the necessity of an additional term in the ϵ -equation when S is large, the particular form of $(G_\epsilon)_{RNG}$ given in Eq. (16-66) is *not* directly derived from the RNG approach, and constitutes another possible weak point in the RNG model. Because $\eta \propto \sqrt{P_k/\epsilon}$, the additional term, $(G_\epsilon)_{RNG}$, can also be interpreted as $c_{2\epsilon}$ being a function varying with P_k/ϵ rather than being a constant as in the standard $k-\epsilon$ model. This recalls the earlier discussion concerning the possibility of the closure constants being made dependent on dimensionless parameters reflecting deviations from the conditions prevailing in the simple calibration flows. In practice, the RNG $k-\epsilon$ model has led to improved predictions in some flows, particularly those in which massive separation has occurred (Lien and Leschziner 1994; Kim and Patel 2000), but not in others (Hanjalic 1994; Lien and Leschziner 1994). Whether it represents a viable general alternative to the standard $k-\epsilon$ model (or the $k-\omega$ model) remains to be established.

In their usual implementation, both the $k-\omega$ and the RNG version of the $k-\epsilon$ models retain the BEVM assumption, so

that the deficiencies, notably the linear stress-strain rate relationship and the insensitivity to normal stresses and anisotropy stemming from it, still remain. Possible turbulence modulation effects from the presence of particles do not seem to have yet received much, if any, attention in the application of either the $k-\omega$ or the RNG models. Although neither model has been as extensively tested as the conventional $k-\epsilon$ model, their availability in commercial computational fluid dynamics codes will likely stimulate increased use in the future.

16.4.6.4 The Mellor-Yamada (or $k-k\mathcal{L}$ Model) Length-Scale Equation Mellor and Yamada (1982) describe a hierarchy of turbulence closure models ranging from a full second-moment model (level 4) to a local-equilibrium model (level 2). The intermediate level $2\frac{1}{2}$ model is described in the next section. Unlike the $k-\epsilon$ model, Mellor-Yamada models eschew the ϵ -equation in favor of either a simple algebraic specification of the length scale, or more generally, an equation directly for the turbulence length scale, \mathcal{L} or equivalently of a quantity $R = 2k$. Although it can be written for more general flows (Mellor and Herring 1973; Rodi 1987), it is often expressed in a form aimed at boundary-layer applications (Mellor and Yamada 1982):

$$\begin{aligned} \frac{DR}{Dt} &= \frac{\partial R}{\partial t} + \frac{\partial(\bar{u}_j R)}{\partial x_j} \\ &= \frac{\partial}{\partial z} \left[\frac{(v_t)_0}{\sigma_R} \frac{\partial R}{\partial z} \right] + \mathcal{L} c_{1R} [P_k + (G_k)_\rho] \\ &\quad - c_{2R} (2k)^{3/2} \left[1 + c_{3MY} \left(\frac{\mathcal{L}}{\kappa L_z} \right) \right] \end{aligned} \quad (16-67)$$

such that only diffusive transport in the vertical z direction is included. The basic eddy viscosity $(v_t)_0 = (2k)^{1/2}\Lambda$, whereas the length scale, L_z , is in general specified externally by an integral. For boundary-layer flow near a wall, the integral simplifies to $L_z = z$, the distance from the wall. The closure constants are $\sigma_R = 5$, $c_{1R} = 1.8$, $c_{2R} = 0.06$, $c_{3MY} = 1.33$. The last term, $\mathcal{L}/(\kappa L_z)$, is necessary for matching the von Kármán constant in the log-law velocity profile. The dissipation term in the k -equation is $\epsilon = c_{2R}(2k)^{3/2}/\mathcal{L}$. As usual, a wall-functions approach may be applied in imposing conditions at a solid boundary. An interesting feature of Eq. (16-67) is the choice of the coefficient of the buoyancy term, equivalent to $c_{3\epsilon}$ in the $k-\epsilon$ model. The choice of unity, tentatively made by Mellor and Yamada (1982), seems to have become the standard in subsequent work, and has not aroused any debate comparable to that surrounding $c_{3\epsilon}$.

Equation (16-67) falls within the class of models, sometimes termed $k-k\mathcal{L}$ (Wilcox 1998), that began with the work of Rotta (1951), who derived an equation for the integral of the two-point correlation function, which can serve to

define a length-scale. Within the classification of length-scale equations in terms of $k^m \mathcal{L}^n$, Eq. (16-67) has $m = 1$, $n = 1$. Somewhat similar length-scale equations have been applied by Sheng and Villaret (1989) and Huynh Thanh and Temperville (1991) for sediment-transport application. Although widely used in geophysical applications, possibly because of its attention to stratification effects, the superiority of Eq. (16-67) to the ϵ -equation in practical engineering computations is controversial. Speziale (1991), for example, concludes that it does not offer any significant advantages over the standard ϵ -equation.

16.4.7 More Sophisticated Models

For the foreseeable future, practical computations of flows involving sediment transport will be dominated by the standard $k-\epsilon$ model, possibly including buoyancy extensions or other ad hoc corrections, or alternative two-equation models, coupled with the advection-diffusion equation for the sediment concentration, Eq. (16-7). Nevertheless, more advanced models continue to be developed, and some have already found or may eventually find their way into leading-edge practice. The two-phase approach to dealing with suspension flows and possible modifications to the $k-\epsilon$ model is very briefly discussed. Nonlinear $k-\epsilon$ models are examined as a possible solution to modelling effects of anisotropy and extra strains. The present state-of-the-art in turbulence modeling for practical computations lies in second-moment closure models, and so these are briefly outlined, though primarily with the aim of deriving simpler algebraic stress models.

16.4.7.1 Two-Phase Flow Turbulence Models The two-phase nature of a suspension flow presents special problems not only for the modeling of the turbulence, but also for the formulation of basic continuity and momentum equations, and the frequent appeal to the stratification analogy deserves greater scrutiny than it has received. Several two-phase flow descriptions of the sediment-transport problem have been given (Drew 1975; McTigue 1981; Kobayashi and Seo 1985; Lamberti et al. 1991; Greimann et al. 1999), but because they have only considered the simplest case of uniform flat-bed flow, they have typically resorted to simple mixing-length closures. Turbulence modification was either ignored or treated via a stratification analogy. The formulation of general numerical models for turbulent two-phase flows and the fundamental problems of averaging and turbulence closure have been reviewed by Crowe et al. (1996). The two-phase formulation starts with separate continuity and momentum equations for each phase, where correlations modeling the kinematic and dynamic interaction between phases already present closure problems (in addition to the turbulence closure problem), which may not be amenable to the standard BEVM approach (Elghobashi 1994). Elghobashi and Abou-Arab (1983) derived two-phase $k-\epsilon$ equations and proposed appropriate closures, with

applications to particulate jet flows. The exact k -equation is found to consist of 38 terms (this may be compared with the 8 terms in Eq. (16-34)), and rather drastic surgery is required to obtain closure. Interestingly, a buoyancy term does *not* explicitly appear in their formulation, though presumably the effect is implicitly captured in correlations involving the instantaneous slip between the two phases. Because of the abstract nature of the concept of interpenetrating continua, experimental determination of correlations or confirmation of detailed predictions is difficult or even impossible, except possibly in numerical simulations.

The near-bed bed-load region poses additional problems because particle-particle interactions become important or dominant, and a dense-phase (as opposed to a dispersed dilute-phase) flow model is necessary. In a single-phase flow approach based on Eq. (16-7), these problems are entirely avoided by using a bed-load transport model that bridges the immobile bed and the suspended-load region where Eq. (16-7) is applied. It is debatable to what extent the traditional views of turbulence can be applied to this region. The possibility of applying granular-fluid models to deal with this dense-phase region has been explored by a number of investigators (Hanes and Bowen 1985; Lamberti et al. 1991; Villaret and Davies 1995).

Example. Villaret and Davies (1995) reported simulations with a two-phase flow model, presumably a version of that described by Simonin (1991). The model incorporates granular-fluid concepts, suspension-induced buoyancy effects, and a low- R model for the near-wall flow, in a $k-\epsilon$ model framework. Figure 16-7 shows the results, including those from simulations with an enhanced version of the Li-Davies one-equation model discussed previously, including buoyancy effects. All of the cases studied did *not* involve an equilibrium bed. The predictions of both models with respect to the velocity profiles agree quite well with measurements, and are clearly superior to the clear-water velocity profiles (the basis of the standard $k-\epsilon$ wall-functions). The simpler one-equation model seems, however, to perform as well as or only marginally worse than the more sophisticated two-phase $k-\epsilon$ model, at least where experimental evidence is available. Larger discrepancies between concentration predictions and measurements can be seen, and the superiority of one or the other model is not clearly established. The simpler one-equation model did benefit from having a measured concentration as its bottom concentration boundary condition, whereas only the depth-averaged concentration was imposed on the two-phase flow model. The comparison suggests that, even for this simplest case of sediment-laden flows, even a very sophisticated model may not necessarily lead to significantly better predictions. Further, improved boundary conditions may play a more important role in better predictions than additional sophistication in turbulence modeling, at least at the present stage of model development.

Hsu et al. (2003) reported predictions using a dilute two-phase-flow $k-\epsilon$ model, which did not include either dense-phase or, at least explicitly, stratification effects, and

so provides a contrast to the two-phase-flow model described in Villaret and Davies (1995). An approximate theoretical solution that agreed with a numerical solution of the resulting model near the bed suggested that effects on the velocity (and also the concentration) profile are $O(\bar{c})$. This seems too weak in general to explain observations, and may indicate that dense-phase and/or stratification effects need to be included.

16.4.7.2 Nonlinear $k-\epsilon$ Models The Boussinesq eddy viscosity model (Eq. (16-14)), relating the Reynolds stress *linearly* to the mean strain rate, analogously to that applied to a Newtonian fluid in laminar flows, is considered one of the major weaknesses of standard turbulence models. Nonlinear constitutive models, analogous to considering turbulent flow as a non-Newtonian fluid, have been proposed as a relatively simple remedy (Speziale 1987, 1996; Launder 1996; Wilcox 1998). An example is a model developed by Craft et al. (1993), which assumes that

$$\begin{aligned} -\overline{\dot{u}_i \dot{u}_j} &= \left(v_t S_{ij}^* - \frac{2}{3} \delta_{ij} k \right) \\ &\quad - v_t \frac{k}{7} \left[c_{1n} \left(S_{ik}^* S_{kj}^* - \frac{1}{3} S_{kl}^* S_{ij}^* \delta_{ij} \right) \right. \\ &\quad + c_{2n} \left(\Omega_{ik} S_{kj}^* + \Omega_{jk} S_{ki}^* \right) \\ &\quad \left. + c_{3n} \left(\Omega_{ik} \Omega_{jk} - \frac{1}{3} \Omega_{ik} \Omega_{lk} \delta_{ij} \right) \right] \\ &\quad - c_\mu v_t \frac{k^2}{7^2} \left[c_{4n} \left(S_{ki}^* \Omega_{lj} + S_{kj}^* \Omega_{li} \right) S_{kl}^* + c_{5n} \right. \\ &\quad \times \left(\Omega_{il} \Omega_{lm} S_{mj}^* + S_{il}^* \Omega_{lm} \Omega_{mj} - \frac{2}{3} S_{lm}^* \Omega_{mn} \Omega_{nl} \delta_{ij} \right) \\ &\quad \left. + c_{6n} S_{ij}^* S_{kl}^* S_{kl}^* + c_{7n} S_{ij}^* \Omega_{kl} \Omega_{kl} \right]. \end{aligned} \quad (16-68)$$

The first bracketed group of terms is the standard BEVM, whereas the second and third bracketed groups are respectively quadratic and cubic terms in $S_{ij}^* = 2S_{ij}$ and a rotation tensor, $\Omega_{ij} = \partial \tilde{u}_i / \partial x_j - \partial \tilde{u}_j / \partial x_i$. There are seven additional closure coefficients, c_{1n}, \dots, c_{7n} . Although the nonlinear constitutive relationship is much more complicated than the Boussinesq model, such a generalization is computationally attractive, because it still permits the use of two-equation models. Apsley et al. (1997) have argued that the early quadratic model of Speziale (1987), although sensitive to anisotropy, is insensitive to flow curvature, which requires at least a cubic model. They also point out that the physical interpretation of nonlinear models that are postulated solely on a formal basis is tenuous, and that the closure coefficient in the viscosity relationship, c_μ , will in general need to be made a function of the strain-rate and rotation tensors. An alternative, more physically based approach to developing nonlinear models simplifies second-moment closure models discussed below.

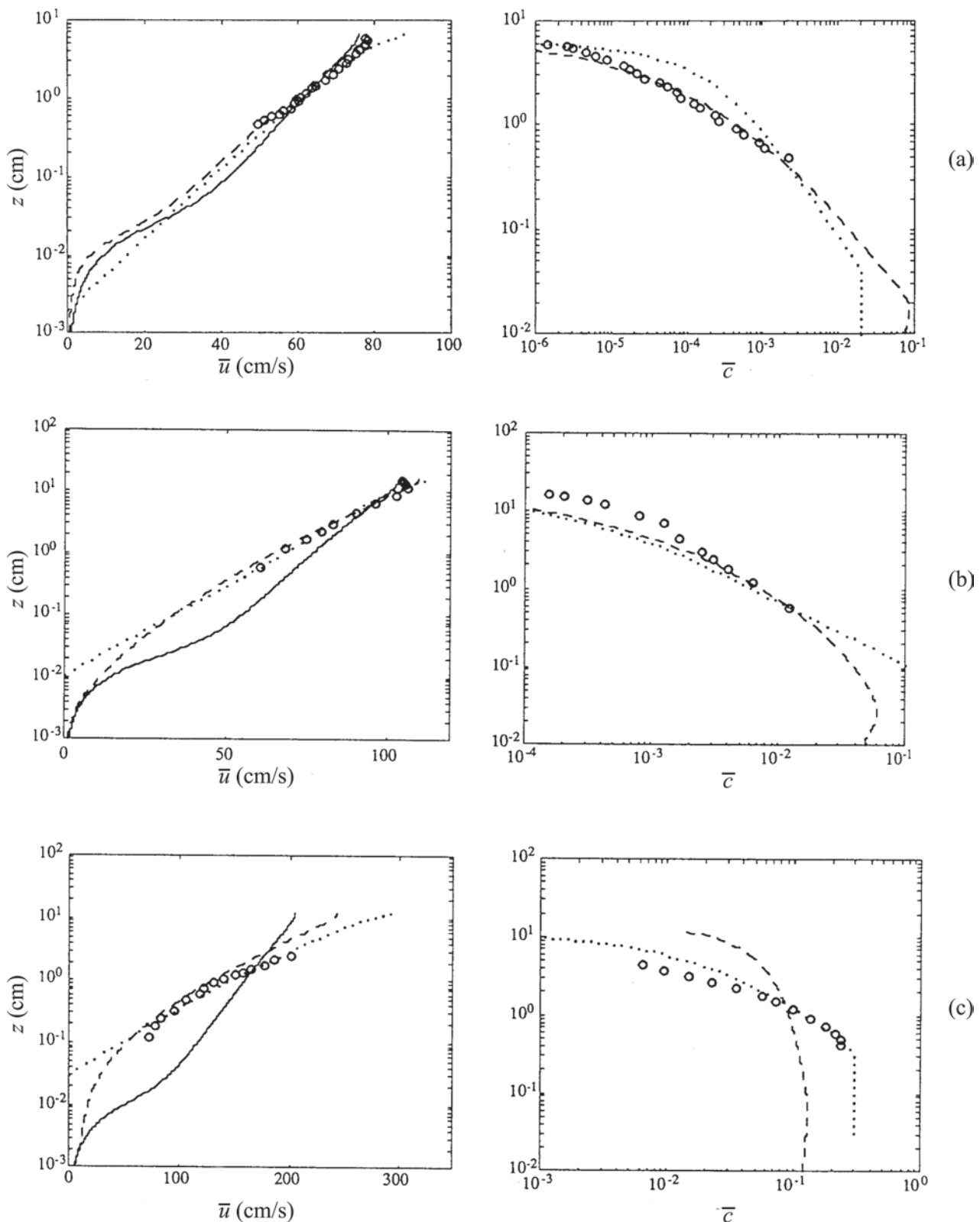


Fig. 16-7. Comparison of velocity (\bar{u}) and concentration (\bar{c}) predictions (Villaret and Davies 1995) and measurements of uniform-flow case: (a) data of Lyn (1988), (b) data of Coleman (1981), and (c) data of Einstein and Chien (1955). Symbols: measurements, — : clear-water prediction; - - : two-phase $k-\epsilon$ model prediction; . . . : one-equation model prediction.

16.4.7.3 Second-Moment Closure and Algebraic Stress Models The original problem posed by the Reynolds averaging of the Navier-Stokes equations is the appearance of unknown Reynolds stress terms. Whereas eddy-viscosity models attempt to relate these unknown terms to the mean fields via constitutive equations and thus resolve the turbulence closure problem, a more direct approach might be considered, namely directly deriving equations for the elements of the Reynolds stress tensor. This approach leads to higher-order correlation terms, which, however, could then be subjected to the type of modeling applied to the lower-order terms in eddy-viscosity models. This forms the theoretical basis of Reynolds stress (RS) or second-moment closure (SMC) models. The equation for $\overline{u'_i u'_j}$ can be written as

$$\begin{aligned} \frac{D(\overline{u'_i u'_j})}{Dt} &= \frac{\partial(\overline{u'_i u'_j})}{\partial t} + \frac{\partial[\overline{u_l}(\overline{u'_i u'_j})]}{\partial x_l} \\ &= P_{ij} + G_{ij} + D_{ij} + \Pi_{ij} - \epsilon_{ij} \end{aligned} \quad (16-69)$$

where D_{ij} denotes diffusive transport terms,

$$P_{ij} = -\overline{u'_i u'_l} \frac{\partial \bar{u}_j}{\partial x_l} - \overline{u'_j u'_l} \frac{\partial \bar{u}_i}{\partial x_l} \quad (16-70)$$

represents the production of $\overline{u'_i u'_j}$ through interaction of the turbulence with the mean strain rate, G_{ij} the production of $\overline{u'_i u'_j}$ by other forces or strains, Π_{ij} the pressure-strain term, and ϵ_{ij} the term representing the viscous dissipation of the Reynolds stresses. If the effects of buoyancy are modeled, then

$$\begin{aligned} (G_p)_{ij} &= \frac{1}{\rho_{ref}} (g_i \overline{p' u'_j} + g_j \overline{p' u'_i}) \\ &= (s-1)(g_i \overline{c' u'_j} + g_j \overline{c' u'_i}) \end{aligned} \quad (16-71)$$

where the second equality invokes the suspension density relation. Besides the basic sediment conservation equation, transport equations for the second-moment quantities involving c' such as $\overline{u'_i c'}$ and $\overline{c'^2}$, are also formulated. The resemblance between Eq. (16-69) and the exact equation for k is not coincidental, since the latter can be derived from the former.

Because the RS model approach solves for each element of the Reynolds stress tensor, and not simply k , anisotropic flow features *should* be better handled. RS models also have the advantage that the production terms, both from shear and from extra strains, are exact, and so flow aspects strongly influenced by such extra strains should be more rationally modeled. This does not of course necessarily extend in a straightforward way to particulate flows, for which the basic models for the momentum equations are still being debated,

though, if the stratification analogy is accepted, the effects of simple stratification should be better modeled. In practice, as will be seen in the next section, the promise of RS models has not yet been satisfactorily fulfilled (see also the general discussion of Bradshaw 1997 and that of Patel 1997 in the context of curvature effects). Apart from the difficulty of modeling the pressure-strain term, Π_{ij} , conventional RS models still use (1) the problematic ϵ -equation, (2) k^2/ϵ for the effective diffusion coefficient for diffusive transport terms, and (3) wall-functions at solid boundaries. Several computations using RS models will be reviewed in Section 16.5.

Although the full second-moment closure offers the promise of resolving some of the well-known problems of two-equation models, the computational demands are much more severe. If only the flow is considered, up to six additional partial differential equations must be solved for a three-dimensional simulation, and if the transport of a scalar, such as a sediment concentration, is also desired, then this may add up to four more partial differential equations, over and above what a two-equation model requires. A further practical problem, especially with sediment transport, is the specification of boundary conditions. The difficulties involved in specifying a bottom boundary condition for c have been discussed already; for an RS model, additional conditions on other second-moment quantities involving c must also be imposed. For such reasons, an intermediate approach may be sought in which Eq. (16-69) is simplified, such that $\overline{u'_i u'_j}$ may ultimately be specified algebraically without the need for solution of partial differential equations. Various algebraic stress (AS) models can be obtained depending on the simplifying assumptions made.

The simplest model makes a local equilibrium assumption in which transport terms in Eq. (16-69) are neglected, and $\overline{u'_i u'_j}$ is determined from the equation

$$P_{ij} + G_{ij} + \Pi_{ij} - \epsilon_{ij} = 0. \quad (16-72)$$

This is the basis of the well-known Mellor-Yamada level $2\frac{1}{2}$ model (Mellor and Yamada 1982), widely used in ocean modeling and more sporadically in hydraulic and coastal engineering (Blumberg et al. 1992; Davies et al. 1997). A feature of this model, absent in the standard or buoyancy-extended $k-\epsilon$ models, but common to AS models including AS $k-\epsilon$ models, is that the closure coefficients (such as c_μ in $k-\epsilon$ models and the stability functions S_M in Mellor-Yamada models) associated with the effective eddy diffusivities for momentum and for buoyancy depend on local dimensionless parameters, such as a gradient Richardson number. Comparisons of the predictions of the Mellor-Yamada level $2\frac{1}{2}$ model and other models have been made by Rodi (1987), and more recently by Burchard and Baumert (1995) and Baumert and Peters (2000), for stratified flows. A variant of the Mellor-Yamada level $2\frac{1}{2}$ model was used by Sheng and Villaret (1989) to study the effect of sediment-induced stratification on erosion of cohesive sediments. Although

the results showed that such stratification could significantly affect erosion, detailed comparisons of flow predictions with experimental data were not given.

The AS model $k-\epsilon$ due to Rodi (1976; 1993) assumes that the sum of the history and transport terms for $\overline{u'_i u'_j}$ is proportional to the corresponding terms for k , with the proportionality factor being $u'_i u'_j/k$, which is not constant. The resulting specification for $\overline{u'_i u'_j}$ can be written as

$$\overline{u'_i u'_j} = k \left[\frac{2}{3} \delta_{ij} + \frac{(1-c_{1A})\{P_{ij} - (2/3)\delta_{ij}P_k\} + (1-c_{2A})\{G_{ij} - (2/3)\delta_{ij}G_k\}}{P_k + G_k - (1-c_{3A})\epsilon} \right] \quad (16-73)$$

with the three additional closure coefficients c_{1A} , c_{2A} , c_{3A} . AS models share some similarities with nonlinear eddy viscosity models, and may be interpreted as a special class of nonlinear models for $\overline{u'_i u'_j}$. Lien and Leschinzer (1994) have argued that, being based on simplifications of the full RS models, they have a stronger physical basis than general nonlinear models in which the relationship between stress and stress is only formally postulated. Mendoza and Shen (1990) applied this model in a study of clear-water flow over nonerodible dunes, and some results are given in Section 16.5.1.

From a similar though rather more involved analysis, involving a number of additional approximations, an analogous specification for concentration flux term, $\overline{u'_i c'}$ can be given,

$$-\overline{u'_i c'} = \frac{k}{\epsilon} \left[\frac{\overline{u'_i u'_j} \left(\frac{\partial \bar{c}}{\partial x_j} \right) + (1-c_{2c}) \overline{u'_i c'} \left\{ \left(\frac{\partial \bar{u}_i}{\partial x_j} \right) - 2c_{3c}(k/\epsilon) g_j (s-1) \left(\frac{\partial \bar{c}}{\partial x_j} \right) \right\}}{c_{1c} + \{P_k + G_k - \epsilon\}/2\epsilon} \right] \quad (16-74)$$

with additional constants, c_{1c} , c_{2c} , and c_{3c} . Launder (1996) notes that, in wall-bounded flows where transport effects are not important, AS models yield results similar to RS models (which does not necessarily mean correct results) for $\approx 60\%$ of the computational effort, but warns that the performance in free turbulent flows is much less satisfactory. As with other aspects of stratified-flow models, the values proposed in the literature for c_{1c} , c_{2c} , and c_{3c} (e.g., Launder 1984; Rodi 1993; Chen and Jaw 1998) have been based on data from thermally stratified flows; to what extent, if at all, these are applicable to sediment-laden flows is still an open question. Velocity-sediment-concentration correlations are rather ill-defined experimentally, and, in any case, extremely difficult to measure.

Example. For a steady uniform plane flow, the algebraic stress model for the flow only (excluding buoyancy effects) can be expressed as

$$0 = g \sin \theta + \frac{\partial (-\overline{u' w'})}{\partial z} \quad (16-75a)$$

$$0 = \frac{\partial}{\partial z} \left(\frac{v_t}{\sigma_k} \frac{\partial k}{\partial z} \right) - \overline{u' w'} \frac{\partial \bar{u}}{\partial z} - \epsilon \quad (16-75b)$$

$$0 = \frac{\partial}{\partial z} \left(\frac{v_t}{\sigma_\epsilon} \frac{\partial \epsilon}{\partial z} \right) + c_{1\epsilon} \frac{\epsilon}{k} \left(-\overline{u' w'} \frac{\partial \bar{u}}{\partial z} \right) - c_{2\epsilon} \frac{\epsilon^2}{k} \quad (16-75c)$$

$$\overline{u'^2} = \frac{2}{3} k \left[1 + \frac{2(1-c_{1A}) \{ -\overline{u' w'} (\partial \bar{u} / \partial z) \}}{-\overline{u' w'} (\partial \bar{u} / \partial z) - (1-c_{3A})\epsilon} \right] \quad (16-75d)$$

$$\overline{v'^2} = \frac{2}{3} k \left[1 - \frac{(1-c_{1A}) \{ -\overline{u' w'} (\partial \bar{u} / \partial z) \}}{-\overline{u' w'} (\partial \bar{u} / \partial z) - (1-c_{3A})\epsilon} \right] \quad (16-75e)$$

$$\overline{w'^2} = \frac{2}{3} k \left[1 - \frac{(1-c_{1A}) \{ -\overline{u' w'} (\partial \bar{u} / \partial z) \}}{-\overline{u' w'} (\partial \bar{u} / \partial z) - (1-c_{3A})\epsilon} \right] \quad (16-75f)$$

$$\overline{u' w'} = \frac{(1-c_{1A})k \{ -\overline{w'^2} (\partial \bar{u} / \partial z) \}}{-\overline{u' w'} (\partial \bar{u} / \partial z) - (1-c_{3A})\epsilon} \quad (16-75g)$$

Again, with the v_t -relationship, Eq. (16-53), the system is closed, with seven equations for the seven unknowns, \bar{u} , k , ϵ , and the four nonzero components of the Reynolds stress tensor, $\overline{u'^2}$, $\overline{v'^2}$, $\overline{w'^2}$, and $\overline{u' w'}$. That the algebraic stress model can reflect anisotropy is seen in the difference between the expression for $\overline{u'^2}$ and $\overline{w'^2}$, with the latter being smaller, as is experimentally observed. Interestingly, $\overline{u'^2}$ and $\overline{w'^2}$ are predicted to be equal, which does not agree with measurements, which indicate that $\overline{u'^2} > \overline{w'^2}$. This incorrect behavior is also produced by the Mellor-Yamada level 2½ model (Mellor and Yamada 1982). The sum of the normal stresses is also seen to yield $2k$, as should be the case. Equation (16-75g) can also be expressed in a form consistent with a BEVM, i.e., $-\overline{u' w'} = c_\mu (k^2/\epsilon) (\partial \bar{u} / \partial z)$, with, however, c_μ being a function of P/ϵ (Rodi 1993), a characteristic of AS models wherein the model constants of the standard $k-\epsilon$ model are found to vary with local parameters, such as P/ϵ or Ri_f .

16.5 APPLICATIONS OF TURBULENCE MODELS TO PROBLEMS RELATED TO SEDIMENT TRANSPORT

In this section, six applications relevant to sediment transport are described in rather more detail. The limited number

of applications necessarily reflect the biases and interests of the author, though studies were chosen to illustrate the capabilities/limitations of turbulence models to simulate different flow features, and where available, to compare the performance of different models. In the following, unless otherwise specified, simulations were performed with the standard $k-\epsilon$ model without buoyancy, the free surface was not modeled (the rigid-lid approximation was invoked), and the turbulent Schmidt number for sediment, is $(\sigma_t)_s = 1/\beta_s = 1$. Four of the six problems involve the simulation of sediment transport, the cases without sediment being a study of flow over bed-forms and a study of flow within model vegetation, both of which exhibit aspects of some relevance to sediment transport modeling. In four cases, the bed is assumed fixed. Even in those cases with sediment transport and with an erodible bed, it is helpful to examine simulations of the corresponding case without sediment and with a fixed bed to investigate possible model deficiencies in a simpler problem. Without the added complications of sediment and a movable bed, the results for the simpler problem of flow over fixed beds provide an upper bound on what can be achieved by turbulence models, as far as the flow is concerned. The first four involve two-dimensional (one-dimensional when horizontal homogeneity is assumed) simulations, whereas, in the last two, three-dimensional computations were undertaken. In both erodible-bed simulations, an Exner equation is applied to determine the temporal evolution of the bed. Experimental data for comparisons have mainly been obtained in laboratory studies, because these offer more detail and control than can usually be achieved in field studies. In two instances, however, field observations were used for comparison.

Cautionary notes must be sounded in comparing the results of numerical simulation with experimental measurements. This concerns, on the one hand, the effects due entirely to numerical choices, such as mesh resolution and treatment of advection, and those due to the turbulence model. The earliest studies and likely most field studies may be criticized for the use of overly coarse numerical grids, often combined with overly diffusive numerical techniques. By the same token, experimental observations may also be contaminated by extraneous features, such as those due to side walls. In the following, the discussion will not dwell on either numerical or experimental shortcomings, though these should be kept in mind.

16.5.1 Flow Over Bed Forms

Bed forms (a definition sketch is given in Fig. 16-8) are ubiquitous in alluvial channels and have posed some of the most challenging problems for those interested in predicting sediment transport. An understanding of flow over bed forms is a prerequisite for reliable transport predictions. The flow over fixed two-dimensional nonerodible bed forms has been studied experimentally (Raudkivi 1963; van Mierlo and de Ruiter 1988; Lyn 1993; McLean et al. 1994; Bennett

and Best 1995; Cellino and Graf 2000). A comprehensive list of experimental work before 1995 is given in Bennett and Best (1995). Before the discussion of fixed-bed flows without sediment, however, the early work of Mendoza and Shen (1988) should be pointed out, in which not only flow but also sediment transport over dunes were simulated using an RS model, with however somewhat limited comparisons to measurements.

With separation, recirculation, and reattachment as prominent features, this flow shares similarities with the classic backward-facing step flow that has become a benchmark of turbulent flow simulation (for a recent study comparing the performance of various turbulence models, see Lien and Leschziner 1994). The quasi-periodic spatial pattern offers, however, simplifications as well as complications. On the one hand, a suitably defined outer flow may be less sensitive to details of bed geometry, somewhat analogously to the effective sand-grain roughness, which justifies to some extent the frequent approximation of treating the bed as being planer but with increased effective roughness (the main difficulty being that the flow region influenced by the bed forms may constitute a substantial fraction of the flow depth). On the other hand, the reattached flow will not have had sufficient time to approach an equilibrium state before separation occurs again, which contrasts with the typical backward-facing-step flow, used in test cases, in which an equilibrium boundary-layer or fully developed channel flow separates.

The pioneering small-scale experiment of Raudkivi (1963) has been the subject of several studies, including those by Johns et al. (1990) using their one-equation model (see Section 16-4.3.3), by Mendoza and Shen (1990) with the AS model of Rodi (1976), by Sajjadi and Aldridge (1995) with one-equation, $k-\epsilon$ and RS models, and by Cheong and Xue (1997) with a $k-\epsilon$ model with a correction term for streamline curvature. The one-equation models have so far proved to be clearly inadequate, reproducing poorly the recirculation region in the mean velocity profile. The Sajjadi and Aldridge (1995) results with a one-equation model also largely overpredicted the magnitude of $\overline{u'w'}$. Some results of Mendoza and Shen (1990), in what seems to be the only study with an AS model (basically that of Rodi 1974), are shown in Fig. 16-9. Quite good agreement of predicted and measured velocity profiles is obtained, and even $\overline{u'w'}$, as well as bed shear

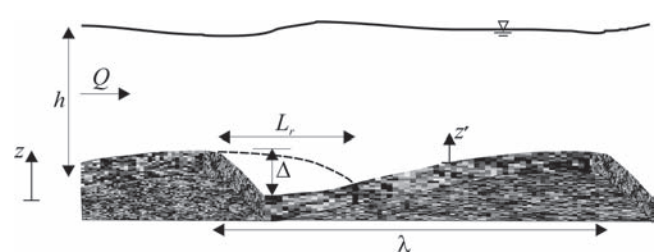


Fig. 16-8. Definition sketch for dune flow.

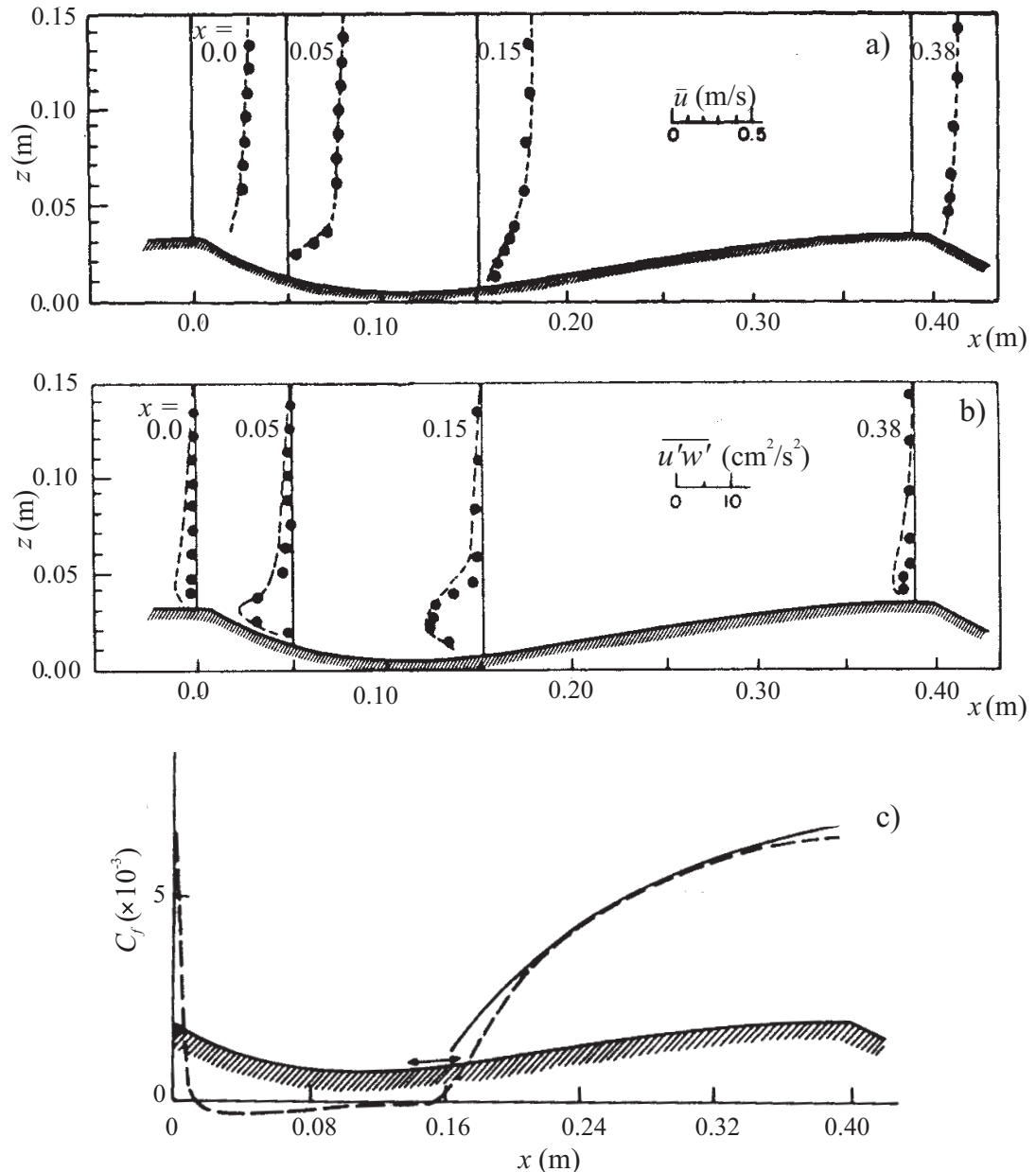


Fig. 16-9. Predictions of \bar{u} , $\overline{u'w'}$, and C_f with an AS $k-\epsilon$ model:—(Mendoza and Shen 1990); symbols and --- (measurements of Raudkivi 1963).

stresses, is quite well reproduced, though some deficiencies are seen, somewhat surprisingly, in regions away from the reattachment point. To a certain extent, this good performance is also found in the Sajjadi and Aldridge (1995) simulations of this case with $k-\epsilon$ and RS models, in contrast to results of more recent studies for other flows, as discussed below. This difference may be explained by the experimental parameters of this particular case, which, as seen in Table 16-3, are quite

distinct from those of the other studies, but might also be due to the limitations of the experimental techniques.

Yoon and Patel (1996) simulated experiment T6 of van Mierlo and de Ruiter (1988) with a $k-\omega$ model, whereas Cheong and Xue (1997) computed the experiment T5 with a $k-\epsilon$ model (Johns et al. (1990) also studied T5 with their one-equation model, but its performance was similar to that already seen for the Raudkivi case). In spite of some

Table 16-3 Experimental Parameters for Flow over Bed Forms

Parameter	Raudkivi (1963; 1966)	van Mierlo de Ruiter (1988)		McLean et al. (Run 2, 1994)
		T5	T6	
λ/h	2.94	6.25	4.76	5
λ/Δ	12.8	20	20	20
L_r/Δ	n.r.	5	5	4.5
$R (10^5)$	0.39	0.99	1.71	0.6
F	0.27	0.25	0.28	0.30
d_r (mm)	0	1.6	1.6	1.5 ^a
Measurement technique	Pitot tube, hot-film	LDV ^b	LDV	LDV

^aAssumed (concrete specified).^bLDV: laser Doppler velocimetry.

differences between the two flows, T5 and T6, the two simulations are compared in Fig. 16-10. A three-layer wall-function approach at the bottom boundary was applied by Cheong and Xue, whereas the $k-\omega$ rough-wall model (Eq. 16-64) was used by Yoon and Patel. The latter report a reattachment length, L_r , in agreement with the measured value, compared to a smaller than measured value (about 20% in the case of the standard $k-\epsilon$ model and 10% in the case of the $k-\epsilon$ model with curvature correction) predicted by Cheong and Xue. The prediction of the bed shear stress, $\bar{\tau}_b$, by the $k-\omega$ model seems notably better, but Yoon and Patel reestimated $\bar{\tau}_b$ from the velocity profile data based on $d_r = 1.6$ mm rather than accepting the values provided by van Mierlo and de Ruiter, which assumed $d_r = 2.6$ mm based on plane-bed measurements. In spite of the good prediction of $\bar{\tau}_b$ and the fair agreement with regards to L_r , the results of Yoon and Patel *underestimated* overall flow resistance by 20%. This is likely associated with the poor performance of *both* models in predicting the peak Reynolds shear stress, $-\overline{u'w'}$, in the separated shear layer, which is markedly underpredicted. This differs from the experience in the backward-facing-step flow problem, where even the standard $k-\epsilon$ model predicts reasonably well the value if not the location of the peak $-\overline{u'w'}$ (Lien and Leschziner 1994), again pointing to subtle but important differences between this flow and the flow over periodic bed forms. An unfortunate characteristic of the van Mierlo and de Ruiter study is that, due to limitations of their optical system, measurements were taken at a location that was relatively far from the flume centerline, such that three-dimensional effects may have played some role.

Because these above studies examined different flows with various numerical grids and techniques, assessing the performance of turbulence models is made difficult. A comparison of four models for the same flow (Run 2 of McLean et al.

1994) with the same grid and numerical solver is given in Fig. 16-11. The computational domain and dune geometry are shown in Fig. 16-11(a). Periodic boundary conditions were imposed at the inlet and outlet, and the rigid-lid approximation was made. The commercial FLUENT (Version 6.0) code was used with second order upwind discretization on a 321×91 (x,y) grid. A roughness height of 1.5 mm was assumed, and an enhanced near-wall model, which, grid permitting and if appropriate, attempts to resolve through to the viscous sublayer by appropriate blending functions and/or a two-layer model, was chosen.

The largest differences in the predicted bed shear stresses (Fig. 16-11(b)) are seen in the region upstream and in the neighborhood of the reattachment point. As seen in other studies, the $k-\epsilon$ model significantly underpredicts L_r , with a slight improvement being achieved with the RNG modification. The L_r predicted by the $k-\omega$ model is approximately the same as that in the earlier Yoon and Patel (1996) study, which, in view of the similarity of the experimental parameters, is not surprising. This, however, exceeds the observed L_r by $\approx 10\%$. The RS model underpredicts L_r by a similar amount, and tends to yield a flatter variation for the reattached internal boundary layer. Because of uncertainties in the estimation of bed shear stress, only a single representative point relatively far from the reattachment point is shown in Fig. 16-11b. All model predictions agree reasonably well with the measurement point in this region.

The results on mean velocity and Reynolds shear stress (Figs. 16-11(c and d)) indicate that the relative performance of a model can be quite variable depending on the region. In general, the standard $k-\epsilon$ model fares the poorest, due in part to and consistent with its worst prediction of the reattachment point. In contrast, the $k-\omega$ and RS models, which

Yoon and Patel (1996)

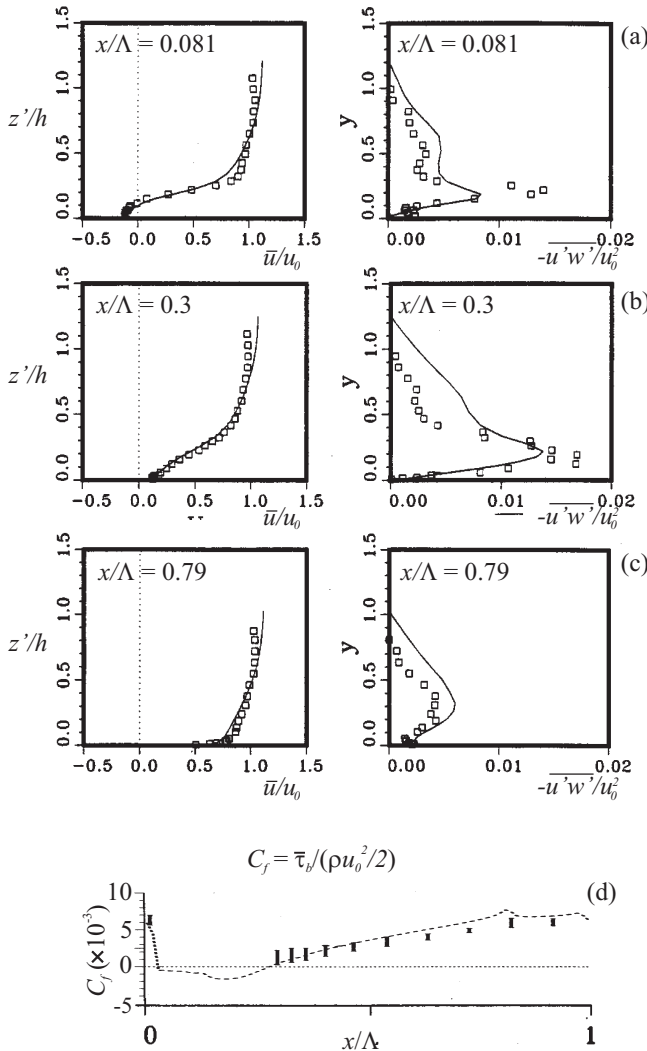
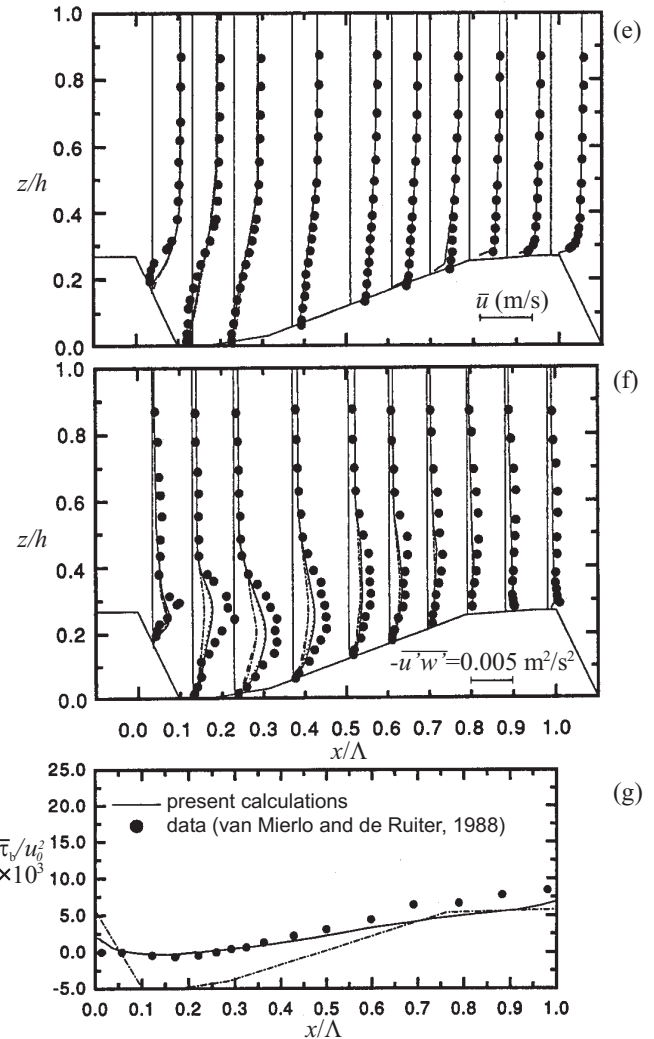


Fig. 16-10. Comparison of $k-\omega$ results (Yoon and Patel 1996; note that z' is measured from the bed) (a), (b), (c), (d) with $k-\epsilon$ model (Cheong and Xue 1997) (e), (f), (g) for van Mierlo and de Ruiter experiments, T6 and T5, respectively.

had best predicted the reattachment point, perform best, but only in the near-bed region. All models substantially underpredicted the peak $-\bar{u}'w'$ associated with the separated shear layer. The RS model consistently performed the best in this regard, but could be in error by more than 50%. This conclusion is consistent with that found in previous studies of the van Mierlo and de Ruiter cases. In the upper half of the flow, however, $-\bar{u}'w'$ was substantially underpredicted by all except the RNG $k-\epsilon$ model. Somewhat surprisingly, the RNG $k-\epsilon$ model did best in the upper half of the flow, particularly with respect to the prediction of $-\bar{u}'w'$. This behavior is rather at odds with previous studies, such as those shown in Fig. 16-10, where even an overprediction of $-\bar{u}'w'$ in this region is seen in the results of Yoon and Patel (1996).

Cheong and Xue (1997)



16.5.2 Flow and Transport in Sedimentation Tanks

Sedimentation tanks are standard equipment in water-treatment plants for the removal of suspended solids. From a broader perspective, lakes and estuaries may be viewed as naturally occurring sedimentation tanks. Turbulent transport in sedimentation tanks or clarifiers may significantly influence their removal performance and hence their reliability. In the present context, this sediment-laden flow presents an example, like turbidity currents, where sediment-induced buoyancy effects may be most clear-cut, and hence where buoyancy extensions to flow and turbulence models may be required. On the other hand, a major simplification compared to the problem of flows in alluvial channels is the negligible

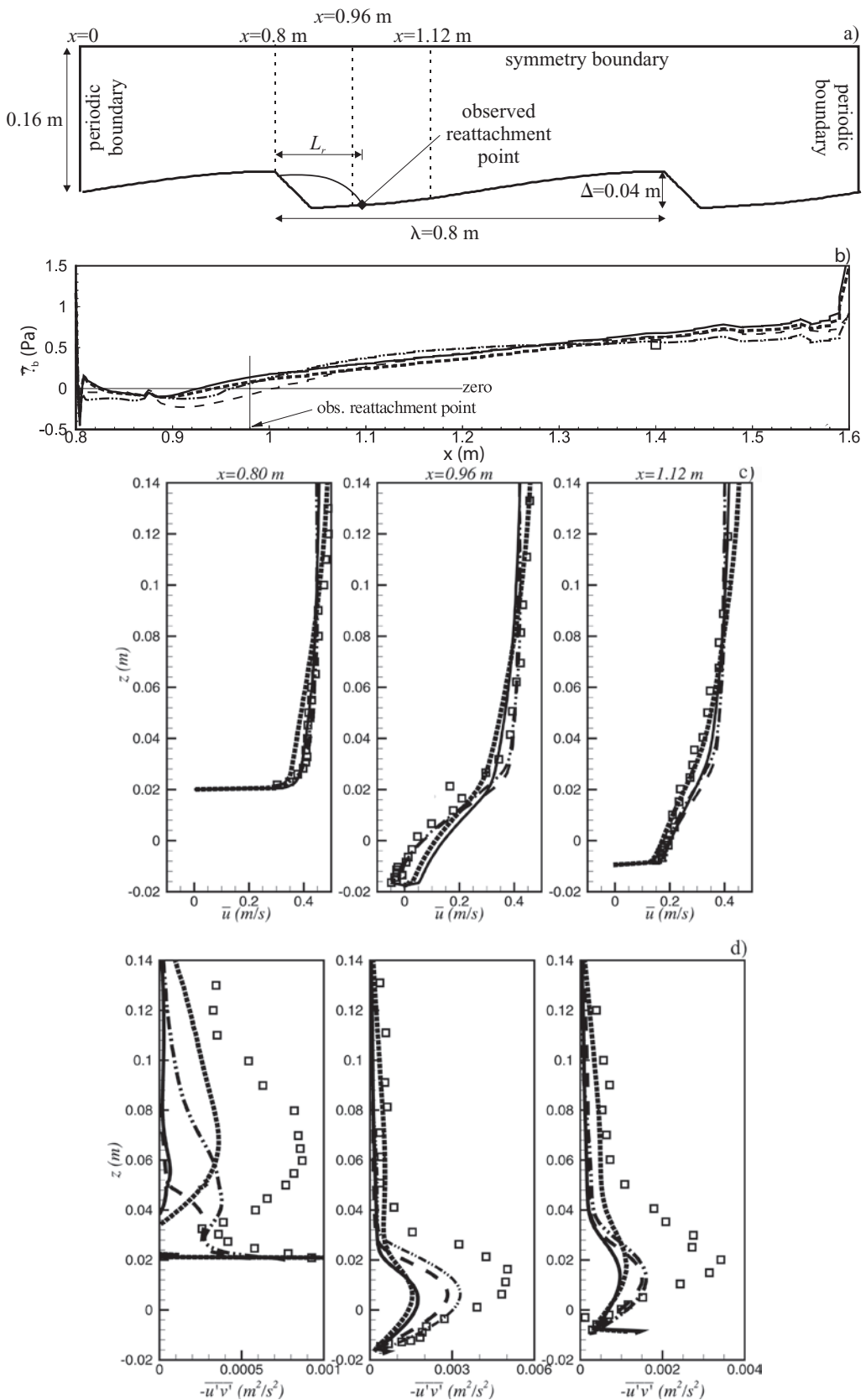


Fig. 16-11. Comparison of four model predictions for the same flow (Run 2 of McLean et al. 1994) using the same numerical grid and scheme: (a) definition sketch, computational domain, and flow geometry; (b) bed shear stress predictions; (c) velocity profiles; (d) Reynolds shear stress profiles; where — is the $k-\epsilon$ model, --- is the $k-\omega$ model, . . . is the RNG $k-\epsilon$ model, and - - - is the Reynolds stress model. Symbols are measurements (or estimates from measurements).

role played by the near-bottom transport and hence the bottom boundary condition for the sediment equation. In this respect, the performance of the turbulence model is more precisely tested (in isolation from the other elements of the transport model) because only suspended load, which is directly related to the turbulence model, is of concern. Various computational studies have examined the flow and transport characteristics in clarifiers, ranging from the early constant eddy-viscosity models of Larsen (1977) and Imam et al. (1982) to the buoyancy-extended $k-\epsilon$ model of Devantier and Larock (1987) to an AS $k-\epsilon$ model in Zhou et al. (1994), with reviews of modeling issues by Krebs (1995) and Matko et al. (1996). Only two cases will be discussed in this section, those of Lyn et al. (1992) and Frey et al. (1993), who simulated the conditions listed in Table 16-4.

Lyn et al. (1992) applied a buoyancy-extended $k-\epsilon$ model with $c_{3\epsilon} = 0$ to predominantly stably stratified horizontal flows. Even at relatively low particle concentrations, suspension-induced buoyancy effects may be significant because of small velocities and hence low shear. The problem of non-uniform-sized particles was dealt with by considering different size classes and solving Eq. (16-7) for each size class. That a solution for ϵ is obtained in a $k-\epsilon$ model was exploited by developing a simple model for flocculation due to turbulent shear, such that the particle concentration in each size class may change not only by deposition but also by flocculation. A zero-diffusive-flux-concentration ($\partial c/\partial z = 0$) condition was imposed at the bottom, under the assumption that reentrainment of deposited sediment does not occur. Results from simulations including and not including sediment-induced buoyancy effects of an actual (tertiary) clarifier are shown in Fig. 16-12. The actual inlet configuration is a series of square jets at the same elevation, and hence the details of the three-dimensional inlet flow cannot be captured by the two-dimensional model. Nevertheless, significant difference in streamline pattern depending on

whether buoyancy effects are or are not included in the model is clearly seen, and comparison with the velocity measurements lends support to the significance of buoyancy effects, though only fair agreement between predicted and observed mean horizontal velocities was achieved. The importance of simulating different sediment size classes when buoyancy effects are included is seen in the comparison with concentration measurements. Because of the presence of small size fractions in the influent, a notable suspended solids concentration is still observed even toward the end of the tank. Interestingly, the concentration predictions, including the effects of different size classes, but without the effects of buoyancy, are found to be, somewhat fortuitously, in reasonable agreement with measurements in spite of obvious discrepancies in the corresponding flow predictions.

When Frey et al. (1993) applied a $k-\epsilon$ model in determining the steady-state flow field, they evaluated the removal efficiency of the clarifier, i.e., the ratio of influent to effluent particle concentration, not by the conventional advection-diffusion equation for the sediment concentration (Eq. (16-7)), but by a Lagrangian model, along the lines of Eqs. (16-9) and (16-10). They also more consistently included a random velocity component to simulate the random motion of particles. In their flow model, the rigid-lid approximation, which could be justified from their very small Froude numbers (Table 16-4), was not made, but buoyancy effects were not included. Fig. 16-13 compares their predictions for the flow field and removal with measurements in a laboratory model experiments with non-uniform-sized particles. Although substantial discrepancies between predicted and measured flow profiles can be seen in the inlet region, surprisingly good agreement is obtained for the predicted particle deposition (Fig. 16-13, the area numbers referring to streamwise stations at which deposited sediment was measured) and the effluent concentration, rather similarly to the previous case. Reasonable prediction

Table 16-4 Experimental Parameters for Flows in Sedimentation Tanks

Parameter	Frey et al. (1993)	Larsen (1977)
Model type	Laboratory	Field
Suspended material	Fine sand	Waste solids
Inlet concentration, C_0 (g/l)	N.r	80
w_s (mm/s)	N.r	0.2–4
d_{50} (μm)	50–100	N.r
$R = (Uh/v) (10^3)$	4.4	9.5
$F = U/\sqrt{gh} (10^{-3})$	11.6	0.49
$Ri_h = g(\Delta\rho_0/\rho)h/U^2$ ^a	N.r	105
Measurement technique	LDV	Ultrasonic current meter

^aBulk Richardson number, based on averaged downstream velocity, U , downstream depth, h , and inlet density difference, $\Delta\rho_0$.

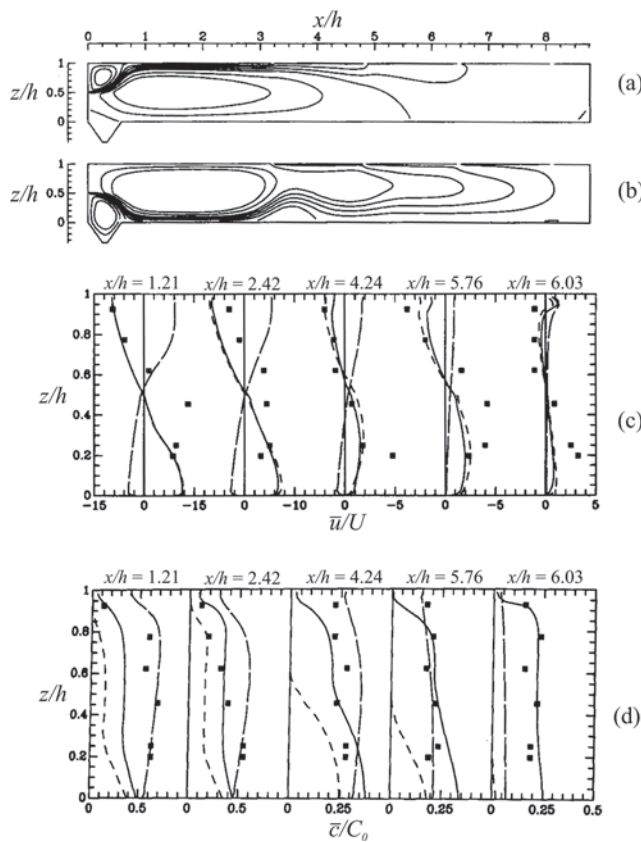


Fig. 16-12. Comparison of predictions (Lyn et al. 1992) of (a) simulated streamlines without (top) and with (bottom) buoyancy effects included, (c) nondimensional horizontal velocity (U is the nominal velocity in the tank), and (d) suspended solids concentration normalized by the inlet concentration, C_0 (—: with buoyancy effects and particle size distribution modeled; ---: with buoyancy effects but monodisperse particles; - - -: without buoyancy effects but with particle size distribution modeled, where symbols are data from Larsen 1977).

of derived overall quantities, such as sediment load, need not imply that detailed flow quantities are well reproduced, and caution is advised in evaluating numerical simulations based solely on derived quantities.

16.5.3 Flow in Vegetated Regions

With increased interest in the hydraulics of wetlands, interest in predicting flow and transport in vegetated areas has grown. Since it would be impractical to model the details of flows through vegetation (Fig. 16-14), questions regarding the appropriate averaging procedure may be raised. In this respect, the problem of predicting the average flow through vegetation resembles the two-phase flow problem in that, in addition to the modeling of turbulence, even the basic momentum balance as well as its effect

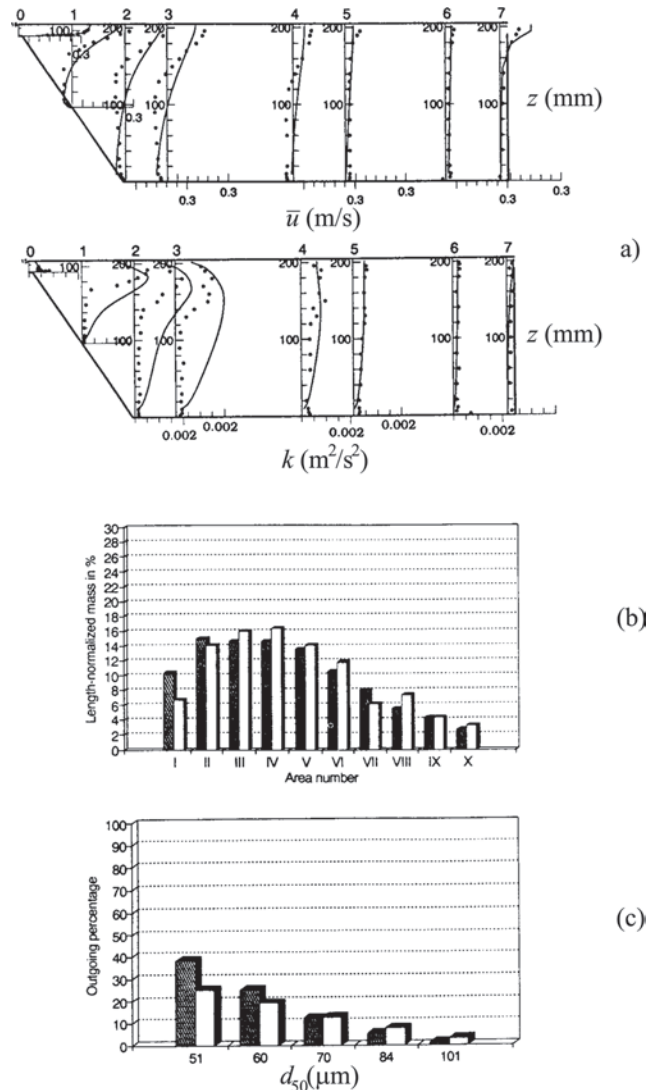


Fig. 16-13. Comparison of measurements in a model sedimentation tank with predictions of the k - ϵ model (Frey et al. 1993): (a) horizontal velocity, \bar{u} , and turbulent kinetic energy, k (symbols are measurements; — — — are predictions); (b) deposition of material at different streamwise stations (shaded bars are measurements; open bars are predictions); (c) effluent particle concentration relative to influent particle concentration as a function of particle diameter (shaded bars are measurements; open bars are predictions). Adapted with permission.

on turbulence characteristics, must be modeled. The usual practice adds a suitably parameterized force term modeling averaged drag forces to the momentum equation (Tsujimoto et al. 1991; Naot et al. 1996), somewhat analogous to the buoyancy-force term if the stratification analogy is invoked for sediment-laden flows. Lopez and Garcia (2001) have pointed out that this approach does not directly deal with the effects of dispersion associated with the spatial averaging process (see the discussion of

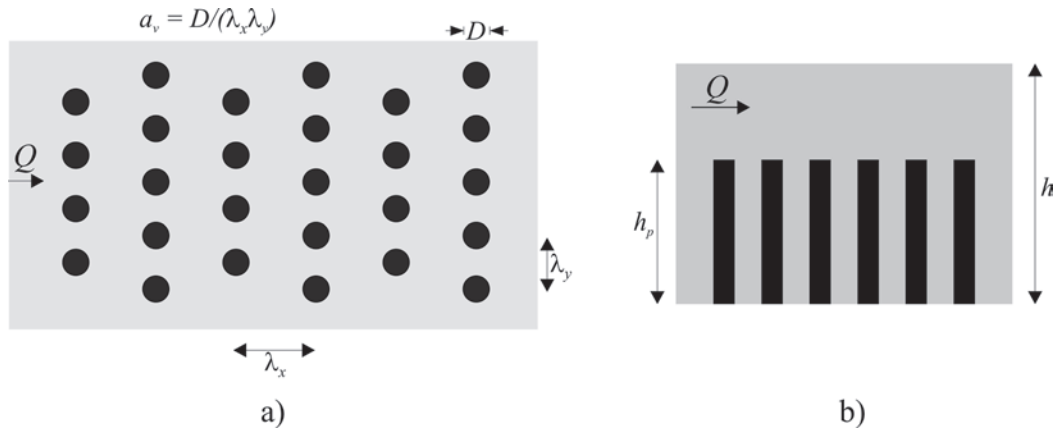


Fig. 16-14. Flow-through model (cylindrical) of nonemergent vegetation: (a) plan view, (b) profile view.

spatially averaged models in Appendix II to this chapter), but ultimately they resorted to the usual practice in their numerical modeling. In this subsection, for clarity, angle brackets will be used to denote variables that are spatially averaged over the horizontal plane.

Provided a model for the momentum equations has been chosen, the modeling of the effect of the vegetation on the turbulence follows essentially the same reasoning as in the development of the standard $k-\epsilon$ equations. If F_i denotes the additional force (per unit mass) term for modeling the effect of vegetation, then a production term, $G_v = c_{vk} F_i u_i$, is added as a source to the k -equation, and a balancing production term, $(G_v)_\epsilon = c_{ve} (\epsilon/k) G_v$, is added to the ϵ -equation (Tsujimoto et al. 1991; Naot et al. 1996;

Lopez and Garcia 2001). As in previous discussions, c_{vk} and c_{ve} denote model constants, and again, for consistency with the limit of local equilibrium, c_{vk} and c_{ve} are related and cannot be chosen independently. There remains some debate as to the appropriate value of c_{vk} which has been taken to be 0.07 by Tsujimoto et al. (1991) and Naot et al. (1996), and to be 1 by Burke and Stolzenbach (1983) and by Lopez and Garcia (2001). As noted by Lopez and Garcia, provided that c_{vk} and c_{ve} are chosen to satisfy the local-equilibrium-limit constraint, the predictions of the eddy viscosity, v_t , may not be particularly sensitive to the particular value of c_{vk} .

Lopez and Garcia applied one-dimensional (horizontal homogeneity of the spatially averaged flow was assumed)

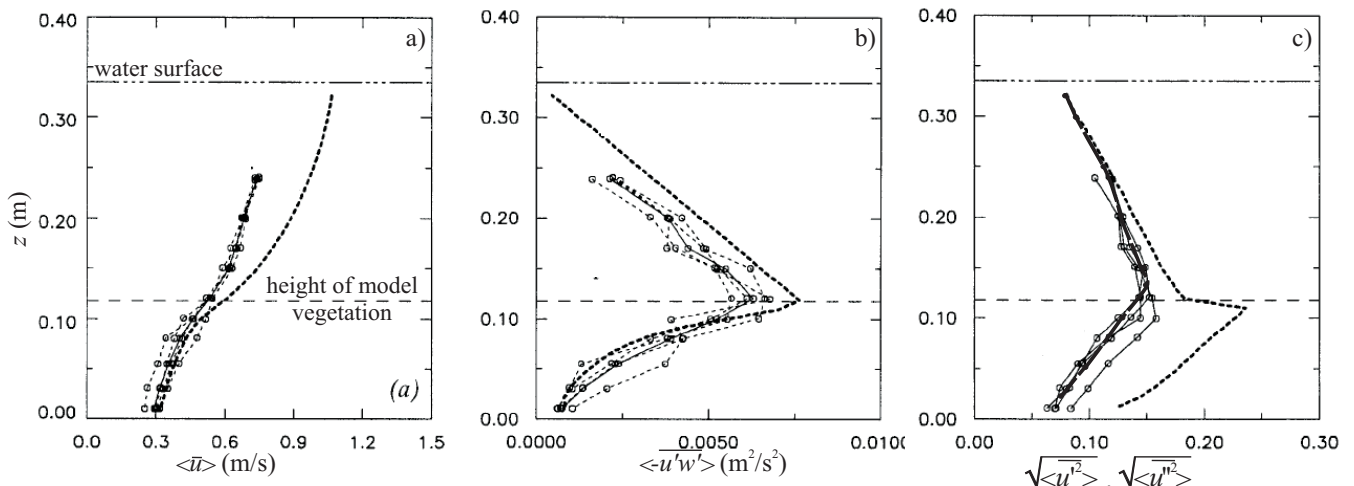


Fig. 16-15. Comparison of measurements (symbols; interpolated lines to aid visualization) and simulation (heavy lines) results for spatially averaged quantities in flow-through model of nonemergent (Lopez and Garcia 2001) (a) mean velocity (—) $k-\epsilon$ model, $k-\omega$ model, (b) Reynolds shear stress; (c) streamwise turbulence intensity (—) $k-\epsilon$ model with $c_{vk} = c_{ve} = 1$, $k-\epsilon$ model with $c_{vk} = c_{ve} = 0$.

$k-\epsilon$ and $k-\omega$ models, with a varying closure coefficient, c_μ , derived from an algebraic stress model, to the case of flow-through nonemergent vegetation without sediment. The results are shown in Fig. 16-15, compared with their own measurements, which were obtained with cylinders of diameter $D = 0.64$ cm and height $h_p = 12$ cm modeling plants. The parameter $a_c \equiv D/(\lambda_x \lambda_y) = 1.09/m$ is used to characterize the areal density of the cylinders, where λ_x and λ_y are the center-to-center cylinder separations in the x and y directions. The mean velocity, $\langle \bar{u} \rangle$, is noticeably overpredicted by the $k-\epsilon$ model in the region above the model vegetation (Fig. 16-15a), which the authors attributed to the effect of three-dimensional motions that are not captured by the one-dimensional model. This by itself seems an inadequate explanation because the actual flow is also three-dimensional within the model vegetation, where the agreement between measurements and predictions is rather better. Similar to the two-phase flow, an incomplete model of the effects of vegetation might have contributed to the discrepancies, though the abrupt change from a vegetated region to vegetation-free region probably played a role. Both models predict similar Reynolds shear stress distributions (only the $k-\epsilon$ predictions are shown), which agree well with the data.

An evaluation of model performance regarding the predictions of k , in this case of the streamwise turbulence intensity, is bound up with the question of the appropriate value of the model constants c_{vk} and c_{ve} (whether $O(1)$ or close to zero). A comparison was made of two model predictions obtained with the $k-\epsilon$ model (similar results were obtained with the $k-\omega$ model), one assuming that $c_{vk} = c_{ve} = 0$, the other assuming that $c_{vk} = 1$ and $c_{ve} = c_{le}$, with $\langle \sqrt{u'^2} \rangle$. The predictions of the former are clearly in closer agreement with the data. Lopez and Garcia, however, argue but do not confirm experimentally that if dispersive effects were included (see Appendix II for a discussion of dispersive effects), as they should be, then the latter predictions would likely be closer to reality.

16.5.4 Oscillatory Flows with Sediment Transport over a Plane Bed

The previous cases examined flows that may be assumed steady in the mean. The effects of unsteadiness may play an important role in the case of sediment transport under waves, where short time scales, such as wave periods, are comparable to important turbulence time scales. The general topic of unsteady turbulent internal flows is reviewed by Brereton and Mankbadi (1995). Problems of sediment transport under waves are discussed broadly in Fredsoe (1993), and with particular attention to unsteady models in Davies (1995). Sediment transport in oscillatory flow over a plane bed has attracted much attention as a fundamental building block to the solution of the more general practical problem. The avail-

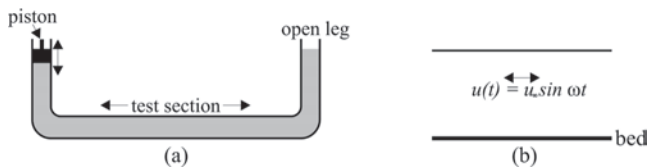


Fig. 16-16. Oscillatory flow: (a) U-tube laboratory channel; (b) profile view of flow in test section.

ability of standard experimental datasets (Jensen et al. 1989, referred to subsequently as JSF; Ribberink and Al-Salem 1994, and 1995, referred to subsequently as RA; Lodahl et al. 1998) makes possible detailed comparison of model predictions with measurements and evaluation of different models. These laboratory studies are performed in a U-tube channel with a closed and an open leg, with the unsteadiness being produced by an oscillating piston in the closed leg of the channel (Fig. 16-16). Under plane-bed (otherwise termed sheet-flow when the bed is erodible) conditions, horizontal homogeneity can be assumed, thus simplifying the problem in that only diffusive (in the vertical direction) transport need be considered, together with the unsteady terms. The experimental conditions for the two cases to be discussed are given in Table 16-5. In both cases, the free-stream flow is purely sinusoidal with zero mean flow; one is a clear-water flow over a fully rough fixed bed, where as the other involves suspended sediment over an erodible but plane transitionally rough bed.

Justesen (1991) compared the performance of the $k-\epsilon$ and a one-equation model (with $\mathcal{L} = \kappa z$) for the JSF clear-water data at various phases, $\phi = \omega t$. The results (Fig. 16-17) suggest that the $k-\epsilon$ is somewhat superior to the one-equation model, at least with this simple specification of \mathcal{L} , but both models yield predictions in reasonable agreement with the measurements for the mean velocity and the bed shear stress, and as might be expected less so for the turbulence quantities. Agreement tends to deteriorate during the deceleration phase, $\phi \gtrsim \pi/2$, possibly indicating difficulties analogous to those encountered for turbulent boundary layers with adverse pressure gradients. Jensen et al. (1989) observed that the (ensemble) mean velocity profile follows a log law at each phase over much of the period, and indeed, for the rough boundary, estimated the bed shear stress from the log-law profile (hence, the good model predictions of bed shear stress are perhaps expected). Thus, since its behavior is so similar to that of a steady wall-bounded flow (over much of the period), and without the massive separation characteristic of the flow over bed forms and the inlet flow into sedimentation tanks, the oscillatory clear-water flow over a rough boundary is comparatively not a severe test of turbulence models, except possibly in the neighborhood of flow reversal ($\phi = 0$ and $\phi = \pi$).

Sana and Tanaka (2000) investigated various near-wall low-Reynolds-number $k-\epsilon$ turbulence models for oscillatory clear-water flows over a smooth bed. They compared

Table 16-5 Experimental Parameters for Oscillatory Flows over Plane Beds

Parameter	Jensen et al. (1989) (JSF, test 13)	Ribberink and Al-Salem (1995) (RA, condition 3)
Median sediment size, d_{50} (mm)	n/a	0.21
Wave period, T (s)	9.7	7.2
Freestream velocity amplitude, U_m (m/s)	2.0	1.7
Freestream particle excursion amplitude, a_{fs} (m)	3.1	2.0
Equivalent roughness, d_r (mm)	0.84	0.52
$R = U_m a_{fs} / v (10^6)$	6.2	3.4
$R_* = (u_*)_{\max} d_r / v$	84	n/a

their predictions with results of direct numerical simulations, thus avoiding uncertainties associated with experimental measurements. As in Justesen (1991), they found that velocity profiles and wall shear stresses were generally well predicted, with weakness during deceleration. Turbulence quantities, such as k and $-\bar{u}'w'$, tended to be less well predicted. As noted previously, the application of low-Reynolds-number near-wall models may be rather limited in sediment-transport problems characterized by rough erodible beds.

Various simulations of the flow studied by Ribberink and Al-Salem (1995) have been reported. Savioli and Justesen (1997a) applied a standard $k-\epsilon$ model, with a bottom concentration condition formulated in terms of a reference concentration, though effectively a flux condition (see discussion in Section 16.4.5.2). Four different models were tested in Davies et al. (1997): (1) a simple mixing-length model ($\mathcal{L}_m = -\kappa z$), (2) a zero-equation eddy-viscosity model based on an unsteady generalization of Eq. (16-27), (3) an enhanced version of the one-equation model of Li and Davies already mentioned, and (4) a two-equation model of Huynh Thanh and Temperville (1991) that seems similar to the Mellor-Yamada level 2½ model. The one-equation and two-equation models incorporate the effect of buoyancy. The bottom concentration boundary condition was essentially the same in all four models, except for the mixing-length model, namely an equilibrium but time-varying reference concentration, though some allowance is made for sediment settling. Three of the four models assumed $(\sigma_t)_s = 1$, the exception being the two-equation model, where $(\sigma_t)_s$ was variable. Brors and Eidsvik (1994) performed an RS model simulation, including buoyancy effects, with a bottom boundary concentration rather similar to that in the Davies et al. study.

The predictions of suspended sediment concentration at various distances from the bed are compared in Fig. 16-18. The simple mixing-length model is clearly inadequate, but the other models examined by Davies et al. are more comparable

in predictive performance. All model predictions suffer from poor phase behavior, which tends to worsen as the distance from the bed increases. This contrasts with the good phase prediction seen earlier with respect to the bed shear stress in clear-water flows. In terms of concentration amplitude, the two-equation models, particularly that of Savioli and Justesen (the observed secondary peak when the flow velocity approaches zero is reproduced, whereas this is absent in the other predictions), performed somewhat better, though the eddy-viscosity model did surprisingly well. The performance of the RS model is not markedly better than that of the other models (again excepting the simple mixing length model), and is arguably worse than the $k-\epsilon$ results of Savioli and Justesen. This better performance of the Savioli-Justesen model may, however, not necessarily be attributable to the turbulence model as such, but rather to the bottom boundary condition, as argued by Savioli and Justesen (1997b). Although Ribberink and Al-Salem (1995) suggested that sediment-induced buoyancy effects might play an important role, Li and Davies (1996) concluded that turbulence damping effects predicted by the one-equation model were observed to be small, and that the representation of turbulence damping may be incomplete. The models including buoyancy effects did not especially distinguish themselves. Davies et al. (1997) attribute the discrepancy in phases to convective effects, though how these might arise in a horizontally homogeneous flow or how they may be different from history effects is not clear. Unfortunately, no predictions of flow characteristics was presented (the discussion by Ribberink and Al-Salem 1995 also was perfunctory with regard to velocity and turbulence statistics), and so whether the flow predictions were any better could not be assessed.

16.5.5 Flow and Transport in a Channel Bend

Natural channels often exhibit a sinuous or meandering longitudinal plan form, and hence flow and transport in

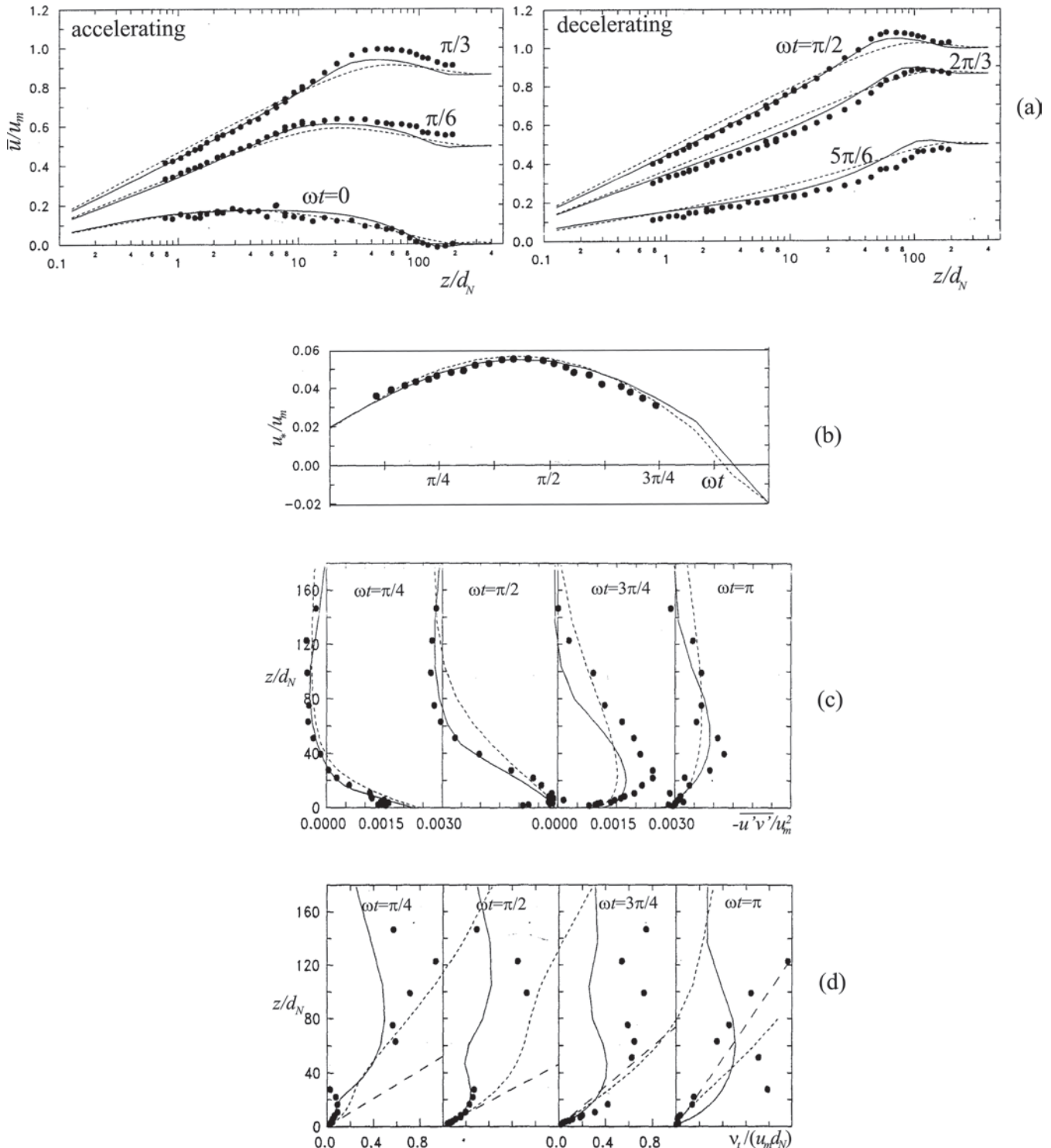


Fig. 16-17. Case of sinusoidally oscillating flow over a plane bed without sediment (Justesen 1991): profile predictions and measurements of (a) velocity, \bar{u}/U_m , (b) shear velocity, u_*/U_m , (c) Reynolds shear stress, $-\bar{u}'v'/u^2_m$, (d) eddy viscosity, $v_t/(U_m d_N)$, U_m a maximum imposed velocity; d_N is the Nikuradse equivalent sand-bed roughness; symbols are measurements of Jensen et al. (1989) and Sumer et al. (1987); — is $k-\epsilon$ model; --- is one-equation model. Adapted with permission.

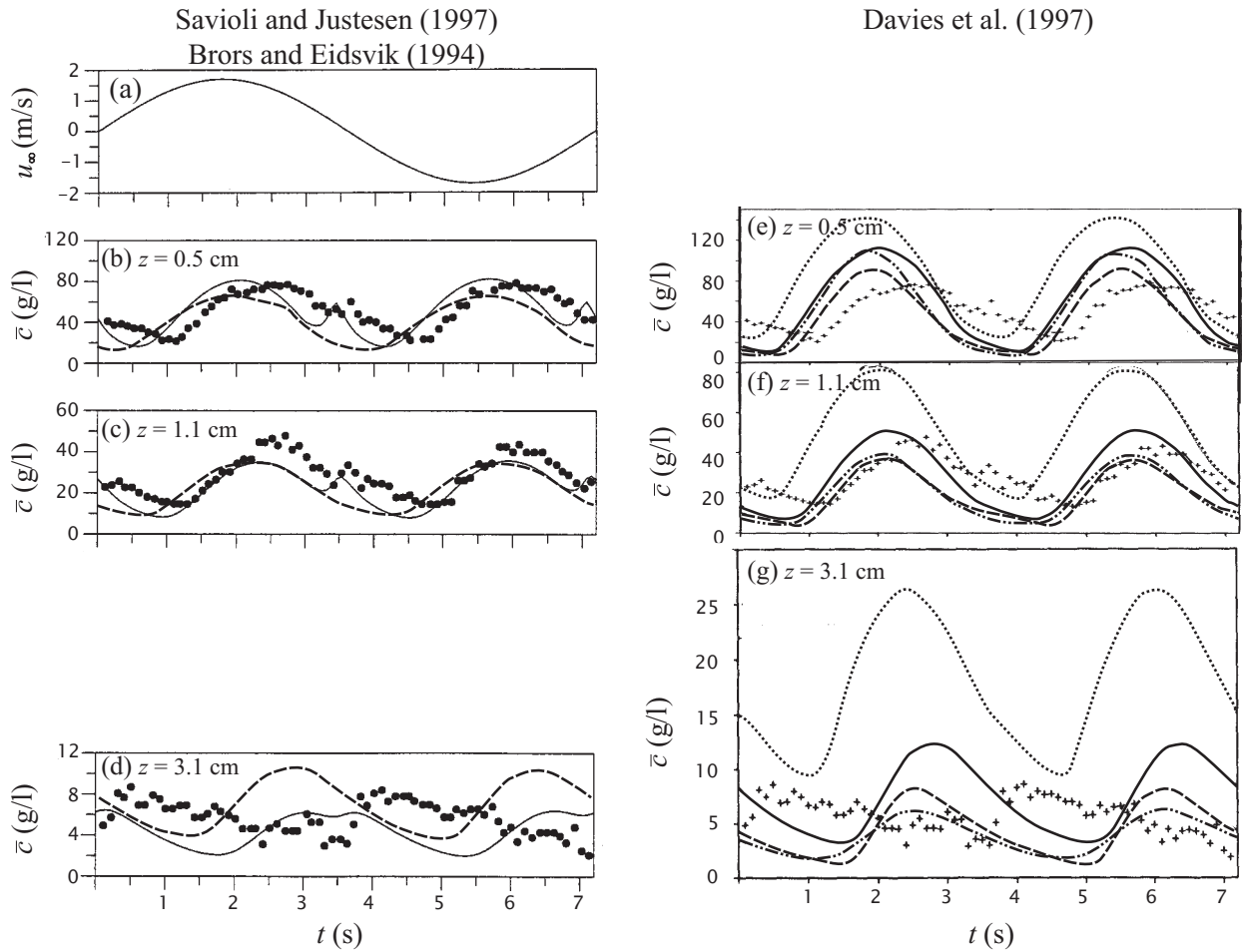


Fig. 16-18. Sinusoidally oscillating flow over a plane erodible bed (symbols are measurements of Ribberink and Al-Salem 1995): (a) imposed freestream velocity, u_∞ ; (b), (c), and (d) measured and predicted (—, $k-\epsilon$ model of Savioli and Justesen 1997a; ---, RS model of Brors and Eidsvik 1994) concentrations; (e), (f), and (g) measured and predicted (—, mixing-length model of Ribberink and Al-Salem 1995; —, one-equation model of Li and Davies 1996; ---, eddy-viscosity model of Fredsoe et al. 1985; -.-., two-equation $k-L$ model of Huynh Thanh et al. 1994) concentrations. Adapted with permission.

bends are of interest to the sediment-transport community (see Chapter 8, which is devoted to various aspects of this topic). The flow is three-dimensional, with some of the basic aspects of sediment transport strongly influenced or even wholly determined by the action of relatively small secondary currents. The main secondary currents result from the opposing centrifugal and pressure forces. The importance of turbulence is more uncertain. Streamline curvature, measured by a radius of curvature, R , is known to have an effect, disproportionately large relative to the size of the curvature terms in the governing equations, on turbulent flow and transport (Patel and Sotiropoulos 1997). The question remains as to their importance relative to the pressure gradient terms, particularly in localized regions, such as regions near the banks. Further, even if its importance

with regard to the gross flow may be minor, its importance for long-term sediment transport, e.g., bank erosion, might be quite significant, and so good predictions of such flow details may be desirable for sediment rather than purely for flow aspects. Two recent experimental studies are suitable for detailed comparisons with numerical predictions (Hicks et al. 1990; Blanckaert and Graf 2001), in that not only mean but also turbulence quantities were obtained, but only the former has so far been the subject of a published simulation. Whereas Hicks et al. (1990) studied the simpler flow over a fixed smooth bed, the other two experimental studies to be dealt with, that of Thorne and Raïs (1983), a field study, and that of Odgaard and Bergs (1988), a laboratory study, investigated flows over an erodible bed, hence with mobile bed forms. In both cases, however, bed-load transport was

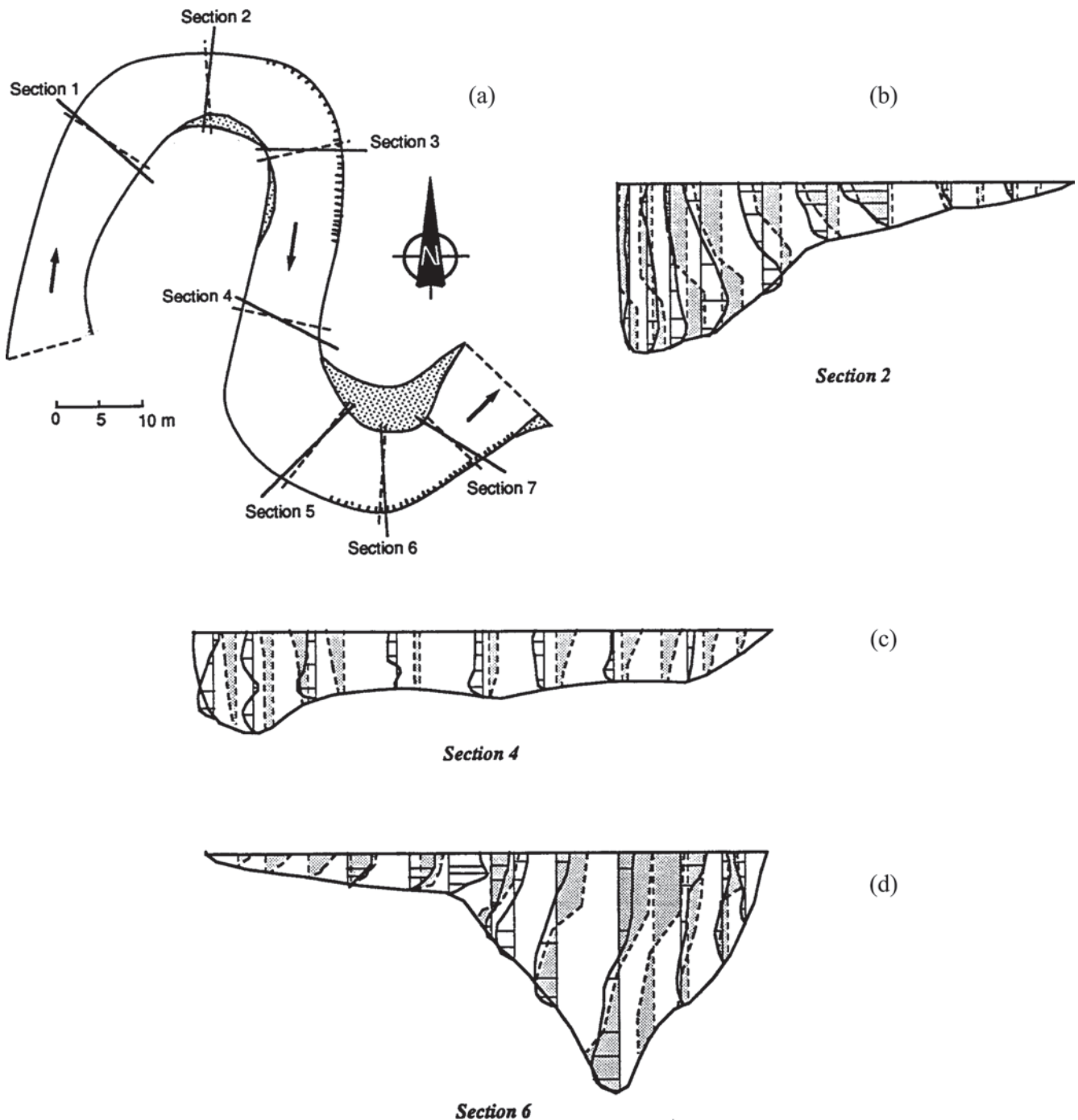


Fig. 16-19. (a) Definition sketch (plan view) of stream (Fall River, Colorado) simulated, (b), (c), and (d) predicted (dashed lines with shaded region) and measured (solid lines) lateral velocity at sections 2, 4, and 6. Predictions, Ghanmi et al. (1997); measurements, Thorne and Raïs (1983). Reproduced with permission.

dominant. The important parameters of the three cases are summarized in Table 16-6.

Only three-dimensional or quasi-three-dimensional models will be discussed since the focus is on turbulence models. Ghanmi et al. (1997) applied a generalized mixing-length closure to simulating the flow in the Fall River in Colorado,

the site of the field study of Thorne and Raïs. A fixed bed, a hydrostatic pressure distribution (hence, this is a quasi-three-dimensional model), and a Manning friction relationship were also assumed. Within the bends, at Sections 2 and 6, there is reasonable *qualitative* agreement in the prediction of the secondary currents, though clear quantitative

Table 16-6 Experimental Parameters for Flows in a Bend

Parameter	Thorne and Raïs (1983)		Odgaard and Bergs (1988)	Hicks et al. (1990) (Run A6)
	Section 2	Section 6		
Experiment type	field		laboratory	laboratory
Bed conditions	migrating dunes		migrating dunes	smooth
Median sediment size, d_{50} (mm)	mixed sand		0.30	n/a
Mean radius of curvature, R_c (m)	11.0	13.5	13.1	3.66
Mean depth, h (m)	0.41	0.44	0.15	0.062
Width, B (m)	6.7	8.25	2.44	0.86
Discharge, Q (m^3/s)	1.7	1.7	0.15	0.022
B/R	0.61	0.61	0.19	0.23
h/R	0.037	0.033	0.011	0.017

discrepancies may be seen, even with the spatially sparse set of measurements (Fig. 16-19). In the straight reach connecting the two successive bends, at Section 4, there are *qualitative* discrepancies in the predicted and observed flow directions. This may indicate that the simple mixing-length model leads to an overly quick relaxation of the flow, such that the simulated flow out of the bend has little or no memory of the bend. The authors give a long list of possible reasons for the disagreement with measurements, though surprisingly the use of an overly simple turbulence model (or even an overly coarse numerical grid) is not mentioned.

The more detailed laboratory measurements of Hicks et al. (1990) for the simpler fixed-bed problem with a sloping outer bank and a vertical inner bank allow a more precise evaluation of flow prediction. Ye and McCorquodale (1998) reported a full three-dimensional simulation, including a free-surface model, of this case. The $k-\epsilon$ model was augmented by corrections to incorporate the effects of curvature and anisotropy near boundaries. The results, for the lateral velocity and turbulence intensity (Fig. 16-20), show quite good agreement with measurements at the different sections along the bed. Significant discrepancies are confined to regions near the free surface, near the outer sloping bank, and, perhaps surprisingly, at the bend entrance for the mean lateral velocity. To some extent, the better agreement may be attributed to the more precise laboratory measurements, though the use of the more sophisticated two-equation turbulence model probably contributed. Ye and McCorquodale also compared the predictions of the modified and the standard $k-\epsilon$ model, and the differences were relatively minor, so the particular corrections for curvature and boundary-induced

anisotropy do not appear to have led to large improvements in predictions.

The erodible-bed laboratory study of Odgaard and Bergs (1988) has been tackled by Wu et al. (2000) in a model incorporating free-surface and erodible-bed models, as well as suspended (though for this particular case, suspended load was practically negligible) and nonequilibrium bed-load models. Typical of erodible-bed models, the sediment model is segregated from the flow model, so that the flow field is first computed, starting for example from an initially guessed bed geometry, then the sediment transport is estimated, and then the bed is adjusted, and the procedure is iterated until an equilibrium bed is attained. Because in the experiment, migrating dunes were observed, the equilibrium bed in the computations, which did not consider bed-form details, must be interpreted in terms of a temporal average. In Fig. 16-21, some computational results are compared with the laboratory measurements. The local flow depths and the equilibrium lateral bed profiles were reproduced fairly well (Figs. 16-21(a–c)). The velocity skew angle (Fig. 16-21(d)), i.e., the angle between the point velocity and the depth-averaged velocity, which characterizes the strength of the lateral velocity relative to the streamwise velocity and hence gives information regarding the relative importance of the secondary currents, was also relatively well predicted. The erodible-bed case was also examined in a simpler three-dimensional model by Shimizu et al. (1990) using the zero-equation parabolic eddy viscosity model (Eq. 16-27), and reasonable predictions of bed topography for a scale model of the Ishikari River were obtained. This raises the question of whether a two-equation model is necessary to predict gross changes in bed levels reliably in the bends of

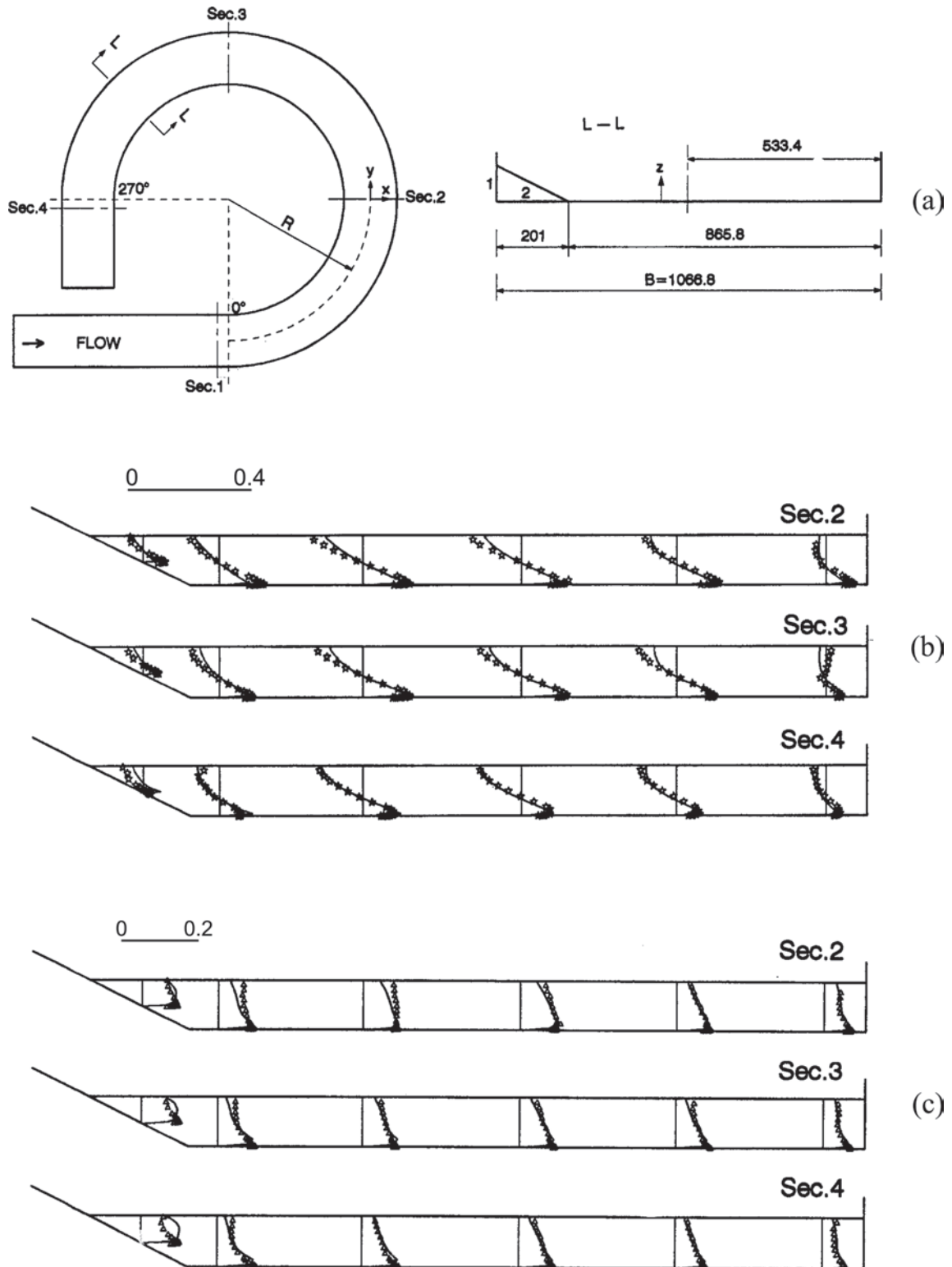


Fig. 16-20. (a) Definition sketch of channel simulated, predicted (solid line), and measured (symbols), (b) lateral velocity, \bar{v} , and (c) lateral turbulence intensity, $\sqrt{v'^2}$, at different sections. Predictions, Ye and McCorquodale (1998); measurements, Hicks et al. (1990).

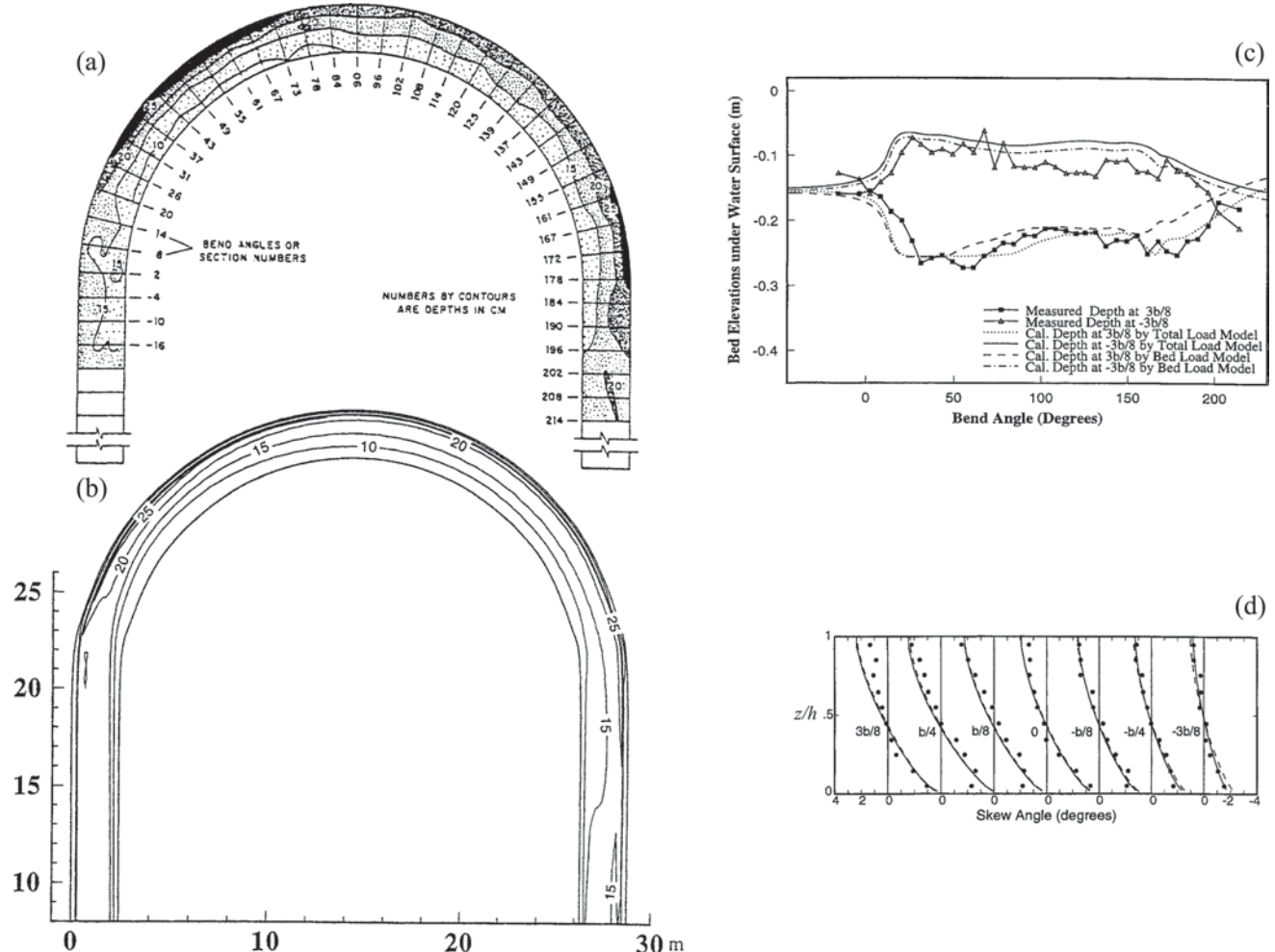


Fig. 16-21. Comparison of measurements (Odgaard and Bergs 1988) and predictions (Wu et al. 2000) in flow through a 180° bend: (a) measured and (b) predicted contours of water depth, (c) streamwise variation of bed elevations at two lateral positions, (d) streamwise averaged (along paths of constant radius) skew angles.

erodible-bed channels, even if detailed flow characteristics are not necessarily reproduced well.

16.5.6 Local Scour around a Circular Bridge Pier

The last application to be considered, local scour around a bridge pier (Fig. 16-22), shares many aspects of the flow and sediment transport discussed in the preceding subsections. As with the flow in bends, interest focuses on the (localized) erosion of the bed, and hence a model of a deformable bed is necessary. The smaller length scales involved, combined with strong three-dimensional features, would seem to pose a more difficult problem for turbulence models. Flow separation and even unsteady large-scale motions, e.g., due to vortex shedding in the wake, will also contribute to difficulties in flow simulation. Local scour occurs as the sediment transport capacity is locally enhanced due to a localized change in the

flow field, e.g., in the presence of a structure, causing sediment to be entrained into the flow, resulting in scour or erosion of the bed (or bank) in a localized area. This section will only consider the classic problem of scour around a circular bridge pier. Traditional discussions of this problem (Raudkivi 1990, or the two chapters 10 and 11 in this volume) have focused on developing correlations of the maximum scour depth with upstream hydraulic conditions, pier geometry, and perhaps sediment parameters. With the notable exception of Melville and Raudkivi (1977), detailed measurements of flow characteristics have only recently appeared (Dargahi 1989; Ahmed and Rajaratnam 1998). Several simulations have nevertheless been reported, mostly, however, without any detailed comparison with experimental measurements of flow and sediment comparable to those in the preceding subsections. Two of the cases to be considered simulated only the flow, without modeling the scour process itself, one over a plane bed, the other over a scour hole approximated as the

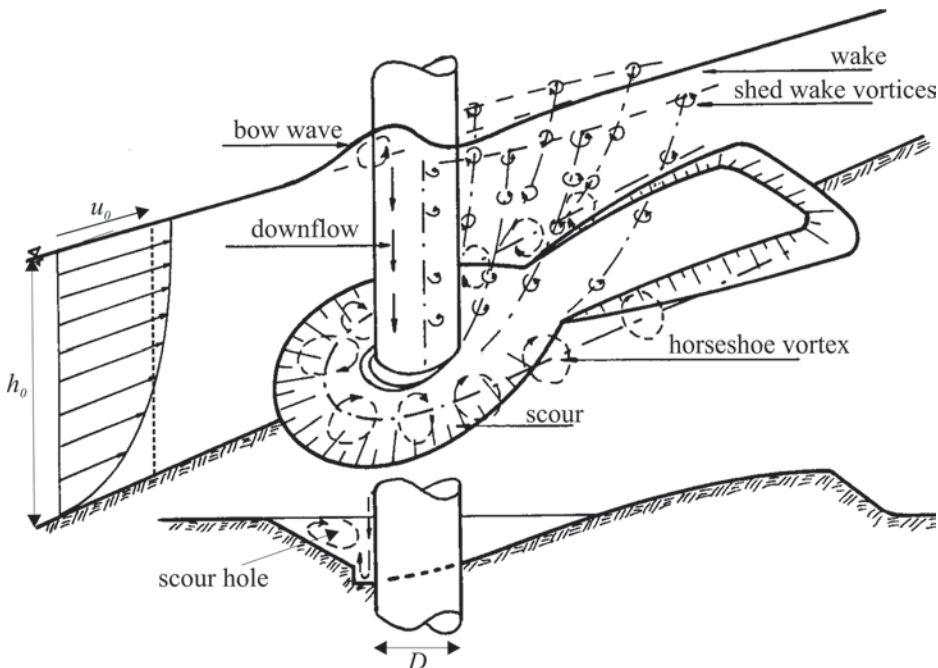


Fig. 16-22. Definition sketch of flow around a cylindrical bridge pier (adapted from Raudkivi 1990). Adapted with permission.

frustum of a cone (therefore radially symmetric about the cylinder axis), whereas the final case included an erodible-bed component, though in the simpler case of clear-water (zero sediment transport upstream of pier) scour. The experimental conditions of the three cases are summarized in Table 16-7. Only three-dimensional computations will be discussed.

Using an eddy-viscosity turbulence model (a Smagorinsky model, often used in large-eddy simulations; see discussion in the next section), with, however, a rigid-lid free-surface, Tseng et al. (2000) performed an unsteady computation of the fixed-plane-bed flow studied experimentally by Dargahi (1989). Because unsteadiness could be modeled, they were able to simulate the periodic vortex shedding occurring in the wake of the cylinder, predicting a shedding frequency of 0.34 Hz compared with a measurement of 0.32 Hz. The measured and predicted bed shear stresses (T_0 is the upstream bed shear stress, and the cylinder center is located at $x / D = 0$) along the streamwise line of symmetry are compared in Fig. 16-23(a). The maximum magnitude is well predicted, though its location is slightly displaced upstream. Unfortunately, comparisons with flow characteristics (velocity and turbulence intensity) were not reported, even though these were measured. The equilibrium-scour flow experiment of Melville and Raudkivi (1977) was simulated by Richardson and Panchang (1998), who tested both a mixing-length and an RNG model. They reported that whereas the latter "appeared to provide a qualitatively more realistic field downstream of the pier, the results of both simulations were largely similar." Because the details of the bed geometry,

particularly those in the cylinder wake, were not available, they assumed a somewhat unrealistic scour hole geometry of a frustum of a cone concentric with the cylinder. The velocity magnitudes at a distance of 2 mm from the bed are of interest because they are expected to be closely correlated with bed shear stresses, and a comparison of predictions and measurements is given in Fig. 16-23(b). Because of likely differences in actual and modeled bed geometries downstream of the cylinder, only results upstream of the cylinder are of interest. Qualitative similarities are seen in an elongated and narrow low-velocity region at the rim of the scour hole and a high-velocity region at an $\approx 70^\circ$ angle from the streamwise symmetry axis. A high degree of uncertainty is associated with these early measurements using thermal anemometry in a highly turbulent recirculation region where such techniques are known to be deficient. An earlier computation by Mendoza-Cabral (1993) with a $k-\epsilon$ model of plane-bed experiments of Melville and Raudkivi (1977) also noted discrepancies between predictions and measurements and attributed these to both experimental uncertainties and deficiencies in turbulence closure.

The erodible-bed case with sediment transport was treated in a decoupled iterative manner by Olsen and Melaaen (1993), who solved alternately the steady flow field with a $k-\epsilon$ model, and then the sediment equations, which included both a suspended-load (modeled by Eq. (16-7)) and a bed-load component, adjusting the bed elevation in the vicinity of the cylinder to ensure sediment conservation in the near-bed region. At the bed, the concentration was specified.

Table 16-7 Experimental Parameters for Flow around a Circular Bridge Pier

Parameter	Melville and Raudkivi (1977)	Dargahi (1989)	Olsen and Melaaen(1993)
Bed conditions	Fixed plane bed (roughness, $d_r = 0.36 \text{ mm}$)	Equilibrium bed (sand)	Equilibrium bed (plastic particles)
Median sediment size, $d_{50} (\text{mm})$	n/a	0.30	3 ($s = 1.04$)
Cylinder diameter, $D (\text{m})$	0.051	0.15	0.75
Upstream depth, $h_0 (\text{m})$	0.15	0.20	0.33
Upstream velocity, $u_0 (\text{m/s})$	0.25	0.26	0.067
$R = u_0 D / v (10^3)$	37.5	39	50
$F = u_0 / \sqrt{gh_0}$	0.21	0.19	0.04

A comparison between measured and computed scour-hole dimensions (Fig. 16-23(c)) showed good agreement. This work was later extended to treat the time-varying scour process in a more realistic manner including unsteady flow and transport as well as a free surface, and the resulting model is more fully described by Olsen and Kjellesvig (1999). While detailed comparisons with flow measurements were not made, the predicted maximum scour depth agreed well with traditional empirical formulae. These encouraging results indicate that the simulations can yield useful engineering results, but whether details of the flow field and the concentration field were predicted well remains to be established.

16.6 DISCUSSION

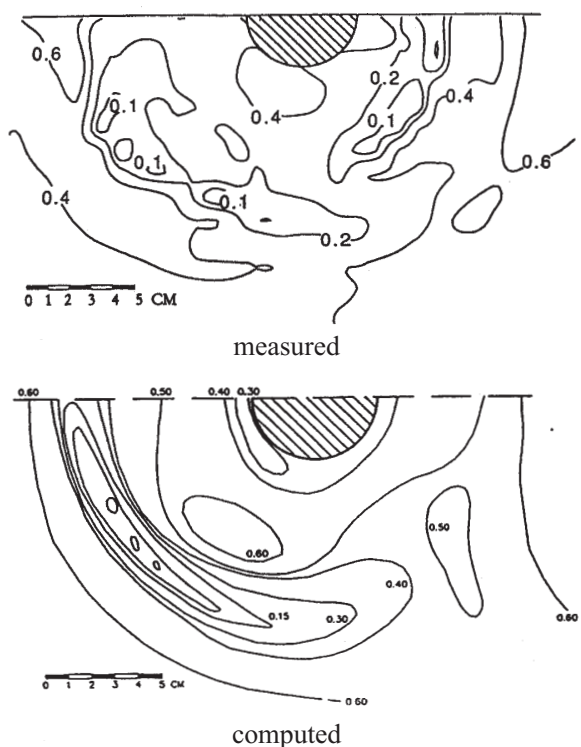
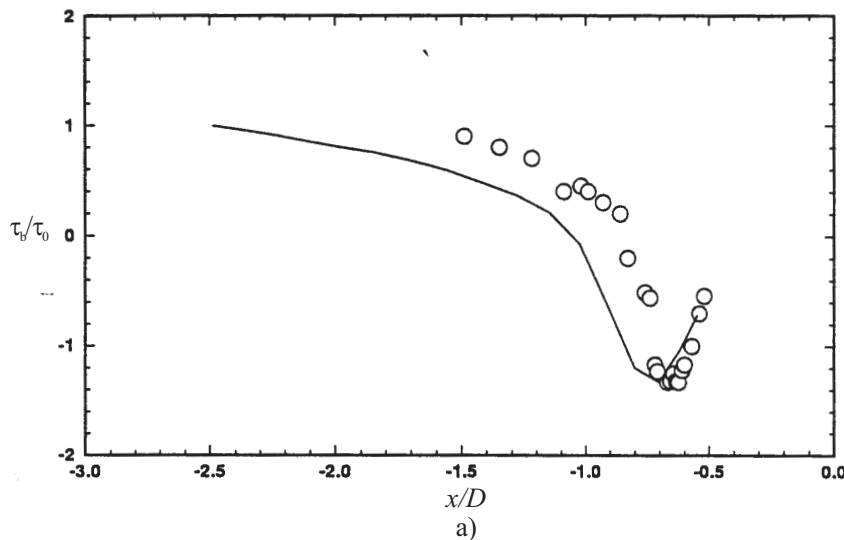
In the preceding sections, the rudiments of turbulence closure models have been described, with particular emphasis on application to problems in sediment transport. Models of varying degrees of sophistication are available, ranging from the simplest constant-eddy-viscosity model through to two-equation models and beyond, and each class of models can, when applied judiciously, provide useful tools for predicting flow and transport. Except in the section on more advanced models, discussion has been restricted to standard models, because these are the most likely to be encountered in the literature, and also most likely to be available in commercial CFD software packages (though these have not particularly catered to those interested in sediment transport). Other models, e.g., CH3D-SED, developed for the U. S. Army Corps of Engineers (Gessler et al. 1999), in which only the vertical diffusivity is computed from a $k-\epsilon$ -type model, and constant horizontal diffusivities are user-specified, may be understood as variants of the standard models, subject to the same or even more limitations, since these have been adapted for a particular class of applications. Although turbulence models have received the bulk of the

attention, these should be recognized as only one element of a flow and transport simulation, and therefore as only one source among others of errors in prediction.

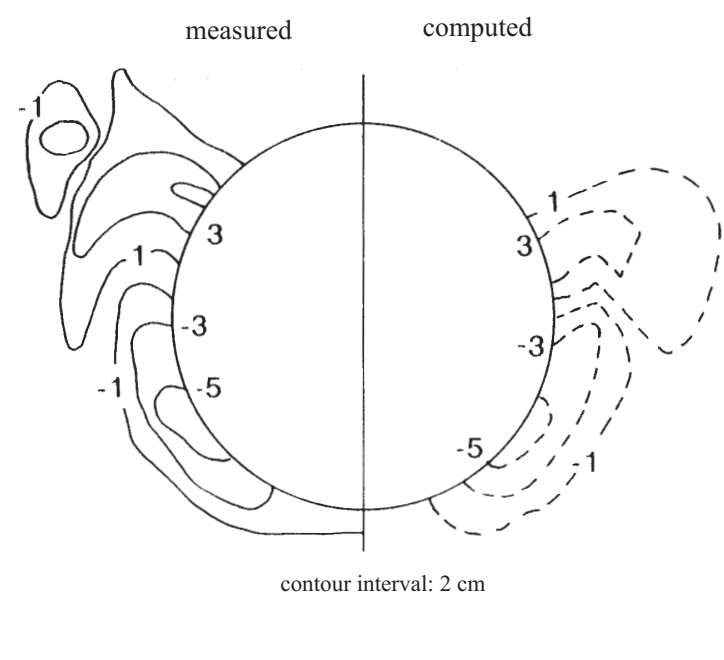
16.6.1 Considerations in the Assessment and Choice of Models

A model should give useful predictions for reasonable effort. In the hands of skilful practitioners, useful predictions can be made with the simplest of models, judiciously complemented by additional empiricism. More complicated models should be adopted when there is reasonable expectation that these bring an increase in accuracy and reliability at least commensurate with the greater effort, which is not necessarily only computational, required. The latter is not always the case, and the point of diminishing returns might be at a rather low level of model sophistication. Qualitative understanding of the specific flow problem is valuable in assessing the importance of the various physical processes contributing to sediment transport and in choosing an appropriate model. What constitutes a reasonable effort is, however, continually changing as advances in computational power are made. Whereas at the time of publication of *ASCE Manual 54*, a one-dimensional model was the limit of what could be expected, at the present time, a fairly complete transport simulation of a steady two-dimensional problem with a two-equation model can be routinely performed with commonly available computer resources. In the not-too-distant future, three-dimensional models may foreseeably become the norm. Another consideration in choosing a more sophisticated model is the possible greater demands in terms of data input for initial and boundary conditions, and for calibration of model parameters.

Traditional prediction methods for one-dimensional cross-sectionally averaged sediment transport are notoriously inaccurate, with measures of merit for prediction typically formulated in terms of the fraction of predictions within 100%



b)



c)

Fig. 16-23. Flow around a cylindrical bridge pier: (a) Smagorinsky eddy-viscosity model predictions (—, Tseng et al. 2000) of normalized bottom shear stress (τ_0 = upstream bed shear stress) compared with the measurements (symbols) of Dargahi (1989); (b) RNG model predictions (Richardson and Panchang 1998) and measurements (Melville and Raudkivi 1977) of near-bed (2 mm from bed) velocity magnitudes; (c) $k-\epsilon$ model predictions and measurements of local scour (Olsen and Melaaen 1993). Adapted with permission.

of the observed values. It is important to recognize that several elements of traditional methods may be imbedded in the models discussed in this chapter in boundary conditions and model parameters, such as the effective roughness height, the equilibrium concentration at a reference elevation, or a sediment-transport function. Errors and uncertainties associated with these elements carry over to predictions made with numerical simulations incorporating sophisticated turbulence models. The turbulence model is directly concerned only with suspended load, and only indirectly affects bed-load transport through the estimate of the shear stress at the bed. Particularly in computations of flows over bed forms, where these are not simulated directly, heavy reliance is placed on traditional results. Here it might be mentioned that one of the classic problems of traditional sediment transport, that of determining the stage or depth of flow for given discharge, channel, and sediment characteristics, has to a large extent been avoided in flow simulations, which frequently assume the depth to be known and apply a rigid-lid model for the free surface. Thus, if the depth must be known prior to the simulation, a rather curious situation could arise in which a traditional method is applied to determine the depth, with all of the uncertainties inherent in such an estimate. Similarly, the determination of whether bed forms are present in any given flow, and if so, their dimensions, so that the specifications of flow and sediment bottom boundary conditions can be done, may rely on traditional procedures. Thus, it would be overly optimistic to expect that the use of sophisticated turbulence models will result in large gains in prediction accuracy and reliability over the entire range of sediment transport problems. Computational fluid dynamics, coupled with turbulence models, has permitted a considerably wider range of sediment transport problems, including multidimensional problems, to be tackled in much greater detail successfully, i.e., with about the same level of accuracy that has been achieved with traditional methods for simple one-dimensional problems. While this may seem disappointing, it should be realized that the problems often could not be tackled at all, so that a prediction within 100% could represent considerable improvement. Nevertheless, the point should be made that the largest errors may be associated with the model elements taken over from traditional methods, rather than with the choice of turbulence models.

The choice of model dimensionality, whether a one- or two- or even three-dimensional modelling approach is taken, may have important implications for the choice of turbulence models. A three-dimensional model at this time may eliminate from consideration more sophisticated turbulence closures due to the computational effort required, so it becomes important to weigh whether increased dimensionality may be more important than a more sophisticated turbulence model. At the same time, if three-dimensional effects on turbulence are strong, then simple turbulence models may be difficult to justify because appropriate length and velocity scales are unknown, and a two-equation model would be attractive. A depth-averaged model (see Appendix II as well as Chapter 15)

might be considered as a workable compromise if the primary turbulence-producing motions of interest are in the horizontal "plane." For steady flows in a channel, with a dominant flow direction and flow separation and reverse flow either absent or not important, a zero-equation model is certainly worth considering as a first step; if the results indicate that important expected flow features are missing or conversely unexpectedly present, a more sophisticated model might be considered for further study. The place of one-equation models is rather questionable; although their limitations vis-à-vis two-equation models are clear, their superiority compared to the zero-equation model is debatable. Of the two-equation models, the $k-\epsilon$ model remains the standard, being the most widely used and hence the most widely tested. This does not mean that its results should be accepted without hesitation. The applications discussed in the previous sections illustrate that the $k-\omega$ and the RNG models can yield, in certain flows and in certain flow regions, performance superior to that of the standard $k-\epsilon$ model, but a blanket recommendation in favor of one or the other cannot yet be made. Full Reynolds stress models have been rather disappointing (it should be admitted that a wide range of RS models have been and continue to be proposed, and lumping them together as has been done here is not altogether fair); the improvements in prediction performance have not always been dramatic. They are likely to remain research rather than practical engineering tools in the foreseeable future. The intermediate algebraic and the related nonlinear turbulence models may, however, be of more practical interest in the near future because of their less severe computational demands.

The value of validation data, either from the field or from laboratory experiments, can hardly be overemphasized. At the same time, it must be recognized that accurate measurements in sediment-transporting flows pose very difficult challenges, in the laboratory but particularly in the field. Certainly, one of the most significant obstacles to improvement in turbulence modeling and prediction of sediment transport lies in the inadequacy of experimental techniques for detailed reliable measurements of flow and, especially, sediment transport, particularly near the bed or boundary. Although turbulence modification has been discussed at some length, the limited experience so far obtained with simulations suggests that, insofar as a stratification model was invoked, the effect is weak, and as a first approximation might be neglected, except in special cases such as a turbidity current or other predominantly sediment-generated flows. The question remains open of whether the actual effects of turbulence modification might be stronger than those predicted by a stratification analogy, and might be manifested in near-bed boundary conditions.

The numerical aspects of flow simulation have received almost no mention in this chapter, though they may exert a

large influence on results as well as choice of models. These are discussed in greater detail in a number of specialized monographs (e.g., Gresho and Sani 2000; Ferziger and Peric 2001). Discretization schemes, particularly the treatment of advection in a high Re flow, may significantly influence the results of simulations because of numerical diffusion. It is now recognized (Speziale and Thangam 1992) that a large part of the discrepancy between measurements and early predictions of the classic turbulent backward-facing-step flow was due to numerical error rather than to the shortcomings of the $k-\epsilon$ model. The use of higher-order discretization schemes and of grid-dependence tests are both strongly recommended in any turbulent simulations. The greater computational effort for more sophisticated turbulence closures stems not only from the larger number of partial differential equations that must be solved, but also from convergence characteristics of their numerical solution being substantially worse than those of simpler models. Second-moment closure models tend to be numerically stiff, such that the additional computational effort may be much larger than might otherwise be thought. Similarly, inclusion of buoyancy effects may in a $k-\epsilon$ model entail difficulties in convergence of the numerical solution.

16.6.2 Other Types of Models

The chapter has focused on Reynolds-averaged Navier-Stokes (RANS) approaches to the problem of predicting turbulent sediment transport, since these are likely to remain dominant in practical computations. Two other general approaches may be mentioned very briefly. Large-eddy simulation (LES) attempts a solution of the unsteady three-dimensional Navier-Stokes equations. Unlike RANS models, time averaging is not applied, but spatial averaging or filtering over small scales is performed. This necessitates modeling on these small subgrid scales, which is thought to be easier because of the more universal characteristics of small-scale motion. Reviews of this approach may be found in the book edited by Galperin and Orszag (1993) and articles by Ferziger (1996) and Piomelli and Chasnov (1996). LES is extremely demanding of computational resources, much more so than even second-moment closure, because sufficient numerical spatial and temporal resolution is needed to ensure realization of a turbulent flow, and the computation must be conducted over a sufficiently long duration for meaningful flow statistics, even for a statistically steady problem. When the typical scale of hydraulic and sediment transport problems is considered, it is doubtful that LES will be applied to problems outside of the laboratory for the foreseeable future. Like the even more extreme direct numerical simulation, where the aim is to resolve all scales with no modeling assumptions being made, one of the main advantages of LES applied to homogeneous fluids is the minimal modeling involved. In its extension to the two-phase sediment-transport problem, however, the modeling involved is much more substantial, and so the attractiveness of LES is

correspondingly diminished. For example, Zedler and Street (2001) performed an LES study of sediment transport over a rippled bed (the size of the larger computational domain was $20.3 \times 2.1 \times 7.7$ cm!), in which an advective-diffusion equation (similar to Eq. (16-7)) is used to model sediment transport. Already a continuum model assumption is made about which some question might be raised (in regions of high concentration, with $c \sim 0.005$, it is estimated that there might have been less than five particles within a numerical cell). Further, a molecular diffusion coefficient (equal to the fluid kinematic viscosity!) was imputed to the sediment for modeling reasons, but its physical origin is dubious. Even for a single-phase flow, LES encounters problems in the flow region near a wall (Ferziger 1996), such that, with the added difficulties posed by high particle concentrations and roughness, not to mention bed forms, the model component become much more substantial. Nevertheless, research results with LES applied to problems related to sediment transport are beginning to appear with greater regularity (Chang and Scotti 2003; Portela and Oliemans 2003).

The last general approach deserving of some mention is less specifically a distinct modeling approach than a conceptual framework for developing models that may ultimately be formally similar to classic models such as a mixing-length model. The central role of coherent structures, especially in wall-bounded turbulence, is emphasized in this framework (Nezu and Nakagawa 1993). Early contributions from researchers in sediment transport include Einstein and Li (1959), Grass (1971), and Jackson (1976), but recent experimental work has attempted to interpret sediment transport in terms of coherent structures (e.g., Müller and Gyr 1986; Wei and Willmarth 1991; Bennett and Best 1995; Nelson et al. 1995; Nino and Garcia 1996; Bennett and Best, 1998), and first attempts have been made to base quantitative predictive models (e.g., Cao 1996) on these concepts. Although these may eventually lead to models competitive with the standard RANS models, experience outside of the sediment transport field is not conducive to optimism (Bradshaw 1997).

APPENDIX I. CARTESIAN TENSOR NOTATION

In this chapter, the governing equations involved scalars (concentration), characterized only by a magnitude, vectors (momentum), characterized by magnitude and direction, with three components, and second-order tensors (stresses), characterized by magnitude, direction, and a surface orientation, with nine components. The use of Cartesian tensor notation offers an economical means of expressing what would in conventional notation be rather lengthy equations.

I.1 Index Notation for Vectors and Tensors

Rather than the conventional use of different symbols for different coordinate directions, the use of a subscripted index

notation is preferred. A position vector, (x, y, z) , is therefore denoted as (x_1, x_2, x_3) , which can be further reduced to x_i , $i = 1, 2, 3$. Similarly, the velocity vector, often denoted by (u, v, w) , is written as (u_1, u_2, u_3) or simply u_i . The benefits are multiplied when the quantity of interest is a tensor quantity, such as stress, which has nine rather than the three components of a vector quantity. It is helpful to view a second-order tensor as a matrix quantity; e.g., the stress tensor, T_{ij} , can be written as

$$T_{ij} = \begin{bmatrix} \tau_{11} & \tau_{12} & \tau_{13} \\ \tau_{21} & \tau_{22} & \tau_{23} \\ \tau_{31} & \tau_{32} & \tau_{33} \end{bmatrix}. \quad (16-76)$$

The tensors discussed in the preceding are symmetric in that the matrix is symmetric; i.e., $\tau_{12} = \tau_{21}$, $\tau_{13} = \tau_{31}$, and $\tau_{23} = \tau_{32}$. For stresses, the first subscript indicate the surface on which the stress acts (the surface is perpendicular to the coordinate direction referred to by the first subscript), where as the second subscript indicate the direction of the stress.

The tensor product of two vectors yields a tensor, such as the Reynolds stress tensor, which is the product of fluctuating velocity vectors, averaged over time. Thus, it can be written as

$$\overline{-u'_i u'_j} = \begin{bmatrix} \overline{-u'_1 u'_1} & \overline{-u'_1 u'_2} & \overline{-u'_1 u'_3} \\ \overline{-u'_2 u'_1} & \overline{-u'_2 u'_2} & \overline{-u'_2 u'_3} \\ \overline{-u'_3 u'_1} & \overline{-u'_3 u'_2} & \overline{-u'_3 u'_3} \end{bmatrix}. \quad (16-77)$$

A useful tensor quantity is the Kronecker delta, δ_{ij} , which can be interpreted as an identity matrix; i.e.,

$$\delta_{ij} = \begin{bmatrix} 1 & 0 & 0 \\ 0 & 1 & 0 \\ 0 & 0 & 1 \end{bmatrix}. \quad (16-78)$$

The Boussinesq eddy-viscosity model can therefore be expressed alternatively as

$$\begin{aligned} & \begin{bmatrix} \overline{-u'_1 u'_1} - \overline{u'_1 u'_2} - \overline{u'_1 u'_3} \\ \overline{-u'_2 u'_1} - \overline{u'_2 u'_2} - \overline{u'_2 u'_3} \\ \overline{-u'_3 u'_1} - \overline{u'_3 u'_2} - \overline{u'_3 u'_3} \end{bmatrix} \\ &= \begin{bmatrix} \nu_t \left(\frac{\partial \bar{u}_1}{\partial x_1} + \frac{\partial \bar{u}_1}{\partial x_1} \right) - \frac{2}{3} k \nu_t \left(\frac{\partial \bar{u}_1}{\partial x_2} + \frac{\partial \bar{u}_2}{\partial x_1} \right) \\ \nu_t \left(\frac{\partial \bar{u}_2}{\partial x_1} + \frac{\partial \bar{u}_1}{\partial x_2} \right) & \nu_t \left(\frac{\partial \bar{u}_2}{\partial x_2} + \frac{\partial \bar{u}_2}{\partial x_2} \right) - \frac{2}{3} k \\ \nu_t \left(\frac{\partial \bar{u}_3}{\partial x_1} + \frac{\partial \bar{u}_1}{\partial x_3} \right) & \nu_t \left(\frac{\partial \bar{u}_3}{\partial x_2} + \frac{\partial \bar{u}_2}{\partial x_3} \right) \end{bmatrix} \end{aligned}$$

$$\begin{bmatrix} \nu_t \left(\frac{\partial \bar{u}_1}{\partial x_3} + \frac{\partial \bar{u}_3}{\partial x_1} \right) \\ \nu_t \left(\frac{\partial \bar{u}_2}{\partial x_3} + \frac{\partial \bar{u}_3}{\partial x_2} \right) \\ \nu_t \left(\frac{\partial \bar{u}_3}{\partial x_3} + \frac{\partial \bar{u}_3}{\partial x_3} \right) - \frac{2}{3} k \end{bmatrix}. \quad (16-79)$$

Equation (16-79) may be compared with Eq. (16-14). It also illustrates more concretely how restrictive the Boussinesq eddy-viscosity assumption is regarding the relationship between the Reynolds stress tensor and the mean strain tensor.

I.2 The Summation Convention

In multidimensional problems, the governing equations often involve sums of contributions from components associated with different coordinate directions. The summation convention provides a conveniently compact manner of expressing sums involving vectors and tensors. In Cartesian coordinates, whenever the same (roman) letter subscript is repeated, then that subscript takes on all possible values and the results are summed. Thus, the fluid continuity equation for an incompressible fluid can be written as

$$\frac{\partial u_j}{\partial x_j} = \frac{\partial u_1}{\partial x_1} + \frac{\partial u_2}{\partial x_2} + \frac{\partial u_3}{\partial x_3} = 0. \quad (16-80)$$

The repeated index, j , takes on all values, $j = 1, 2, 3$, and the respective quantities are summed. Another example is the advection term in the momentum equation, e.g.,

$$\frac{\partial(u_i u_j)}{\partial x_j} = \frac{\partial(u_i u_1)}{\partial x_1} + \frac{\partial(u_i u_2)}{\partial x_2} + \frac{\partial(u_i u_3)}{\partial x_3} \quad (16-81)$$

Here, although there are two indices, i and j , only j is repeated, so that u_i remained unchanged, but j again takes on all values and the results are summed. For $i = 1$, this would be the advection term for the momentum balance in the x_1 -direction. A final example is given by the production term, $P_k = -\overline{u'_i u'_j} S_{ij}$, in the turbulent kinetic energy equation. Because the k -equation is a scalar equation, P_k is necessarily a scalar, but it is a product of two tensors, the Reynolds stress tensor, $-\overline{u'_i u'_j}$, and the mean strain rate tensor, S_{ij} . The procedure of arriving at a scalar from a (scalar) product of second-order tensors is sometimes termed a contraction, and is signaled by two repeated indices, both i and j . Because there are two repeated indices rather than one, a total of nine rather than three terms are included in the summation. If expanded, Eq. (16-35) would appear as

$$\begin{aligned}
P_k = & -\overline{u'_1 u'_1} \left[\frac{1}{2} \left(\frac{\partial u_1}{\partial x_1} + \frac{\partial u_1}{\partial x_1} \right) \right] - \overline{u'_1 u'_2} \left[\frac{1}{2} \left(\frac{\partial u_1}{\partial x_2} + \frac{\partial u_2}{\partial x_1} \right) \right] \\
& - \overline{u'_2 u'_1} \left[\frac{1}{2} \left(\frac{\partial u_2}{\partial x_1} + \frac{\partial u_1}{\partial x_2} \right) \right] - \overline{u'_2 u'_2} \left[\frac{1}{2} \left(\frac{\partial u_2}{\partial x_2} + \frac{\partial u_2}{\partial x_2} \right) \right] \\
& - \overline{u'_3 u'_1} \left[\frac{1}{2} \left(\frac{\partial u_3}{\partial x_1} + \frac{\partial u_1}{\partial x_3} \right) \right] - \overline{u'_3 u'_2} \left[\frac{1}{2} \left(\frac{\partial u_3}{\partial x_2} + \frac{\partial u_2}{\partial x_3} \right) \right] \\
& - \overline{u'_1 u'_3} \left[\frac{1}{2} \left(\frac{\partial u_1}{\partial x_3} + \frac{\partial u_3}{\partial x_1} \right) \right] - \overline{u'_2 u'_3} \left[\frac{1}{2} \left(\frac{\partial u_2}{\partial x_3} + \frac{\partial u_3}{\partial x_2} \right) \right] \\
& - \overline{u'_3 u'_3} \left[\frac{1}{2} \left(\frac{\partial u_3}{\partial x_3} + \frac{\partial u_3}{\partial x_3} \right) \right]. \tag{16-82}
\end{aligned}$$

The first three terms on the right hand side hold $i = 1$, while j takes on all three values; the next three terms hold $i = 2$, while j takes on all three values; and so on. P_k is sometimes written in an alternative manner, namely, $P_k = -\overline{u'_i u'_j} (\partial \bar{u}_i / \partial x_j)$, which can be shown to lead ultimately to the same expression for P_k .

Although tensor notation has been exploited here primarily for convenience, much of the current development of new turbulence models relies heavily on the language associated with tensors, such as invariance and material frame indifference, which arises in the development of constitutive equations in continuum mechanics. An introduction to such concepts is given in Malvern (1969).

APPENDIX II. SPATIALLY AVERAGED MODELS

The problem of turbulence closure arose from a simplification of the Navier-Stokes equations in which temporal averages were taken. A similar though quite distinct problem arises when simplification by spatial averaging is sought. In traditional one-dimensional (sediment-free) hydraulics, cross-sectional averaging leads to momentum and kinetic energy correction coefficients that vary with the degree of spatial heterogeneity of bulk flow velocity at any specific cross section. Model equation(s) must be developed for these coefficients if these play any significant role. The classic problem of longitudinal shear dispersion in a pipe or channel provides another example of the effects of spatial averaging, which is more directly comparable to the turbulence problem. In this case, a cross-sectionally averaged model leads to apparently substantially increased (longitudinal) transport, which under certain conditions can be effectively modeled by a gradient-transport relationship with a constant *dispersion coefficient* (Fischer et al. 1979). Apart from cross-sectional averaging, the most common form of spatial averaging

is averaging over the depth, which can often be justified because vertical variations in flow quantities are much less important than variations in the plan or horizontal directions. Less frequently encountered, width averaging may have special appeal for sediment-transport problems because the vertical direction, central to the sedimentation process, retains an explicit role in the simulation. Other, more subtle forms of spatial averaging are often implicitly applied. Approaches where bed forms are present in a flow but are not explicitly modeled may be viewed as implicitly spatially averaging or filtering out bed details. The following is limited to depth-averaged models, but similar issues would arise in other spatially averaged models. Further discussion of spatially averaged and depth-averaged models may be found in Chapter 15, as well as in the review by the ASCE Task Committee on Turbulence Models in Hydraulic Computations (1988).

Similarly to a time-averaged variable (recall Eq. (16-1)), the depth-averaged variable, $\langle f \rangle$, can be obtained by integration over the local depth, $h(X, Y, t)$,

$$\langle f \rangle(X, Y, t) = \frac{1}{h(X, Y, t)} \int_{Z_{\text{bed}}(X, Y, t)}^{Z_{\text{bed}}(X, Y, t) + h(X, Y, t)} f(X, Y, Z, t) dZ \tag{16-83}$$

where X and Y denote the plan location in the streamwise and in the lateral direction, and Z_{bed} is the local elevation of the bed (see Fig. 16-24). The deviation of f from $\langle f \rangle$ along the vertical coordinate, Z , is denoted as f^* , so that f can be decomposed as $f = \langle f \rangle + f^*$. In much the same way as in Reynolds averaging, problems arise from the nonlinear advection terms when the momentum equations are integrated over the depth. Consider, for example, the depth-averaging of the advective flux of streamwise momentum over the depth,

$$\langle uu \rangle = \langle ((u) + u^*)((u) + u^*) \rangle = \langle u \rangle^2 + \langle u^* u^* \rangle \tag{16-84}$$

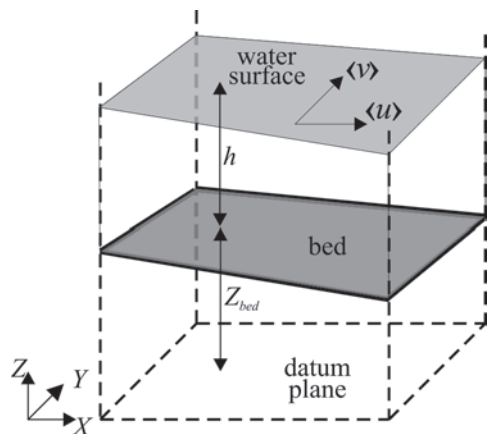


Fig. 16-24. Definition sketch for depth-averaged model.

where

$$\langle u^* u^* \rangle = \frac{1}{h(X, Y, t)} \int_{z_{\text{bed}}}^{z_{\text{bed}} + h(X, Y, t)} (u - \langle u \rangle)^2 dZ. \quad (16-85)$$

The spatial correlation terms such as $\langle u^* u^* \rangle$ are not necessarily zero, and when they are not negligible should be included in the transport equations.

Almost invariably, depth-averaged models invoke the shallow-water-wave approximation, i.e., neglect of vertical accelerations such that the vertical momentum equation reduces to the equation of hydrostatics, with the resulting governing equations

$$\frac{\partial h}{\partial t} + \frac{\partial(h\langle u \rangle)}{\partial X} + \frac{\partial(h\langle v \rangle)}{\partial Y} = 0 \quad (16-86a)$$

$$\begin{aligned} & \frac{\partial(h\langle u \rangle)}{\partial t} + \frac{\partial(h\langle u \rangle^2)}{\partial X} + \frac{\partial(h\langle u \rangle\langle v \rangle)}{\partial Y} \\ &= -gh \frac{\partial}{\partial X}(h + Z_{\text{bed}}) + \frac{(\tau_{sx} - \tau_{bx})}{\rho} \\ &+ \frac{1}{\rho} \left[\frac{\partial}{\partial X} \left\{ h \left(\bar{\tau}_{xx} - \rho \langle u^* u^* \rangle \right) \right\} \right] \\ &+ \frac{1}{\rho} \left[\frac{\partial}{\partial Y} \left\{ h \left(\bar{\tau}_{xy} - \rho \langle u^* v^* \rangle \right) \right\} \right] \end{aligned} \quad (16-86b)$$

$$\begin{aligned} & \frac{\partial(h\langle v \rangle)}{\partial t} + \frac{\partial(h\langle u \rangle\langle v \rangle)}{\partial X} + \frac{\partial(h\langle v \rangle^2)}{\partial Y} \\ &= -gh \frac{\partial}{\partial Y}(h + Z_{\text{bed}}) + \frac{\tau_{sy} - \tau_{by}}{\rho} \\ &+ \frac{1}{\rho} \left[\frac{\partial}{\partial X} \left\{ h \left(\bar{\tau}_{xy} - \rho \langle u^* v^* \rangle \right) \right\} \right] \\ &+ \frac{1}{\rho} \left[\frac{\partial}{\partial Y} \left\{ h \left(\bar{\tau}_{yy} - \rho \langle u^* v^* \rangle \right) \right\} \right]. \end{aligned} \quad (16-86c)$$

The shear stresses at the bed and at the water surface, τ_{bx} and τ_{sx} , τ_{by} and τ_{sy} , follow from integration over the depth, and flow-resistance relationships specifying these in terms of the other variables, such as $\langle u \rangle$ and $\langle v \rangle$, must be externally provided. In many practical cases where the flow may be considered well-mixed over the depth, the deviation or dispersion terms, $\langle u^* u^* \rangle$, $\langle u^* v^* \rangle$, and $\langle v^* v^* \rangle$, are small and can be justifiably neglected. As suggested by the form of Eq. (16-86), these terms act like effective stresses, but, unlike Reynolds stresses, are not related to turbulence, but rather, as should be clear from Eq. (16-85), stem entirely from spatial averaging over nonuniformities in time-averaged quantities in the vertical direction. If these are important, then separate models, most likely problem-specific, must be provided for

them. As might be expected from Taylor dispersion (Fischer et al. 1979), a gradient-transport model, possibly with a constant dispersion coefficient, might under certain conditions be appropriate. For expedience, such a model assumption is frequently made in practice, even when a theoretical justification cannot be rigorously made, to account for the dispersion terms if these are not altogether ignored. More sophisticated models of dispersion make specific assumptions regarding the vertical distributions of mean velocity and concentration, and compute the dispersive transport by integration, similarly to Eq. (16-85). Lane (1998) discusses the modeling of dispersive transport in depth-averaged models. Evidently vertical motion features, e.g., due to buoyancy effects, are not captured in Eq. (16-86), except possibly indirectly in the dispersion terms, so that if these are of interest, a depth-averaged model is unlikely to be appropriate.

A depth-averaged turbulence model is concerned solely with determining the remaining stress terms, $\bar{\tau}_{xx}$, $\bar{\tau}_{xy}$, $\bar{\tau}_{yy}$. Turbulence models ranging from zero- to two-equation models may be considered for this purpose in a manner analogous to the non-depth-averaged models already discussed. Zero-equation constant-eddy-viscosity and mixing-length models have been applied. Depth-averaged two-equation models could conceivably be derived in the same way as the continuity and momentum equations by integrating the equations, say for k and ϵ , over the depth. This would pose difficulties in the treatment of the important production and destruction source/sink terms, as well as in the definition of eddy viscosity, which must be related, preferably in a computationally simple manner, to depth-averaged quantities, such as $\langle u \rangle$. Thus, a more heuristic approach is taken in formulating turbulence two-equation model equations that are analogous to those applied in non-depth-averaged models. A $k-\epsilon$ model for depth-averaged simulations (Rastogi and Rodi 1978; Rodi 1993) may therefore be given as

$$\begin{aligned} & \frac{\partial(\langle k \rangle)}{\partial t} + \frac{\partial(\langle u \rangle\langle k \rangle)}{\partial X} + \frac{\partial(\langle v \rangle\langle k \rangle)}{\partial Y} \\ &= \frac{\partial}{\partial X} \left(\frac{\langle v_t \rangle}{\sigma_{\langle k \rangle}} \frac{\partial \langle k \rangle}{\partial X} \right) + \frac{\partial}{\partial Y} \left(\frac{\langle v_t \rangle}{\sigma_{\langle k \rangle}} \frac{\partial \langle k \rangle}{\partial Y} \right) \\ &+ \langle P_k \rangle + (\langle P_{k \rangle}_b - \langle \epsilon \rangle) \end{aligned} \quad (16-87a)$$

$$\begin{aligned} & \frac{\partial(\langle \epsilon \rangle)}{\partial t} + \frac{\partial(\langle u \rangle\langle \epsilon \rangle)}{\partial X} + \frac{\partial(\langle v \rangle\langle \epsilon \rangle)}{\partial Y} \\ &= \frac{\partial}{\partial X} \left(\frac{\langle v_t \rangle}{\sigma_{\langle \epsilon \rangle}} \frac{\partial \langle \epsilon \rangle}{\partial X} \right) + \frac{\partial}{\partial Y} \left(\frac{\langle v_t \rangle}{\sigma_{\langle \epsilon \rangle}} \frac{\partial \langle \epsilon \rangle}{\partial Y} \right) \\ &+ c_{1(\epsilon)} \langle P_k \rangle + (\langle P_{\epsilon \rangle}_b - c_{2(\epsilon)} \frac{\langle \epsilon \rangle^2}{\langle k \rangle}) \end{aligned} \quad (16-87b)$$

The term $\langle P_k \rangle$, modeling the production of the depth-averaged turbulent kinetic energy $\langle k \rangle$ by gradients in $\langle u \rangle$ and $\langle v \rangle$, is the two-dimensional version of Eq. (16-35) (or Eq. (16-82)); i.e.,

$$\begin{aligned} \langle P_k \rangle = \langle v_t \rangle & \left[2 \left(\frac{\partial \langle u \rangle}{\partial X} \right)^2 + 2 \left(\frac{\partial \langle v \rangle}{\partial Y} \right)^2 \right. \\ & \left. + \left(\frac{\partial \langle u \rangle}{\partial Y} + \frac{\partial \langle v \rangle}{\partial X} \right)^2 \right]. \end{aligned} \quad (16-88)$$

Equations (16-87) are *not* derived from integrating the corresponding three-dimensional equations over depth, but rather may be more precisely viewed as a plausible but ad hoc extension to a two-dimensional model. As such, $\langle k \rangle$, $\langle \epsilon \rangle$, and $\langle v_t \rangle$ should *not* be interpreted literally as depth-averaged analogues of the three-dimensional k and ϵ . Equations (16-87) are therefore most appropriate in simulating flows where the turbulent flow features of greatest interest are those in the horizontal plane.

The constitutive relationship between stress and “rate of strain” is sometimes written in the same manner as Eq. (16-14), namely,

$$\begin{aligned} \frac{\bar{\tau}_{xx}}{\rho} &= 2 \langle v_t \rangle \left(\frac{\partial \langle u \rangle}{\partial X} \right) - \frac{2}{3} \langle k \rangle, \\ \frac{\bar{\tau}_{yy}}{\rho} &= 2 \langle v_t \rangle \left(\frac{\partial \langle v \rangle}{\partial Y} \right) - \frac{2}{3} \langle k \rangle, \\ \frac{\bar{\tau}_{xy}}{\rho} &= \langle v_t \rangle \left(\frac{\partial \langle u \rangle}{\partial Y} + \frac{\partial \langle v \rangle}{\partial X} \right). \end{aligned} \quad (16-89)$$

A difficulty is apparent in Eq. (16-89) in that the term $-2\langle k \rangle/3$ no longer serves the purpose of ensuring consistency between the stress-rate-of-strain relationship and the definition of $\langle k \rangle$ (note the difference in continuity equations, Eq. (16-2a) and Eq. (16-86a)). An alternative constitutive relationship, due to Chapman and Kuo (1985), and adopted by Biglari and Sturm (1998) in a study of flow around bridge abutments, expresses, e.g., $h\bar{\tau}_{xx}$ in terms of gradients of $\partial(h\langle u \rangle)/\partial X$ and so on; it is consistent only for steady flows, and its basis in the physics of turbulent flows is somewhat tenuous. As seen before with buoyancy and vegetation effects, the presence of additional forcing terms in the momentum equations, i.e., the stresses at the bottom (and presumably at the water surface, though this is generally ignored) requires additional source terms,

$$\langle P_{\langle k \rangle} \rangle_b = \langle c_{\langle k \rangle} \rangle_b u_*^3/h, \quad \langle P_{\langle \epsilon \rangle} \rangle_b = \langle c_{\langle \epsilon \rangle} \rangle_b u_*^4/h^2 \quad (16-90)$$

where u_* is a bottom shear velocity obtained from the same friction relationship used to obtain τ_{bx} .

The closure constants, $c\langle k \rangle$, $c\langle \epsilon \rangle$, $\sigma\langle k \rangle$, and $\sigma\langle \epsilon \rangle$, are rather boldly chosen to be the same as in the standard model (Table 16-2), whereas the remaining closure constants, $\langle c_{\langle k \rangle} \rangle_b$ and $\langle c_{\langle \epsilon \rangle} \rangle_b$, are chosen for consistency with results for the simple case of unidirectional steady uniform channel flow. In the latter case, where $\langle P_k \rangle \equiv 0$ and transport terms are either zero or negligible, with a local-equilibrium balance being established between production and dissipation, the usual relationships, $\langle \epsilon \rangle \sim u_*^3$ and $\langle k \rangle \sim u_*^2$, are obtained:

$$\begin{aligned} u_* &= \left[c_f (\langle u \rangle^2 + \langle v \rangle^2) \right]^{1/2}, \\ \langle c_{\langle k \rangle} \rangle_b &= c_f^{-1/2}, \quad \langle c_{\langle \epsilon \rangle} \rangle_b = E_* \frac{c_{2\epsilon} c_\mu^{1/2}}{c_f^{3/4}} \end{aligned} \quad (16-91)$$

where c_f is a friction coefficient and E_* is a constant that may be used for calibration (Minh Duc et al. 1998; Rodi 1993 gave $E_* = 3.6$). The eddy viscosity for the depth-averaged model is obtained exactly as before, $v_t^* = c_\mu \langle k \rangle^{2/3}/\langle \epsilon \rangle$. Again, in the simple case of unidirectional steady uniform channel flow, this reduces to a constant-coefficient zero-equation model, $v_t^* \sim u_* h$.

The depth-averaged equation for suspended sediment transport can be similarly expressed as

$$\begin{aligned} \frac{\partial(h\langle c \rangle)}{\partial t} &+ \frac{\partial(h\langle u \rangle\langle c \rangle)}{\partial X} + \frac{\partial(h\langle v \rangle\langle c \rangle)}{\partial Y} \\ &= \frac{\partial}{\partial X} \left[h \left(\frac{v_t^*}{\sigma_c} \frac{\partial \langle c \rangle}{\partial X} - \langle u^* c^* \rangle \right) \right] \\ &\quad + \frac{\partial}{\partial Y} \left[h \left(\frac{v_t^*}{\sigma_c} \frac{\partial \langle c \rangle}{\partial Y} - \langle v^* c^* \rangle \right) \right] + B \end{aligned} \quad (16-92)$$

where $\langle u^* c^* \rangle$ and $\langle v^* c^* \rangle$ are the dispersion terms, and B is a source/sink term analogous to the terms involving τ_{bx} and τ_{by} in Eq. (16-86) representing entrainment and deposition at the bed, essentially equivalent to $\langle J_s \rangle_b$ of Eq. (16-57). It is reiterated that the dispersion terms, $\langle u^* c^* \rangle$ and $\langle v^* c^* \rangle$, may not necessarily be well described by a simple gradient-transport model. The difficulty of defining an appropriate bottom boundary condition for sediment remains in depth-averaged models, and is compounded by the need to express this in terms, not of local bottom concentration, c_b , as in Eq. (16-57), but of the modeled depth-averaged concentration, $\langle c \rangle$. Similarly to the more complete model, a bed-load model may also be needed.

The commonly used depth-averaged models described above are undoubtedly useful tools, but they constitute engineering compromises, the limitations of which should be recognized. If vertical nonuniformities and motion are important, then neglect of dispersion terms can really not

be justified. For sediment transport applications where suspended load is significant, the vertical distribution of suspended sediment is likely to be much more nonuniform than that of velocity. Even with dispersion terms included, the effects of vertical motion may only be quite imperfectly modeled, because flow is constrained to be in the $X-Y$ plane. Differences in the *direction* of the depth-averaged velocity vector and the point velocity (non-zero-velocity skewness angles) will be important in sediment transport, not only for the suspended load, but also for the bed load, since the direction of the bottom shear force may differ from the direction of the depth-averaged velocity. Additional model elements, typically involving specific models of vertical velocity distributions, can be introduced in order to sensitize the standard depth-averaged $k-\epsilon$ model to effects due to flow and nonuniformities in the vertical direction. The depth-averaged model clearly involves a greater number of modeling assumptions, based largely on the convenience and simplicity of the resulting model equations and empirical experience.

REFERENCES

- Ahmed, F., and Rajaratnam, N. (1998). "Flow around bridge piers." *Journal of Hydraulic Engineering, ASCE*, 124, (3), 288–300.
- Alonso, C. V. (1981). "Stochastic models of suspended-sediment dispersion." *Journal of the Hydraulics Divisions., ASCE*, 107 (HY6), 733–757.
- Apsley, D., Chen, W.-L., Leschziner, M., and Lien, F.-S. (1997). "Non-linear eddy-viscosity modeling of separated flows." *Journal of Hydraulic Research*, 35(6), 723–748.
- Armanini, A., and DiSilvio, G. (1988). "A one-dimensional model for the transport of a sediment mixture in non-equilibrium conditions." *Journal of Hydraulic Research*, 26(3), 275–292.
- ASCE Task Committee on Turbulence Models in Hydraulic Computations (1988). "Turbulence modeling of surface water flow and transport: I, II, III, IV, and V." *Journal of Hydraulic Engineering, ASCE*, 114(9), 970–1073.
- Barenblatt, G. I. (1953). "On the motion of suspended particles in a turbulent flow." *Prikladnaya Matematika Mekhanika*, 16 (1), 67–78.
- Barenblatt, G. I. (1996). *Scaling, self-similarity, and intermediate asymptotics*. Cambridge University Press, Cambridge, U.K.
- Barton, J. R., and Lin, P.-N. (1955). *A study of the sediment transport in alluvial streams*. Civil Engineering Dept., Colorado A & M College, Fort Collins, Colo.
- Baumert, H., and Peters, H. (2000). "Second-moment closures and length scales for weakly stratified turbulent shear flows." *Journal of Geophysical Research*, 105, (C3), 6453–6568.
- Bennett, S. J., and Best, J. L. (1995). "Mean flow and turbulence structure over fixed, two-dimensional dunes: Implications for sediment transport and bedform stability." *Sedimentology*, 42, 491–513.
- Bennett, S. J., Bridge, J. S., and Best, J. L. (1998). "Fluid and sediment dynamics of upper-stage plane beds." *Journal of Geophysical Research*, 103, (C1), 1239–1274.
- Biglari, B., and Sturm, T. W. (1998). "Numerical modeling of flow around bridge abutments in compound channel." *Journal of Hydraulic Engineering ASCE*, 124, (2), 156–164.
- Blanckaert, K., and Graf, W. H. (2001). "Mean flow and turbulence in open channel bend." *Journal of Hydraulic Engineering, ASCE*, 127, (10), 835–847.
- Blumberg, A. F., Galperin, B., and O'Connor, D. J. (1992). "Modeling vertical structure of open channel flow." *Journal of Hydraulic Engineering, ASCE*, 118, (8), 1119–1134.
- Boillat, J. L., and Graf, W. H. (1981). "Settling velocity of spherical particles in calm water." *Journal of the Hydraulics Divisions, ASCE*, 107(HY10), 1123–1131.
- Boillat, J. L., and Graf, W. R. (1982). "Vitesse de sédimentation de particules sphériques en milieu turbulent [Settling velocities of spherical particles in turbulent media]." *Journal of Hydraulic Research*, 20(5), 395–413.
- Boivin, M., Simonin, O., and Squires, K. D. (1998). "Direct numerical simulation of turbulence modulation by particles in isotropic turbulence." *Journal of Fluid Mechanics*, 375, 235–263.
- Bradshaw, P. (1997). "Understanding and prediction of turbulent flows—1996." *International Journal of Heat and Fluid Flow*, 18, 45–54.
- Brereton, G. J., and Mankbadi, R. R. (1995). "Review of recent advances in the study of unsteady turbulent internal flows." *Applied Mechanics Review*, 48, (4), April, 189–212.
- Brors, B., and Eidsvik, K. J. (1994). "Oscillatory boundary layer flows modelled with dynamic Reynolds stress turbulence closure." *Continental Shelf Research*, 14, (13/14), 1455–1475.
- Burchard, H., and Baumert, H. (1995). "On the performance of a mixed-layer model based on the $k-\epsilon$ turbulence closure." *Journal of Geophysical Research*, 100, (C5), 8523–8540.
- Burchard, H., Petersen, O., Rippeth, T. P. (1998). "Comparing the performance of the Mellor-Yamada and the $k-\epsilon$ two-equation turbulence models." *Journal of Geophysical Research* 103, (C5), 10543–10554.
- Burke, R. W., and Stolzenbach, K. D. (1983). *Free surface flow through salt marsh grass*, Sea Grant Rep. MITSG 83–16, Massachusetts Institute of Psychology, Cambridge, Mass.
- Cao, Z., Zhang, X., and Xi, H. (1996). "Turbulent bursting-based diffusion model for suspended sediment in open-channel flows." *Journal of Hydraulic Research*, 34, (4), 457–472.
- Cebeci, T., and Bradshaw, P. (1977). *Momentum transfer in boundary layers*. Hemisphere, Washington, D.C.
- Celik, I. (1982). "Discussion of 'Mixture theory for suspended sediment transport' by D. F. McTigue." *Journal of the Hydraulics Division., ASCE*, 108, (HY3), 467–468.
- Celik, I., and Rodi, W. (1984). "Simulation of free-surface effects in turbulent channel flows." *Physicochemical Hydrodynamics*, 5, (3/4), 217–227.
- Celik, I., and Rodi, W. (1988). "Modeling suspended sediment transport in nonequilibrium situations." *Journal of Hydraulic Engineering, ASCE*, 114, (10), 1157–1191.
- Cellino, M., and Graf, W. H. (1999). "Sediment-laden flow in open-channels under noncapacity and capacity conditions." *Journal of Hydraulic Engineering, ASCE*, 125, (5), 455–462.
- Cellino, M., and Graf, W. H. (2000). "Experiments on suspension flow in open channels with bed forms." *Journal of Hydraulic Research*, 38, (4), 289–298.
- Chang, Y. S., and Scotti, A. (2003). "Entrainment and suspension of sediments into a turbulent flow over ripples." *Journal of Turbulence*, 4, 1–22.
- Chapman, R. S., and Kuo, C. Y. (1985). "Application of the two-equation $k-\epsilon$ turbulent model to a two-dimensional, steady, free

- surface flow problem with separation." *International Journal of Numerical Methods in Fluids*, 5, 257–268.
- Chen, C.-J., and Jaw, S.-Y. (1998). *Fundamentals of turbulence modeling*. Taylor & Francis, Washington, D.C.
- Cheong, H. F., and Xue, H. (1997). "Turbulence model for water flow over two-dimensional bed forms." *Journal of Hydraulic Engineering, ASCE*, 123, (5), 402–409.
- Clift, R., Grace, J. R., and Weber, M. E. (1978). *Bubbles, drops, and particles*. Academic Press, New York.
- Coleman, N. L. (1970). "Flume studies of the sediment transfer coefficient." *Water Resources Research*, 6, (3), 801–809.
- Coleman, N. L. (1981). "Velocity profiles with suspended sediment." *Journal of Hydraulic Research*, 19, (3), 211–229.
- Craft, T. J., Suga, K., and Launder, B. E. (1993). "Extending the applicability of eddy viscosity models through the use of deformation invariants and non-linear elements." *Proc., 5th International Symposium on Refined Modeling and Turbulence Measurements*, International Association for Hydraulic Research, Paris, France, 125–132.
- Crowe, C. T., Troutt, T. R., and Chung, J. N. (1996). "Numerical models for two-phase turbulent flows." *Annual Reviews of Fluid Mechanics*, 28, 11–44.
- Crowe, C., Sommerfeld, M., and Tsuji, Y. (1998). *Multiphase flows with droplets and particles*. CRC Press, Boca Raton, Fla.
- Dargahi, B. (1989). "The turbulent flow field around a circular cylinder." *Experiments in Fluids*, 8, 1–12.
- Davies, A. G. (1995). "Effects of unsteadiness on the suspended sediment flux in co-linear wave-current flow." *Continental Shelf Research*, 15, (8), 949–979.
- Davies, A. M., Jones, J. E., and Xing, J. (1997). "Review of recent developments in tidal hydrodynamics modeling. II: Turbulence energy models." *Journal of Hydraulic Engineering, ASCE*, 123, (4), 293–302.
- Davies, A. G., Ribberink, J. S., Temperville, A., and Zyberman, J. A. (1997). "Comparison between sediment transport models and observations made in wave and current flows above plane beds." *Coastal Engineering*, 31, 163–198.
- Devantier, B. A., and Larock, B. E. (1987). "Modeling sediment-induced density currents in sedimentation basins." *Journal of Hydraulic Engineering, ASCE*, 113, (1), 80–94.
- Devenport, W. J., and Sutton, E. P. (1991). "Near-wall behavior of separated and reattaching flows." *AIAA Journal*, 29, (1), 25–31.
- Dietrich, W. D. (1982). "Flow, boundary shear stress, and sediment transport in a river meander." Ph.D. dissertation, University of Washington, Seattle, Wash.
- Drew, D. A. (1975). "Turbulent sediment transport over a flat bottom using momentum balance." *Journal of Applied Mechanics, Transaction of the ASME*, 38–44.
- Drew, D. A. (1983). "Mathematical modeling of two-phase flows." *Annual Reviews of Fluid Mechanics*, 15, 261–291.
- Durbin, P. A., and Petterson Reif, B. A. (2001). *Statistical theory and modeling for turbulent flows*. Wiley, Chichester, U.K.
- Einstein, H. A., and Chien, N. (1954). Second approximation to the solution of the suspended load theory. *Research Rep. No. 3*, University of California, Berkeley, Calif.
- Einstein, H. A., and Chien, N. (1955). "Effects of heavy sediment concentration near the bed on velocity and sediment distribution." *M. R. D. Sediment Series, No. 8*, Univ. of Calif. Inst. of Eng. Research, U.S. Army Eng. Div., Missouri River.
- Einstein, H. A., and Li, H. (1959). "The viscous sublayer along a smooth boundary." *Proceeding of the ASCE 82*, Paper 945, 1–27.
- Elghobashi, S. (1994). "On predicting particle-laden turbulent flows." *Applied Science Research*, 52, 309–329.
- Elghobashi, S. E., and Abou-Arab, T. W. (1983). "A two-equation turbulence model for two-phase flows." *Physics of Fluids*, 26, (4), 931–938.
- Elghobashi, S. E., and Truesdell, G. C. (1993). "On the two-way interaction between homogeneous turbulence and dispersed solid particles. 1: Turbulence modification." *Physics of Fluids A*, 5, (7), 1790–1801.
- Ferziger, J. H. (1996). "Large eddy simulation." *Simulation and modeling of turbulent flows*, T. B. Gatski, M. Y. Hussaini, and J. L. Lumley, eds., Oxford Univ. Press, New York.
- Ferziger, J. H., and Peric, M. (2001). *Computational fluid dynamics*, 3rd Rev. Ed., Springer-Verlag, Berlin.
- Fischer, H. B., List, E. J., Koh, R. C. Y., Imberger, J., and Brooks, N. H. (1979). *Mixing in inland and coastal waters*, Academic Press, New York.
- Fredsoe, J. (1993). "Modeling of non-cohesive sediment transport processes in the marine environment." *Coastal Engineering*, 21, 71–103.
- Fredsoe, J., Andersen, O. H., and Silberg, S. (1985). "Distribution of suspended sediment in large waves." *Journal of Waterway, Port, Coastal and Ocean Engineering, ASCE*, 111, (6), 1041–1059.
- Frey, P., Champagne, J. Y., Morel, R., and Gay, B. (1993). "Hydrodynamics fields and solid particles transport in a settling tank." *Journal of Hydraulic Research*, 31, (6), 763–776.
- Galperin, B., Kantha, L. H., Hassid, S., and Rosati, A. (1988). "A quasi-equilibrium turbulent energy model for geophysical flows." *Journal of the Atmospheric Sciences*, 45, (1), 55–62.
- Galperin, B., and Orszag, S., eds. (1993). *Large eddy simulation of complex engineering and geophysical flows*. Cambridge Univ. Press, New York.
- Gessler, D., Hall, B., Spasojevic, M., Holly, F., Pourtaheri, H., and Raphelt, N. (1999). "Application of 3D mobile bed, hydrodynamic model." *Journal of Hydraulic Engineering, ASCE*, 125, (7), 737–749.
- Ghanmi, A., Robert, J.-L., and Khelifi, M. (1997). "Three-dimensional finite element model to simulate secondary flows: Development and validation." *Journal of Hydraulic Research*, 35, (3), 291–300.
- Grass, A. J. (1971). "Structural features of turbulent flow over smooth and rough boundaries." *Journal of Fluid Mechanics*, 50, (2), 233–255.
- Greimann, B. P., Muste, M., and Holly, F. M., Jr., (1999). "Two-phase formulation of suspended sediment transport." *Journal of Hydraulic Research*, 37, (4), 479–500.
- Gresho, P. M., and Sani, R. L. (2000). *Incompressible flow and the finite element method*. Wiley, New York.
- Hagatun, K., and Eidsvik, K. J. (1986). "Oscillating turbulent boundary layer with suspended sediments." *Journal of Geophysical Research*, 91, (C11), 13,045–13,055.
- Hallbäck, M., Hennigsson, D. S., Johansson, A. V., and Alfredsson, P.H., eds. (1996) *Turbulence and transition modelling*. ERCOFTAC Series, Kluwer Academics, Dordrecht, The Netherlands.
- Hanes, D. M., and Bowen, A. J. (1985). "A granular-fluid model for steady intense bedload transport." *Journal of Geophysical Research*, 90, (C5), 9149–9158.
- Hanjalic, K. (1994). "Advanced turbulence closure models: A view of current status and future prospects." *International Journal of Heat and Fluid Flow*, 15, (3), June, 178–203.

- Haroutunian, V., and Engelman, M. S. (1993). "Two-equation simulations of turbulent flows: A commentary on physical and numerical aspects." *Advances in finite element analysis in fluid dynamics*, M. N. Dhaubhadel, M. S. Engelman, and W. G. Habashi, eds., ASME Fluids Eng. Div., New York, 171, 95–105.
- Hicks, F. E., Jin, Y. C., and Steffler, P. M. (1990). "Flow near sloped bank in curved channel." *Journal of Hydraulic Engineering, ASCE*, 116, (1), 55–70.
- Hinze, J. (1975). *Turbulence*. McGraw-Hill, New York.
- Hsu, T. J., Jenkins, J. T., and Liu, P. L. F. (2003). "On two-phase sediment transport: Dilute flow." *Journal of Geophysical Research—Oceans*, 108, (C3), No. 3057.
- Huynh Thanh, S., and Temperville, A. (1991). "A numerical model of the rough turbulent boundary layer in combined wave and current interaction." *Euromech 262—Sand transport in rivers, estuaries and the sea*, R. Soulsby and R. Bettess, eds., Balkema, Rotterdam, The Netherlands, 93–102.
- Huynh Thanh, S., Tran Thu, T., and Temperville, A. (1994). "A numerical model for suspended sediment in combined currents and waves." *Sediment Transport Mechanisms in Coastal Environment and Rivers*, World Scientific, Singapore, 122–130.
- Imam, E., McCorquodale, J. A., and Bewtra, J. K. (1982). "Numerical modeling of sedimentation tanks." *Journal of Hydraulic Engineering, ASCE*, 109, (12), 1740–1754.
- Itakura, T., and Kishi, T. (1980). "Open channel flow with suspended sediments." *Journal of the Hydraulics Division, ASCE*, 106 (HY8), 1325–1343.
- Jackson, R. G. (1976). "Sedimentological and fluid dynamical implications of the turbulent bursting phenomenon in geophysical flows." *Journal of Fluid Mechanics*, 77, 531–560.
- Jensen, B. L., Sumer, B. M., and Fredsoe, J. (1989). "Turbulent oscillatory boundary layers at high Reynolds number flow." *Journal of Fluid Mechanics*, 206, 265–297.
- Jobson, H. E., and Sayre, W. W. (1970). "Vertical transfer in open channel flow." *Journal of Hydraulic Engineering, ASCE*, 114, (10), 1157–1191.
- Johns, B., Soulsby, R. L., and Chesher, T. J. (1990). "The modeling of sandwave evolution resulting from suspended and bed load transport of sediment." *Journal of Hydraulic Research*, 28 (3), 355–374.
- Jovic, S., and Driver, D. (1995). "Reynolds number effect on the skin friction in separated flows behind a backward-facing step." *Experiments in Fluids*, 18, 464–467.
- Justesen, P. (1991). "A note on turbulence calculations in the wave boundary layer." *Journal of Hydraulic Research*, 29 (5), 699–711.
- Kim, H. G., and Patel, V. C. (2000). "Test of turbulence models for wind flow over terrain with separation and recirculation." *Boundary-Layer Meteorology*, 94, 5–21.
- Kobayashi, N., and Seo, S. N. (1985). "Fluid and sediment interaction over a plane bed." *Journal of Hydraulic Engineering, ASCE*, 111 (6), 903–921.
- Krebs, P. (1995). "Success and shortcomings of clarifier modeling." *Water Research*, 31, (2), 181–191.
- Kundu, P. K. (1990). *Fluid Mechanics*. Academic Press, San Diego.
- Lamberti, A., Montefusco, L., and Valiani, A. (1991). "A granular-fluid model of the stress transfer from the fluid to the bed." *Euromech 262—Sand transport in rivers, estuaries and the sea*, R. Soulsby and R. Bettess, eds. Balkema, Rotterdam, The Netherlands, 209–214.
- Lane, S. N. (1998). "Hydraulic modeling in hydrology and geomorphology: A review of high resolution approaches." *Hydrological Processes*, 12, 1131–1150.
- Larsen, P. (1977). "On the hydraulics of rectangular settling basins, experimental and theoretical studies." *Rep. 1001*, Dept. of Water Resources Eng., Lund Institute of Technology, Lund University, Lund, Sweden.
- Lauder, B. E. (1978). "Heat and mass transport." In *Turbulence*, 2nd Ed., P. Bradshaw, ed., Springer-Verlag, Berlin.
- Lauder, B. E. (1984). "Second-moment closure: Methodology and practice." *Turbulence models and their applications*, Vol. 2, Editions Eyrolles, Paris.
- Lauder, B. E. (1996). "An introduction to single-point closure methodology." *Simulation and modeling of turbulent flows*, T. B. Gatski, M. Y. Hussaini, and J. L. Lumley, eds., Oxford Univ. Press, New York.
- Le, H., Moin, P., and Kim, P. (1997). "Direct numerical simulation of turbulent flow over a backward-facing step." *Journal of Fluid Mechanics*, 330, 349–374.
- Li, Z., and Davies, A. G. (1996). "Towards predicting sediment transport in combined wave-current flow." *Journal of Waterway, Port, Coastal, and Ocean Engineering, ASCE*, 122 (4), 157–164.
- Lien, F. S., and Leschziner, M. A. (1994). "Assessment of turbulence-transport models including non-linear RNG eddy-viscosity and second-moment closure for flow over a backward-facing step." *Computers and Fluids*, 23, (8), 983–1004.
- Liggett, J. A. (1994). *Fluid mechanics*. McGraw-Hill, New York.
- Lodahl, C. R., Sumer, B. M., and Fredsoe, J. (1998). "Turbulent combined oscillatory flow and current in a pipe." *Journal of Fluid Mechanics*, 373, 313–348.
- Lopez, F., and Garcia, M. H. (2001). "Mean flow and turbulence structure of open-channel flow through submerged vegetation." *Journal of Hydraulic Engineering, ASCE*, 127, (5), 392–402.
- Lumley, J. L. (1973). "Two-phase and non-Newtonian flows." In *Turbulence*, P. Bradshaw, ed., Springer, New York.
- Lumley, J. L., and Panofsky, H. A. (1964). *The structure of atmospheric turbulence*. Interscience, New York.
- Lyn, D. A. (1988). "A similarity approach to turbulent sediment-laden flows in open channels." *Journal of Fluid Mechanics*, 193, 1–26.
- Lyn, D. A. (1991). "Resistance in flat-bed sediment-laden flows." *Journal of Hydraulic Engineering, ASCE*, 117 (1), 94–115.
- Lyn, D. A. (1993). "Turbulence measurements in open-channel flows over artificial bed forms." *Journal of Hydraulic Engineering, ASCE*, 119 (3), 306–326.
- Lyn, D. A., Stamou, A. I., and Rodi, W. (1992). "Density currents and shear-induced flocculation in sedimentation tanks." *Journal of Hydraulic Engineering, ASCE*, 118 (6), 849–867.
- Malvern, L. E. (1969). *Introduction to the mechanics of a continuous medium*. Prentice-Hall, Englewood Cliffs, N.J.
- Matko, T., Fawcett, N., Sharp, A., and Stephenson, T. (1996). "Process safety and environmental protection." *Transactions of the Institute of Chemical Engineering*, 74, 245–258.
- Maxey, M. R. (1993). "The equations of motion for a small rigid sphere in a non-uniform flow." *ASME/FED Gas-Solid Flows*, 166, 57–62.

- McComb, W. D. (1990). *The physics of fluid turbulence*. Clarendon, Oxford, U.K.
- McLean, S. R. (1992). "On the calculation of suspended load for noncohesive sediments." *Journal of Geophysical Research*, 97, (C4), 5759–5770.
- McLean, S. R., Nelson, J. M., and Wolfe, S. R. (1994). "Turbulence structure over two-dimensional bed forms: Implications for sediment transport." *Journal of Geophysical Research*, 99, (C6), 12729–12747.
- McTigue, D. F. (1981). "Mixture theory for suspended sediment transport." *Journal of the Hydraulics Division, ASCE*, 107, (HY6), 659–673.
- McTigue, D. F. (1982). "Closure to 'Mixture theory for suspended sediment transport' by D. F. McTigue," *Journal of the Hydraulics Division, ASCE*, 108, (HY10), 1245–1247.
- Mei, R., and Adrian, R. J. (1995). "Effects of Reynolds number on isotropic turbulent dispersion." *Journal of Fluids Engineering, ASME*, 117, 402–409.
- Mellor, G. L., and Herring, H. J. (1973). "A survey of the mean turbulence field closure models." *AIAA Journal*, 11, (5), 590–599.
- Mellor, G. L., and Yamada, T. (1982). "Development of a turbulence closure model for geophysical fluid problems." *Reviews of Geophysics and Space Physics*, 20, (4), 851–875.
- Melville, B. W., and Raudkivi, A. J. (1977). "Flow characteristics in local scour at bridge piers." *Journal of Hydraulic Research*, 15, (4), 373–380.
- Mendoza-Cabral, C. (1993). "Computation of flow past a cylinder mounted on a flat plate." *Proc., Hydraulic Eng. '93*, H. W. Shen, S. T. Su, and F. Wen, eds., ASCE, New York, 899–904.
- Mendoza, C., and Shen, H. W. (1988). "Modeling of turbulent two-phase flow over dunes." *First National Fluid Dynamics Congress*. AIAA, New York.
- Mendoza, C., and Shen H. W. (1990). "Investigation of turbulent flow over dunes." *Journal of Hydraulic Engineering, ASCE*, 116, (4), 459–477.
- Minh Duc, B., Wenka, T., and Rodi, W. (1998). "Depth-average numerical modeling of flow and sediment transport in the Elbe River." *Proc., Third Int. Conf. Hydroscience and Eng.* National Center for Computational Hydroscience and Engineering, University of Mississippi, Oxford, Miss.
- Monin, A. S., and Yaglom, A. M. (1971). *Statistical fluid mechanics. mechanics of turbulence*, Vol. 1, MIT Press, Cambridge, Mass.
- Müller, A., and Gyr, A. (1986). "On the vortex formation in the mixing layer behind dunes." *Journal of Hydraulic Research*, 24, (5), 359–375.
- Murray, P. B., Davies, A. G., and Soulsby, R. L. (1991). "Sediment pick-up in wave and current flows." *EuroMech 262—Sand transport in rivers, estuaries and the sea*, R. Soulsby and R. Bettess, eds., Balkema, Rotterdam, The Netherlands, 37–44.
- Muste, M., and Patel, V. C. (1997). "Velocity profiles for particles and liquid in open-channel flows." *Journal of Hydraulic Engineering, ASCE*, 123, (9), 742–751.
- Naot, D., Nezu, I., Nakagawa, H. (1996). "Hydrodynamic behavior of partly vegetated open-channels." *Journal of Hydraulic Engineering, ASCE*, 122, (11), 625–633.
- Nelson, J. M., Shreve, S. R., McLean, S. R., and Drake, T. G. (1995). "Role of near-bed turbulence structure in bedload transport and bedform mechanics." *Water Resources Research*, 31, 2071–2086.
- Nezu, I., and Nakagawa, H. (1993). *Turbulence in open channel flows*, IAHR Monograph Series, Balkema, Rotterdam, The Netherlands.
- Nezu, I., and Rodi, W. (1986). "Open-channel flow measurements with a laser-Doppler anemometer." *Journal of Hydraulic Engineering, ASCE*, 112, (5), 335–355.
- Niño, Y., and Garcia, M. H. (1996). "Experiments on particle-turbulence interactions in the near-wall region of an open-channel flow: Implications for sediment transport." *Journal of Fluid Mechanics*, 326, 285–319.
- Odgaard, A. J., and Bergs, M. A. (1988). "Flow processes in a curved alluvial channel." *Water Resources Research*, 24, (1), 45–56.
- Olsen, N. R. B., and Melaaen, O. (1993) "Three-dimensional calculation of scour around cylinders. *Journal of Hydraulic Engineering, ASCE*, 119, (9), 1048–1054.
- Olsen, N. R. B., and Kjellesvig, H. M. (1999). "Three-dimensional numerical modeling of bed changes in a sand trap." *Journal of Hydraulic Research*, 37, (2), 189–198.
- Ouillon, S., and le Guennec, B. (1996). "Modeling non-cohesive suspended sediment transport in 2D vertical free-surface flows." *Journal of Hydraulic Research*, 34, (2), 219–236.
- Patel, V. C. (1997). "Longitudinal curvature effects in turbulent boundary layers." *Progress in Aerospace Sciences*, 33, 1–70.
- Patel, V. C. (1998). "Perspective: Flow at high Reynolds number and over rough surfaces—Achilles heel of CFD." *Journal of Fluids Engineering, ASME*, 120, 434–444.
- Patel, V. C., Rodi, W., and Scheuerer, G. (1985). "A review and evaluation of evaluation of turbulent models for near-wall and low-Reynolds-number flows." *AIAA Journal*, 23, (9), 1308–1319.
- Patel, V. C. and Sotiropoulos, F. (1997). "Longitudinal curvature effects in turbulent boundary layers." *Progress in Aerospace Sciences*, 33 (½), 1–70.
- Piomelli, U., and Chasnov, J. R. (1996). "Large-eddy simulations: Theory and application." *Turbulence and transition modelling*, M. Hallbäck, D. S. Henningson, A. V. Johansson, and P. H. Alfredsson, eds., ERCOFTAC series, Kluwer, Dordrecht, The Netherlands.
- Piquet, J. (1999). *Turbulent flows: Models and physics*. Springer, Berlin.
- Portela, L. M., and Oliemans, R. V. A. (2003). "Eulerian-Lagrangian DNS/LES of particle-turbulence interactions in wall-bounded flows." *International Journal for Numerical Methods in Fluids*, 43, 1045–1065.
- Prandtl, L. (1925). "Über die ausgebildete Turbulenz." *Zeitschrift für angewandte Mathematik und Mechanik* (5), 136–139.
- Rastogi, A., and Rodi, W. (1978). "Predictions of heat and mass transfer in open channels." *Journal of the Hydraulics Division, ASCE*, 104, (HY3), 397–420.
- Raudkivi, A. J. (1963). "Study of sediment ripple formation." *Journal of the Hydraulics Division, ASCE*, 69, (HY6), 15–33.
- Raudkivi, A. J. (1966). "Bedforms in alluvial channels." *Journal of Fluid Mechanics*, 26, (3), 507–514.
- Raudkivi, A. J. (1990). *Loose boundary hydraulics*. Pergamon, Oxford, England.
- Ribberink, J. S., and Al-Salem, A. A. (1994). "Sediment transport in oscillatory boundary layers in cases of rippled beds and sheet flow." *Journal of Geophysical Research*, 99, (C6), 12707–12727.

- Ribberink, J. S., and Al-Salem, A. A. (1995). "Sheet flow and suspension of sand in oscillatory boundary layers." *Coastal Engineering*, 25, 205–225.
- Richards, K. J. (1980). "The formation of ripples and dunes on an erodible bed." *Journal of Fluid Mechanics*, 99, (2), 597–618.
- Richardson, J. E., and Panchang, V. G. (1998). "Three-dimensional simulation of scourinducing flow at bridge piers." *Journal of Hydraulic Engineering, ASCE*, 124, (5), 530–541.
- Rodi, W. (1976). "A new algebraic relation for calculating Reynolds stress." *Zeitschrift für Angewandte Mathematik und Mechanik*, 56, 219–221.
- Rodi, W. (1987). "Examples of calculations methods for flow and mixing in stratified fluids." *Journal of Geophysical Research*, 92, (C5), 5305–5328.
- Rodi, W. (1993). *Turbulence models and their application in hydraulics*, 3rd Ed., Balkema, Rotterdam, The Netherlands.
- Rodi, W. (1995). "Impact of Reynolds-average modeling in hydraulics." *Proceedings of the Royal Society of London*, series 451, 141–164.
- Rotta, J. C. (1951). "Statistische Theorie nichthomogener Turbulenz." *Zeitschrift für Physik*, 129, 547–572.
- Rotta, J. C. (1964). "Temperaturverteilungen in der turbulenten Grenzschicht an der ebenen Platte." *International Journal of Heat and Mass Transfer*, 7, 215–228.
- Sajjadi, S. G., and Aldridge, J. N. (1995). "Prediction of turbulent flow over rough asymmetrical bed forms." *Applied Mathematical Modeling*, 19, 139–152.
- Sana, A., and Tanaka, H. (2000). "Review of $k-\epsilon$ models to analyze oscillatory boundary layers." *Journal of Hydraulic Engineering, ASCE*, 126, (9), 701–710.
- Savioli, J., and Justesen, P. (1997a). "Sediment in oscillatory flows over a plane bed." *Journal of Hydraulic Research* 35 (2), 177–190.
- Savioli, J., and Justesen, P. (1997b). "Discussion of 'Towards predicting sediment transport in combined wave-current flow.'" *Journal of Waterway, Port, Coastal, and Ocean Engineering, ASCE*, 123, (6), 362–363.
- Sekine, M., and Kikkawa, H. (1992). "Mechanics of saltating grains. II." *Journal of Hydraulic Engineering, ASCE*, 118, (4), 536–558.
- Sheng, Y. P., and Villaret, C. (1989). "Modeling the effect of suspended sediment stratification on bottom exchange processes." *Journal of Geophysical Research*, 94, (C10), 14429–14444.
- Simonin, O. (1991). "Predictions of the dispersed phase turbulence in particle-laden jets." *Gas-solid flows*, D. E. Stock, Y. Tsuji, J. T. Jurewicz, M. W. Reeks, and M. Gautam, eds., ASME, New York, vol. 121, 197–206.
- Smith, J. D., and McLean, S. R. (1977). "Spatially averaged flow over a wavy surface." *Journal of Geophysical Research*, 82, (12), 1735–1746.
- Soulsby, R. L., and Wainwright, B. L. S. A. (1987). "A criterion for the effect of suspended sediment on near-bottom velocity profiles." *Journal of Hydraulic Research*, 25, (3), 341–356.
- Spalart, P. R. (2000). "Strategies for turbulence modeling and simulations." *International Journal of Heat and Fluid Flow*, 21, 252–263.
- Spalart, P. R., and Allmaras, S. R. (1992). "A one-equation turbulence model for aeronautical flows." *AIAA Paper 92–439*, AIAA, Roitton, Va.
- Speziale, C. G. (1987). "On nonlinear $k-l$ and $k-\epsilon$ models of turbulence." *Journal of Fluid Mechanics*, 178, 459–475.
- Speziale, C. G. (1991). "Analytical models for the development of Reynolds stress closures in turbulence." *Annual Reviews of Fluid Mechanics*, Annual Reviews, Palo Alto, Calif.
- Speziale, C. G. (1996). "Modeling of turbulent transport equations." *Simulation and modeling of turbulent flows*, T. B. Gatski, M. Y. Hussaini, and J. L. Lumley, eds., Oxford Univ. Press, New York.
- Speziale, C. G., and Bernard, P. S. (1992). "The energy decay in self-preserving isotropic turbulence revisited." *Journal of Fluid Mechanics*, 241, 645–667.
- Speziale, C. G. and Thangam, S. (1992). "Analysis of an RNG based turbulence model for separated flows." *International Journal of Engineering Science*, 30, (10) 1379–1388.
- Squires, K. D., and Eaton J. K. (1991). "Measurement of particle dispersion obtained from numerical simulations of isotropic turbulence." *Journal of Fluid Mechanics*, 226, 1–35.
- Stock, D. E. (1996). "Particle dispersion in flowing gases—1994 Freeman Scholar Lecture." *ASME Journal of Fluids Engineering*, 118, 4–17.
- Sumer, B.M., Jensen, B.L., and Fredse, J. (1987). "Turbulence in oscillatory boundary layers." *Advances in Turbulence, Proc. 1st European Conf.*, G. Comte-Bellot and J. Mathieu, eds., Springer-Verlag, New York, 556–567.
- Tennekes, H. (1989). "Two- and three-dimensional turbulence." *Lecture notes from the NCAR-GTP Summer School, June 1987*, World Scientific, Singapore, 1–73.
- Tennekes, H., and Lumley, J. L. (1972). *A first course in turbulence*, MIT Press, Cambridge, Mass.
- Thorne, C. R., and Raïs, S. (1983). "Secondary current measurement in a meander river." *Proc. ASCE Inter. Conf. on River Meandering*, ASCE, New York, 675–686.
- Tseng, M.-H., Yen, C. L., and Song, C. C. S. (2000). "Computation of three-dimensional flow around square and circular piers." *International Journal of Numerical Methods in Fluids*, 34, 207–227.
- Tsujimoto, T., Shimizu, Y., and Nakagawa, H. (1991). "Concentration distribution of suspended sediment in vegetated sand bed channel." *International symposium on transport of suspended sediment and its mathematical modeling*.
- Turner, J. S. (1973). *Buoyancy effects in fluids*. Cambridge Univ. Press, Cambridge, U.K.
- Van Mierlo, M. C. L. M., and de Ruiter, J. C. C. (1988). "Turbulence measurements above artificial dunes." *Rept. Q789*, Delft Hydraulics Laboratory, Delft, The Netherlands.
- Van Rijn, L. (1982). "Equivalent roughness of alluvial bed." *Journal of Hydraulics Division, ASCE*, 108, (HY10), 1215–1218.
- Van Rijn, L. (1984b). "Sediment transport, I: Bed load transport." *Journal of Hydraulic Engineering, ASCE*, 110 (10), 1431–1456.
- Van Rijn, L. (1984a). "Sediment pick-up functions." *Journal of Hydraulic Engineering, ASCE*, 110, (10), 1494–1502.
- Van Rijn, L. (1984c). "Sediment transport. Suspended load transport." *Journal of Hydraulic Engineering, ASCE*, 110, (11), 1613–1641.
- Vanoni, V. A. (1946). "Transportation of suspended sediment by water." *Transactions of the ASCE*, 111, Paper 2267, 67–133.
- Vanoni, V. A., ed. (1975). *Sedimentation Engineering*, ASCE Manual no. 54, ASCE, New York.

- Villaret, C., and Davies, A. G. (1995). "Modeling sediment-turbulent flow interactions." *Applied Mechanics Review*, 48, (9), 601–609.
- Villaret, C., and Trowbridge, J. H. (1991). "Effects of stratification by suspended sediments on turbulent shear flows." *Journal of Geophysical Research*, 96, (C6), 10659–10680.
- Wang, L.-P., and Maxey, M. R. (1993). "Settling velocity and concentration distribution of heavy particles in homogeneous isotropic turbulence." *Journal of Fluid Mechanics*, 256, 27–68.
- Wei, T., and Willmarth, W. (1991). "Examination of v -velocity fluctuations in a turbulent channel flow in the context of sediment transport." *Journal of Fluid Mechanics*, 223, 241–252.
- Wiberg, P. L., and Rubin, D. M. (1989). "Bed roughness produced by saltating sediment." *Journal of Geophysical Research*, 94, (C4), 5011–5016.
- Wiberg, P. L., and Smith, J. D. (1985). "A theoretical model for saltating grains in water." *Journal of Geophysical Research*, 90, (C4), 7341–7354.
- Wiberg, P. L., and Smith, J. D. (1989). "Model for calculating bed load transport of sediment." *Journal of Hydraulic Engineering, ASCE*, 115, (1), 101–123.
- Wilcox, D. C. (1998). *Turbulence modeling for CFD*, 2nd Ed., DCW Industries, La Cañada, Calif.
- Wu, W., Rodi, W., and Wenka, T. (2000). "3D numerical modeling of flow and sediment transport in open channels." *Journal of Hydraulic Engineering, ASCE*, 126, (1), 4–15.
- Yakhot, V., and Orszag, S. A. (1986). "Renormalization group analysis of turbulence. 1: Basic theory." *Journal of Scientific Computing*, 1, (1), 3–51.
- Yang, T. S., and Shy, S. S. (2003). "The settling velocity of heavy particles in an aqueous near-isotropic turbulence." *Physics of Fluids*, 15, (4), 868–880.
- Ye, J., and McCorquodale, J. A. (1998). "Simulation of curved open channel flows by 3D hydrodynamic model." *Journal of Hydraulic Engineering, ASCE*, 124, (7), 687–698.
- Yoon, J. Y., and Patel, V. C. (1996). "Numerical model of turbulent flow over a sand dune." *Journal of Hydraulic Engineering, ASCE*, 122, (1), 10–18.
- Zedler, E. A., and Street, R. L. (2001). "Large eddy simulations of sediment transport: currents over ripples." *Journal of Hydraulic Engineering*, 127, (6), 444–452.
- Zhou, S. P., McConquodale, J. A., and Godo, A. M. (1994). "Short circuiting and density interface in primary classifiers." *Journal of Hydraulic Engineering*, 120, (9), 1060–1080.

This page intentionally left blank